Experimental Investigation on Tapping Noise in EVAP System of a Motor Vehicle

by

Zhe Li

A thesis
presented to the University of Waterloo
in fulfillment of the
thesis requirement for the degree of
Master of Applied Science
in
Mechanical Engineering

Waterloo, Ontario, Canada, 2014

AUTHOR'S DECLARATION

I hereby declare that I am the sole author of this thesis. This is a true copy of the thesis, including any required final revisions, as accepted by my examiners.

I understand that my thesis may be made electronically available to the public.

Abstract

Within automotive industry, Noise, Vibration and Harshness (NVH) has emerged to be one of the main research topics. Unlike attributes such as vehicle safety, drivability, and durability which are functionality criteria, NVH is closely tied to quality and comfort of the ride. The recent trend in consumer market shows that NVH is becoming increasingly important in purchasing decisions and can significantly affect competitive edge of vehicles.

Among various factors that contribute to vehicle noise, pressure pulsation inside vehicle fuel system has been subject to studies for several decades. In gasoline vehicles, with the introduction and wide spread of returnless fuel delivery system, the pressure pulsation phenomenon has become more and more prominent and has raised several issues, including noise. Similar phenomenon can be found in EVAP system where pressure is small. However, the information regarding pressure pulsation and noise issue in EVAP system is very limited.

This thesis investigated the noise issue caused by pressure pulsation inside EVAP system of a current production vehicle by one of the major automotive Original Equipment Manufacturers (OEM). There are two main parts in this research. First part is to build a test stand integrating the original parts provided by the OEM to re-create the noise, then to observe and collect data on the noise issue to understand the noise generation mechanism. Second part of this research is to, through literature survey, generate ideas on noise reduction, and then to test these ideas. Due to limited information, literature survey was focused on researches done on the fuel delivery system.

By collecting and analyzing pressure data on various running conditions, utilizing inspection camera, and carefully designed experiments, this research made findings on pressure pulsation and noise phenomenon, examined possible scenarios for the noise generation mechanism, and provided key evidences regarding various components and their effects on the pressure pulsation/noise. This thesis presented 8 different approaches to achieve noise reduction. Among those, 5 focused on pressure pulsation attenuation, which heavily drew inspiration from pulsation attenuation methods used in fuel delivery system. The methods tested in this thesis achieved various degree of success in noise reduction. However, each had its own drawbacks: they caused flow restriction in the line, and/or reduced the vacuum level going to the fuel tank system, and/or required design changes on critical parts in the system.

Acknowledgements

I would like to thank Professor Fue-Sang Lien for offering me this great opportunity to explore further into the world of fluid mechanics. This collaboration with the Automotive OEM was not possible if not by Professor Lien's tireless work.

I also would like to thank Professor Zhongchao Tan for providing me guidance throughout my research. His help on sharing his expertise and knowledge in experimental work was instrumental for the success of this research.

I greatly appreciate the time and effort from Professor Fue-Sang Lien to help me go through my thesis for editing, also from Professor Amir Khajepour and Professor Zhongchao Tan for being my thesis readers.

Also my sincerest gratitude goes to my group members, colleagues, 4 coop students who assisted me with this research, and those who helped me, supported me, and/or made my past 5-term experience fun, enjoyable, and memorable; also to the engineers and technical experts from the OEM, who shall remain anonymous, for providing me with parts, insights, resources, and information I needed.

Last but not the least, my deepest feeling goes to my family, my farther and my mother, without whom this thesis would not be possible.

Dedication

To my parents, Kaizhong Li, Qiju Pan.

Table of Contents

List of Figures

List of Tables

List of Symbols

AF	**Air Fuel Ratio**
CFD	**computational fluid dynamics**
CPV	**canister purge valve**
DAQ	**data acquisition**
DC	**duty cycle**
EVAP	**evaporative emission**
FDM	**fuel delivery module**
FEM	**finite element method**
FLVV	**flow limiting vent valve**
FWD	**front wheel drive**
GVV	**grade vent valve**
HVAC	**heating, ventilation, and air conditioning**
ID	**inner diameter**
LPM	**liters per minute**
LVM	**logical volume management**
MPI	**multiport fuel injection**
MS	**Microsoft®**
NAFTA	**North America Free Trade Agreement**
NI	**National Instruments**
NVH	**noise, vibration, and harshness**
OEM	**original equipment manufacturer**
ORVR	**On-Board Refueling Vapor Recovery**
PCM	**powertrain control module**
PP	**peak-to-peak**
PWM	**pulse width modulation**
RPM	**revolution per minute**
ULC	**Underwriters Laboratories of Canada**

Chapter 1
Introduction

1.1 Background

1886 was the year widely regarded as the birth of the modern automobile when Karl Benz patented his invention which is now known as the "Benz Patent-Motorwagen". Ever since then, the automotive industry has seen itself steadily growing into one of the most important components in global economy. Today, more than 8 million people are employed in directly making motor vehicles and parts, accounting for over 5 percent of the entire global manufacturing employment. In addition, there are about 5 times more employed in the related manufacturing and service provision. 84 million motor vehicles were produced in the year 2012 alone [1].

As of 2011, there are just fewer than 1.1 billion motor vehicles in use around the world-that is 165 vehicles per 1000 people. In Europe, the motorization rate is just under one vehicle for every two people. The number goes higher in NAFTA (Canada, Mexico, and United States of America) with 644 vehicles per 1000 people [2], [3]. With this many cars in use, people are spending more and more time on road inside vehicles. In the US, the average time people spend in their car is 20 hours per week and the average travel distance is 200 miles per week [3].

Because of its importance, immensely abundant amount of resources have been invested into vehicle-related researches. Aside from functional criteria of the vehicle, more and more researches have been focusing on other aspects, including EVAP [4], fuel consumption [5], ride quality [6]–[9], and many other attributes. The term "attribute" is a commonly used terminology in automotive industry. It covers a variety of engineering areas such as craftsmanship, styling, package, performance, safety, aerodynamics, climate control, ride and handling, and NVH. All of above mentioned are "attributes" which are experienced, one way or another, by the driver/passenger at vehicle level [10].

Quality of ride is important not only because of the comfort level perceived by the drivers and passengers, it also attributes to vehicle safety in two main aspects. First, uncomfortable vehicles will cause driver fatigue, especially during long journeys [11]. Second, driver's ability to control the vehicle can be compromised due to poor ride quality [6]–[9]. There are several attributes to the ride quality: entertainment ,such as audio system, gaming, video, DVD, MP3, USB, navigation and internet connectivity [12]–[14], ergonomics, such as seat design [15], HVAC such as thermal comfort, and in-cabin air quality [16], and NVH [10].

It has been observed that NVH, especially in-cabin noise, is a critical factor towards the comfort and usability for the end user. Thus, it is becoming increasingly important in purchasing decision and can affect the competitive edge of products in market place significantly [10]. Therefore, many major OEMs have started including NVH attribute into early design cycle in order to avoid costly and ineffective patches afterwards should issues arise [17]–[23].

NVH is by itself a very complicated problem that can be roughly divided into three components: problem source (noise source), transmission/travel path, and receiver (human ear). Within vehicle NVH, there are two main noise transmission paths: structure borne, and air borne. Three major noise sources have been identified: visual noise (wind), road noise (tires, road conditions, etc.), and engine noise (transmission, power train, etc.) [17].

In modern vehicle fuel system design, returnless fuel delivery system is currently most common in gasoline vehicles, replacing the full return fuel system [24]. The wide adoption of returnless fuel system design was a means for meeting emission requirements [4], [25]–[27]. However, a side effect of this returnless fuel delivery system is the potential for injector induced flow ripples to create high pressure pulsations [24]. Fuel delivery system is a prime factor inside the vehicle, affecting its efficiency, performance, and emissions [28]. Pressure pulsations inside vehicle fuel system can cause several issues. For example, inside fuel delivery system, pressure pulsation can cause fuel maldistribution which leads to increase in harmful emission and consumption while deteriorating the drivability, undesirable air-fuel ratio which can greatly decrease the efficiency of the catalytic converter, and unwanted noise [29].

Another important development for the gasoline fuel system is the EVAP (Evaporative Emission Control) system. The main purpose of the EVAP system is to minimize the gasoline vapor leaking into the ambient atmosphere [25]. This is very important because gasoline vapor not only causes environmental damages, it also has detrimental effects on human health [30]. However, studies on pressure pulsation inside EVAP system and related issues are very limited. One possible explanation is the high-pressure nature of the fuel delivery line, compared to low pressure nature of the EVAP line. The EVAP line is subject to vacuum pressure from engine side, while the typical pressure in gasoline fuel delivery line is 300-400kPa (gauge) [31].

In diesel vehicles (compression ignition engine), both returnless fuel delivery system and EVAP system are not adopted due to low evaporative nature of the fuel. Although diesel vehicles have full return fuel delivery system and no EVAP system in place, they still suffer pressure-pulsation-caused issues [32]. However, this research mainly focuses on gasoline vehicle with a brief cover on diesel vehicles.

Vehicles that run on alternative fuels or electrical vehicles also face NVH issues of their own. However, the fuel system NVH is relatively unique in the conventional vehicles, that is, vehicles that rely on gasoline, diesel, or some formula of blend. From the current trend, the gasoline/diesel-fuel based vehicles will still be the major components in the global vehicle markets, accounting for at least 70% to 80% in the year 2030 [33]. Thus, it is important and relevant to keep researching the NVH issue in the fuel system: fuel delivery and EVAP systems.

Additional research value in looking into pressure pulsation and noise issue inside EVAP system is that it is not confined within gasoline vehicles only. It can also apply to certain flex-fueled engine vehicles that has similar fuel system design, including returnless fuel delivery system, as well as EVAP system [34]. Another potential for this topic is that its results may help guide future research in gas-fuel vehicles, for example, hydrogen-fueled cars [35].

1.2 Motivation

In gasoline fuel system, there are two fuel lines going into the engine [26], [36], [37]: the liquid fuel supply line which is the fuel delivery system, and the vapor fuel line which is EVAP system. The liquid fuel is being supplied via the fuel pump to the engine under high pressure. The vapor fuel line is illustrated in Figure 1-1. The EVAP system also serves the purpose for On-Board Refueling Vapor Recovery (ORVR), which ensures the vapor created during the refueling process does not leak out into the ambient atmosphere [38]. Its main purpose is for vehicle evaporative emission control, thus it is also called EVAP system.

In EVAP system, the Canister Purging Valve (CPV) is normally closed. Due to the evaporative nature of the gasoline fuel, it evaporates into vapor state. The excess fuel vapor then exits the fuel tank via the valve system inside the fuel tank. The “T” connection between the filler pipe, canister and fuel tank is to allow some of the fuel vapor to condense back into liquid form during refilling (ORVR). When vapor enters the canister, which is filled with active carbon, it is stored inside. The canister has a sensor inside which keeps track of its capacity. When pre-determined conditions are met, the sensor sends the signal to the Powertrain Control Module (PCM), which then signals CPV to open. Opening of CPV will subject the system under the vacuum pressure created by the engine. The fresh air is drawn into the canister, flushing out the fuel vapor. The vapor fuel/air mixture is then fed into the engine. On the engine side, there is another system that ensures the correct air-fuel ratio is achieved.

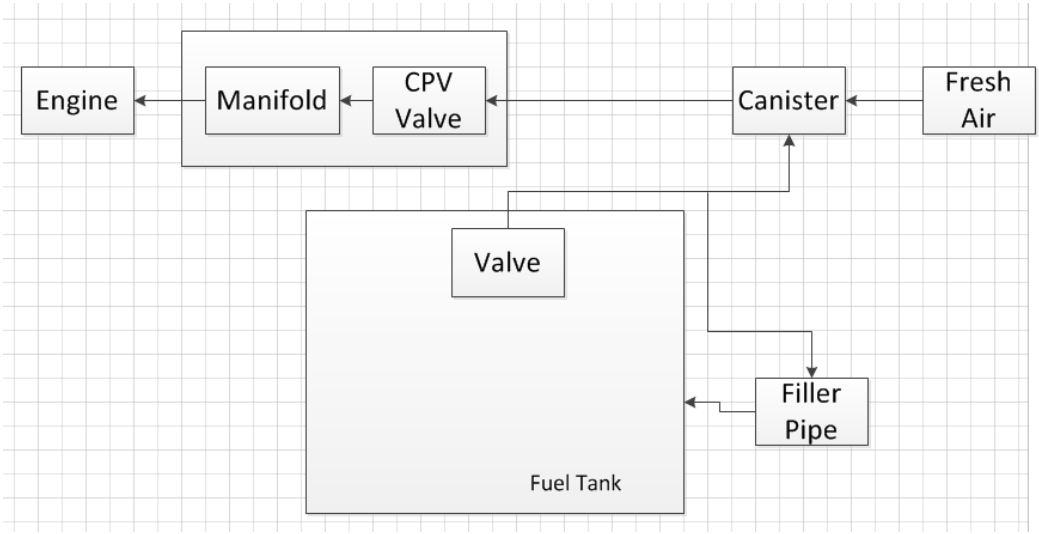

Figure 1-1: Schematics of a typical vehicle EVAP system

There is a current production vehicle designed and assembled by a major OEM that is having in-cabin noise issue. Based on preliminary test performed by the OEM, it was narrowed down that the noise source is from the vehicle EVAP system. The EVAP system utilizes the negative pressure (lower than ambient atmospheric pressure) as a driving force to pull the vapor from the carbon canister. Figure 1-2 shows an overview of the EVAP system, including the fuel tank and the valves inside the fuel tank. The numbers shown in the figure each corresponds to a part and the list of the parts is shown in Table 1-1 below. No. 10 part, which is the straps and bolts, is not shown in the schematics. It is integrated as part of the fuel tank in the actual experimental setup.

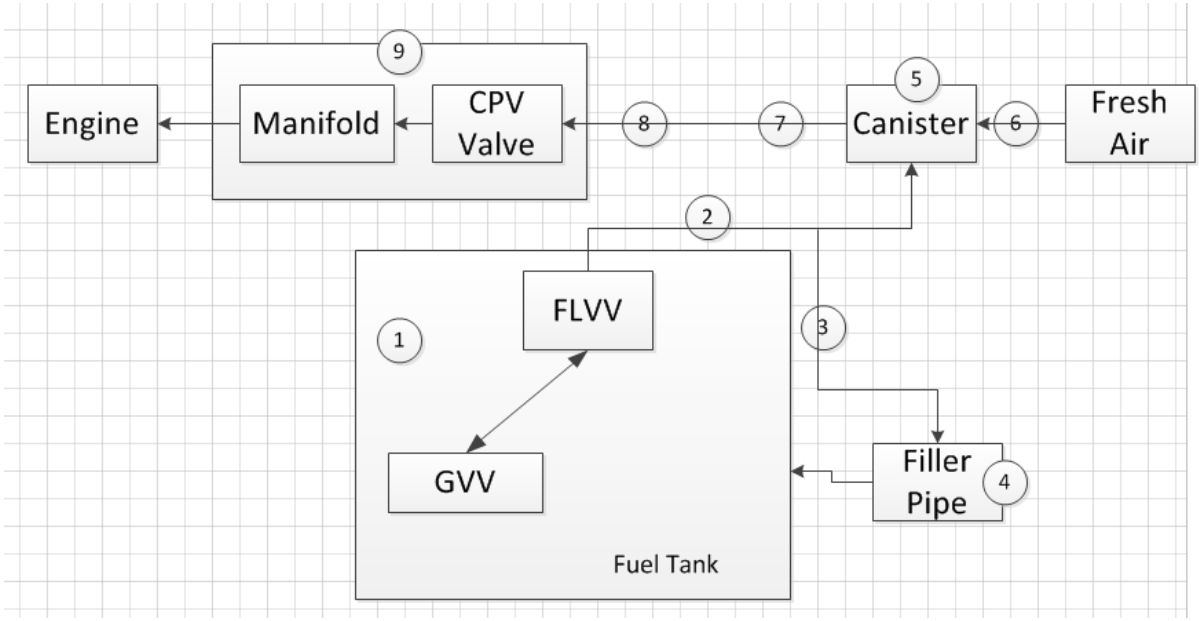

Figure 1-2: Fuel tank and EVAP system

Table 1-1: Fuel tank and EVAP system parts list

#	Part Description
1	Fuel tank, with the FLVV (flow limiting vent valve), and GVV (grade vent valve) valve system built-in
2	Tank to canister line
3	Re-circulation line
4	Filler pipe
5	Carbon canister
6	Fresh air tube
7	Canister to front line
8	Main vapor line
9	Manifold with CPV (canister purging valve)
10	Straps and bolts to secure fuel tank

The gasoline fuel inside fuel tank (①) evaporates, causing vapor inside the fuel tank to build up. The FLVV and GVV inside the fuel tank act together to regulate the vapor and to create a pathway for the vapor to leave the fuel tank. The vapor then passes through tank to canister line (②), and is stored inside the carbon canister (⑤), which is filled with active carbon. When canister reaches its capacity, a signal is sent to the PCM (powertrain control module), which in turn opens CPV (canister purging valve) to purge

the vapor inside the canister. The running engine provides a negative pressure which causes the vapor to flow towards the engine, as illustrated by the arrows in Figure 1-2. The fuel vapor, being purged out of the canister and mixed with incoming fresh air through fresh air tube (⑥), goes through canister to front line (⑦), main vapor line (⑧), manifold (⑨), and finally enters the engine as part of the fuel supply. The precise fuel-air ratio is realized by a system of sensors and valves controlled by the PCM. The re-circulation line (③) and filler pipe (④) provides another path for the vapor to flow, for ORVR purpose.

The CPV is a solenoid valve controlled by a PWM (pulse-width modulation) driver. It controls the vapor flow rate by varying the duty cycle. The frequency of the PWM signal is fixed during vehicle calibration. Due to its nature of operation, CPV creates pressure pulsation. This pressure pulsation travels through the vapor lines, canister, and back into the fuel tank. Given the right condition, the pressure pulsation can excite the valves inside the fuel tank (FLVV, and/or GVV), making tapping noise. This tapping noise was arbitrarily named "Woodpecker noise" for its tapping nature similar to a woodpecker pecking a tree trunk.

The conditions that the tapping noise would occur and became audible inside the cabin are as follows:

- full fuel +0.2-0.3 gallons after 3rd "click" or almost full (95%+);
- idle condition/ No fan On/ No Radio ON and with right fuel level, right purge condition, FLVV flapper gets excited and creates vapor/air pulsation balance issue;
- low speed stop triggers noise and continuous for a while if purge is still on that time;
- the CPV is operating at 20Hz (or 17Hz); it was observed that at lower frequency (14Hz or lower) the noise disappears; and
- it was observed that when the car is on a nose-down position, even at a small angle (roughly between 1-2 degrees), the noise seems to be worsened**.**

1.3 Objectives

The objectives of this research are:

- to develop and build an experimental setup that integrates the OEM parts and other equipment/sensors, such that it can simulate the noise condition;
- to study the noise generation mechanism and understand the phenomena;
- to investigate several potential methods to minimize/eliminate the noise; and
- to give assessments, either qualitatively or quantitatively, whichever was possible, of each noise minimization/elimination method.

Due to safety reason, the experiment used water instead of actual gasoline. There were concerns that replacing gasoline with water would affect the nature of the system to a degree that noise could not be re-created. However, test results showed that using water could still produce noise. More detailed descriptions and findings are included in Chapter 3 and Chapter 4.

1.4 Overall Structure of the Thesis

The overall structure of this thesis is as follows:

Chapter 1 provides brief background on the automotive industry as a whole, and then discusses the importance of NVH attribute to this industry. Also, the noise issue that is studied in this thesis was described in full details. Finally, the objectives of this research were listed.

Chapter 2 covers a comprehensive review of the researches done previously regarding the noise issue caused by pressure pulsation inside vehicle fuel system with a focus on gasoline vehicles. Diesel vehicles were also briefly mentioned. Due to limited information regarding EVAP system, the review was thus focused on fuel delivery system. This chapter is further divided into three main topics of research: noise issue in the vehicle, pressure pulsation issue in vehicle, and noise issue caused by pressure pulsation in vehicle.

Chapter 3 explains the methodology this research used to study the noise phenomenon. First, a simple test setup was built for preliminary testing. This is covered in the first sub-section. Then there are 6 more subsections that detailed the full experimental setup, including equipment/sensor specs, test layout, measurements, data acquisition, data post-processing, and system running conditions monitoring/controlling. This chapter ends with a thorough description of the baseline running scenario.

Chapter 4 covers results obtained during noise re-creation and related discussions. Pressure readings revealed important information. This was the focal point for discussion in this chapter. Then, a theory was proposed to potentially explain the noise generation mechanism. The role of GVV and its impact on noise generation was studied as well. Visualization achieved by utilizing inspection camera was discussed next. Finally, another phenomenon which related to external force causing deformation of the tank, and its effect on noise was discussed.

Chapter 5 presents testing results on 8 different approaches for noise reduction. Among them, 5 were pressure pulsation attenuation strategy. The pressure pulsation attenuation methods were inspired from methods used in the fuel delivery system. The pressure pulsations were quantified using peak-to-peak value. The effect on flow restriction was also monitored for each method.

Chapter 6 summarizes the findings as well as assessments of noise reduction methods from previous chapter, and then provides recommendations for possible future investigations.

Lastly, Bibliography lists the papers and resources this thesis referenced.

Chapter 2
Literature Review

Very few information regarding the noise issue created in the EVAP system is available. Thus, the literature review was focused on the similar issue in the fuel delivery system. The pressure pulsations inside the fuel delivery line have known to cause issues such as noise, unevenly distributed fuel throughout different engine piston cylinders (maldistribution), and negatively affecting air-fuel ratio [31], [39]. And these issues are known to exist in both gasoline and diesel vehicles [32].

There are two main parts in this chapter. First, two aspects related to the research topic were reviewed. One is about vehicle noise and its impact on people, including some of the leading causes for vehicle noise and its effect on person inside the vehicle. The other aspect is researches done about the pressure pulsation phenomenon in vehicle. Second, previous studies on vehicle noise caused by pressure pulsations inside vehicle fuel system were reviewed, including existing methodology in monitoring the pressure pulsation, as well as different approaches for noise reduction, including pressure pulsation attenuation strategies. The second part was focused on fuel delivery system, because information regarding the pulsation issue in EVAP system is limited.

However, some external resources were also surveyed regarding pressure pulsation attenuation methods. Chang et al. [40] suggested that when flow permeates through a porous wall, the pressure pulsation decreases linearly. The porous material was not mentioned as a means for pressure pulsation attenuation in automotive industry, probably due to practical considerations.

La et al. [19] noted that as the automotive industry starts to shift from internal combustion engines toward zero emission vehicles, it brings its own NVH challenges because of its unique dynamic feature of the powertrain and driveline system. The most common dynamic driveline NVH issues with 100% electric vehicle manifests themselves as groans, rattles and clunks. However, many researchers pointed out that the conventional gasoline/diese vehicles will remain the dominant component in global vehicle productions for at least the next several decades [33], [41], [42]. Thus, this thesis will only focus on gasoline vehicles and the NVH issue that is related to the gasoline fuel system.

2.1 Studies on Vehicle Noise

Quality of ride is an important factor that influences the car-buyers' purchasing decisions. Among many aspects in ride quality, NVH has become such a vital component that it alone can affect the competitive edge of the products in market place significantly [10]. Thus, the automotive industry has invested vast amount of resources into vehicle NVH issue [17]–[23]. Depends on the noise source, some studies on NVH combined the vibration and noise together [18], [20], [23], while other studies focused on the noise issue alone [17], [19], [21], [22].

2.1.1 Common Causes of Vehicle Noise

Williams et al. [22] in their study very detailed listed the different factors that contributes to the vehicle noise. This comprehensive study enabled the exact re-creation of the noise in their NVH simulator. There are three levels in the hierarchy of noise generation: contribution level, source level, and vehicle level.

Within contribution level, there are three contributions: body panel contributions, local source contributions, and powertrain surface contributions. The body panel contributions contain floor, roof, firewall, and closures. The local contributions contain glass, aerodynamics, and sealing. The powertrain surface contributions consist of engine and gearbox surfaces, exhaust surfaces, and intake surfaces. These contributions were transmitted through either structure-borne (engine mounts, and suspension bushes) or air-borne path (intake orifice, exhaust orifice, and tyres).

On the source level, there are 6 sources: base engine, intake, exhaust, road noise, tyre noise, and wind noise. The first three sources are grouped together as engine noise, while the remaining three noise sources are grouped together as masking noise.

On the vehicle level, the noises are mixed with secondary sounds to become the total noise. The secondary sound can include gear whining, key-on during starting, horn, indicator, rattles, and discrete impact event from the road surface or traffic.

2.1.2 Vehicle Noise Impact

From the automakers' point of view, since NVH directly affects consumers' purchasing decisions, they have put more and more resources into related researches. A recent trend is to include NVH in the early design phase to avoid costly patch work after [10], [22], [23], [43], [44]. Traditionally, customer

perception of the annoyance of noise is characterized by calculating the loudness of such sounds [45], [46].

William et al. [22] developed a vehicle simulator, indicating that aside from collecting objective data, researchers are also paying attention to customer perception of the vehicle noise. Some sounds are regarded as favorable by customers, and there are automotive engineers and NVH experts dedicated on tuning the vehicle to produce such pleasant sounds. Amman et al. [21] conducted a study on subjective quantification of wind buffeting noise. They focused on how a customer would react to time-varying wind noise. Hatti et al. [10] noticed that the demands by the customers concerning comfort, driving pleasure, and design appears sometimes supersede the functionality criteria. Thus, the automobile makers are now trying to meet these requirements on quality, comfort, and often emotional aspects. Among these different attributes, NVH is considered to be one of the key factors.

Thus, in summary, the NVH does not fall under the vehicle functionality criteria but rather quality and comfort of ride. The main impact for the noise on the customer is the perception of annoyance rather than other detrimental hazards. However, since it has become so important that it may swing customers' purchasing decisions, it should continue to be the focus of research within automotive industry.

2.2 Studies on Pressure Pulsations in Vehicle Fuel System

There are many existing and publicly available information regarding pressure pulsation inside the fuel delivery system. This is partially due to the high pressure nature of the fuel delivery line. The pressure pulsation is more offensive and thus causing issues that are more prevalent [24], [31], [39], [47]. Because very few information were found on pressure pulsations in EVAP system which is under negative vacuum pressure, this review is focused on the fuel delivery line. Some of the approaches for pressure pulsation attenuation methods used in fuel delivery system were tested in the EVAP supply line.

2.2.1 Common Causes of Pressure Pulsations in Vehicle Fuel System

In a returnless fuel delivery system, flow ripples are created in the fuel rail when injectors are firing. Each injector creates individual pressure pulsation, which may be increased due to the deadheaded architecture (the fuel rail). Another reason behind an increase in pressure variation in the returnless fuel system is the relocation of the pressure regulator from the engine side to the fuel tank compared with the full return fuel delivery system. A common practice in the automobile design is to integrate the pressure regulator with the liquid fuel pump inside fuel tank. This pressure pulsation may be further worsened at sub 0^{o}C temperatures due to increased fuel line stiffness and fuel density [24], [29], [31], [39]. In

addition, low pressure or high pressure pump pulses, sudden cross section changes in flow path can also contribution to pulsation generations in vehicle fuel supply system [32]. Figure 2-1 and Figure 2-2 below illustrate the fuel rail system and a typical returnless fuel delivery system.

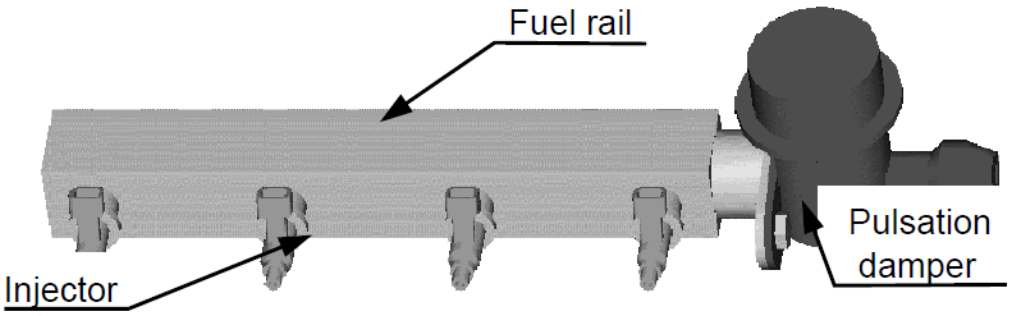

Figure 2-1: A typical fuel rail with pulsation damper (reproduced from [31]**).**

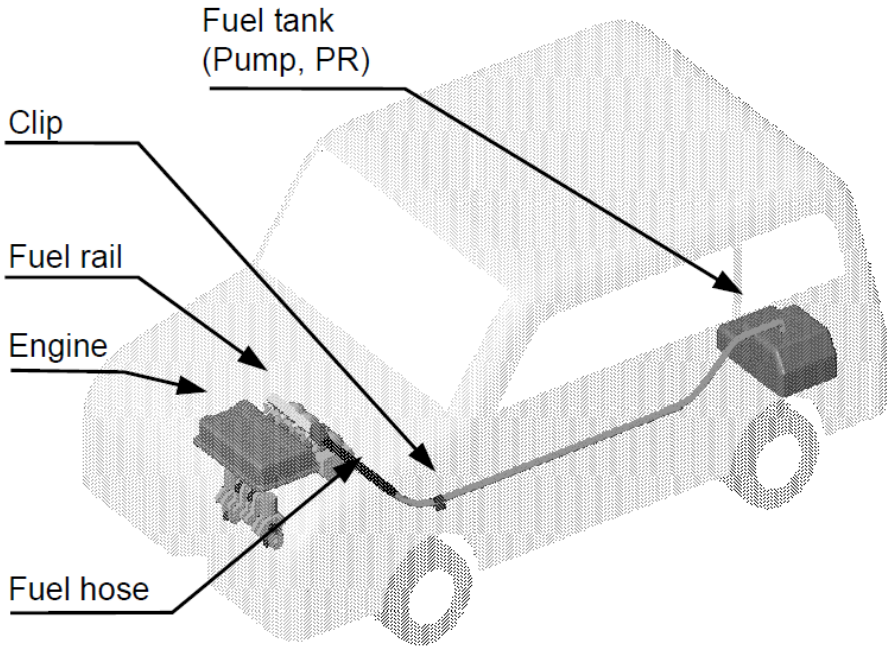

Figure 2-2: A typical returnless fuel delivery system (reproduced from [31]**).**

In most automotive application, the primary source for pressure pulsation is the pump and the injectors. Furthermore, high pressure pump is the major noise source in diesel system, while the injector is the major noise source in gasoline system [32].

In diesel system, the high pressure fuel pump takes a finite amount of fuel into its chamber and them rapidly compresses it. This action produces fluctuations of sinusoidal pattern on both the pressure and

flow around the mean system pressure and flow. Once the fluid, under high pressure and high speed, exits the pump, it produces a compression wave. The wave travels through the fuel supply line, meeting bends or restriction on its path. Some of the wave's energy is absorbed, some keeps passing along with the flow, and the rest is reflected back against the flow coming from the pump. This back-and-forth effect of the compression wave creates the fuel pressure pulsation, noise, and lowers the service time of the pump [32].

In gasoline system the injector closes and opens in a very short period of time, in the order of milliseconds. This rapid closing and opening of injectors causes fuel pressure pulsation inside fuel rail and may create noise. The noise in gasoline engines can be distinguished from those from diesel engines. The noise from gasoline fuel injector is a very short click with broad frequency content and it can propagate as fluid-borne or structure-borne [32].

In EVAP system the negative vacuum pressure, which is the "driving force", is supplied by the engine. If the CPV is a solenoid type valve that is controlled by PWM driver, its closing and opening will cause flow ripple effect, which in turn causes pressure pulsations [25], [37], [48]–[53]. However, this highly depends on the nature of the CPV design. Some OEMs utilizes "gate valve" design for their CPVs and subsequently there is no pressure pulsation inside the EVAP line.

2.2.2 Issues caused by Pressure Pulsations in Vehicle Fuel System

Maldistribution of fuel

The pressure variation on the fuel delivery system can cause maldistribution on the fuel injectors [24], [29], [31], [39], [47], [54]. The imbalance of the fuel delivered through each fuel injector was studied in great details. It was observed that although pressure pulsation is the cause, the magnitude of the pulsation (peak-to-peak) is inversely related to the amount of imbalance of fuel. Thus, smaller pressure pulsation causes bigger maldistribution.

Kim et al. [29], and Chen and Yang [54] pointed out that the maldistribution of fuel is unavoidable in reality, because of the production tolerance of each injector, aging of injectors, as well as breathing behaviour of individual cylinders by the intake manifold structure and valve characteristics. However, it is responsible for causing deterioration of drivability, and increase in harmful emission and fuel consumption.

Air-Fuel (AF) ratio

Air-fuel ratio is crucial in engine combustion. Ideally the air-fuel ratio is controlled to be around the stoichiometric ratio. A small deviation away from this ratio can lead to large degradation of the

conversion efficiency of the catalytic converter. This in turn adversely affects the emission, as well as fuel consumption [29], [54].

Noise

The pressure pulsation in the fuel delivery system can cause undesired noise [24], [31], [39], [47]. The noise is usually audible during vehicle idle conditions as the background noise is less. Aside from pressure attenuation approach to address the noise issue, vibration-isolation-clips and under-floor tubes are also used to reduce vehicle noise [31].

2.3 Studies on Vehicle Noise Caused by Pressure Pulsations in Fuel System

The pressure pulsation inside the fuel system is an ongoing issue in the automotive industry and has been subject to studies by many researchers. With the introduction of the returnless fuel system, pressure pulsation was worsened. Vehicle noise is one of the issues that fuel system pressure pulsations can cause [31], [39].

Due to its high pressure nature, the pressure pulsations inside the fuel delivery line are more offensive and can cause more severe problems, including loud noise, fuel maldistribution and undesired air-fuel ratio, which causes emission and fuel consumption concerns [29].

The EVAP system is subject to negative vacuum pressure. The information regarding studies on the noise caused by pressure pulsations in the EVAP system is very limited. Thus the review is focused on the studies done on the fuel delivery line.

2.3.1 Approach

There are two main approaches to study the noise caused by fuel system pressure pulsations: experimental work, or numerical simulations (FEA, CFD). Most experimental work was focused on the fuel rail, the injectors, and the pulsation damper design [31], [39], [55]. The simulation also focused on these three things but with more cases covered [17], [28], [47], [56], [57].

Cortese [39] performed experiments with a relative large quantity of runs. She tested 6 different types of injectors on a test fuel rail. With pulse width of 9 different settings, she did a continuous sweep of engine speed change from 500 to 8000 RPM. However, she acknowledged that the resultant data was so large that a more comprehensive model was needed to fully study the correlations between the parameters. It was also very difficult to reduce this data to a readily understandable format.

Mizuno et al. [31] in their experiment tested the fuel rail geometry and its effect on the pressure pulsation. They studied three factors: volume, cross-section shape, and width-to-height aspect ratio. But they could only perform 3 cases for each parameter. During each patameter testing, the other parameters were fixed. Thus, their work could not show if there were any combined effect between these three factors.

Ogata et al. [47] continued on Mizuno et al.'s work [31] using experimental approach, they were able to consider more factors: the sound speed, fuel rail length, supply line length, and cross-section area ratio. These factors, especially the sound speed is difficult to monitor and change in real life. Thus, numerical methods provided a means to study these factors. The change on the other three factors in experimental approach will require machining of new parts. They used finite element methods to simulate the fuel delivery system, including the fuel supply line and fuel rail with two different configurations.

Recently in 2013, Tariq and Tripathi [32] summarized previous researchers' work on fuel system pressure pulsation attenuation and used robust engineering methodology to design a noise-free fuel supply system without the use of pressure pulsation damper. They focused on the material of the fuel rail, fuel rail length, fuel rail volume, as well as the fuel inlet radius.

Roberts and Cui [28] utilized numerical simulations to investigate the "Hockey Puck" style damper. Based on previous empirical data, they focused on three parameters that affect the damper performance: angle between the entrance and exit ducts, height-to-diameter aspect ratio, as well as inlet-to-outlet offsets. They first compared their simulation results with the experimental results to validate the CFD model. Then, they were able to run simulation under different parameter settings to study the correlations.

Roberts and Cui [28] noted that currently the optimal design iteration comes from trial and error, and that the science behind the correlations between these parameters are not fully understood. This brings another degree of difficulty to the design engineers as they cannot follow a certain pattern to determine the maximum damper performance and thus have to rely on testing results. Numerical simulation provides a faster and cheaper way.

Similar to Roberts and Cui's work [28], Heo et al. [57] used numerical simulation to study the pressure pulsation characteristics based on the fuel rail geometry. They were able to run many cases with different parameter settings. The simulation enabled them to study more parameters. Aside from the internal volume, aspect ratio, shape of the fuel rail, they included the effect of the fuel rail bulk modulus on the pressure pulsations. They realized this by changing the fuel rail wall thickness and material. They

also utilized design of experiments methodology to minimize the number of runs and provided a way to look into the combined effect among the parameters.

Orand and Rhote-Vaney [17] used lumped-parameter model approach of fluid dynamics to simulate fuel supply and delivery system. Their work included a much complex numerical model which integrated the entire fuel system. The system is capable of modeling not only the whole system but also each subpart, including pump, pressure regulator, pulsation damper, and filter. They concluded that the numerical simulation is superior in terms of couplings between different dynamic subsystems, which make the experimental approach cumbersome.

In summary, the experimental approach usually did not cover many cases due to limitations on time and cost, while numerical simulation can provide multiple runs with numerous factors under investigation. However, the data post-processing proved to be more difficult. As Cortese [39] pointed out, to perform large scale tests is one thing, while to analyze the data and to reduce it to a format that is readily understandable can be even more challenging. Table 2-1 below summarizes the approaches used by different researchers in chronological order.

Table 2-1-Approach Summary

Researcher and Year	Approach	Description
Chen and Yang 1998 [54]	Numerical with Experimental Validation	They improved a numerical model in FuelNet, which included an acoustics model to enable both liquid fuel pressure pulsation and acoustic noise prediction. This improved model was validated against 8 sets of test data for four important variables.
Hu et al. 1999 [56]	Numerical with Experimental Validation	The developed a computer model for predicting pressure pulsations inside a 6-injector fuel rail system, based on previous work of single-injector model. The model was validated against experimental data under same situation, which is different opening/closing sequence of the 6 injectors and pressure readings were measured at various points inside the fuel rail.
Izydorek and Maroney 2000 [24]	Experimental	They proposed a standard testing methodology to evaluate the pulsation damper attenuation, as well as noise reduction effect.
Mizuno et al. 2002 [31]	Experimental	Their test setup included the entire fuel delivery system, including fuel tank, fuel pump, fuel supply line, injector, fuel rail, as well as fuel injector pulse generator. They tried to adjust the fuel rail geometry to achieve pressure pulsation attenuation without the use of pressure pulsation damper.

Researcher and Year	Approach	Description
Ogata et al. 2003 [47]	Numerical	Based on Mizuno et al.'s work [31], they used numerical simulation to further study the pressure pulsation reduction in fuel rails. Numerical simulation (FEM) enabled them to look into parameters such as speed of sound in fuel rail, fuel rail length, supply line/connection line length, and different fuel rail configurations.
Cortese 2004 [39]	Experimental	Used a 4-injector fuel rail, tested 6 different injectors, with 9 pulse width time settings for injectors, and engine speed from 500-8000 RPM sweep.
Roberts and Cui 2006 [28]	Numerical	Roberts and Cui focused on the pressure pulsation damper and used numerical simulation (CFD) for design optimization for "Hockey Puck" damper.
Huang 2009 [55]	Experimental	He focused on injector design, including studying how different parameters affect the injector performance. .
Orand and Rhote-Vaney 2009 [17]	Numerical	Orand and Rhote-Vaney developed model that utilized lumped-parameter approach of the fluid dynamics on the fuel supply and delivery system. The model was validated against test results.
Kim et al. 2010 [29]	Numerical	They proposed an individual cylinder air-fuel ratio estimation algorithm for individual cylinder air-fuel ratio control. This algorithm was then validated with a 1-D engine simulation tool.
Spegar 2011 [58]	Numerical	He used quasi-1D simulation to study three control factors and to optimize fuel rail assembly design in an in-line 3 cylinder engine, using Robust Engineering Methodology.
Heo et al. 2012 [57]	Numerical	They used oil hammer simulation technique to investigate the pressure pulsation characteristics inside the fuel rail.
Tariq and Tripathi 2013 [32]	Experimental	They summarized previous works done on fuel rail design to reduce pressure pulsation without the use of pulsation damper. Using Robust Engineering Methodology, they came up with an optimum fuel rail design for a production vehicle in India.

2.3.2 Parameters Monitored

Peak-to-Peak Pressure

Izydorek and Maroney [24] proposed a standard way to measure the fuel system pulse damper attenuation and they used peak-to-peak value to quantify the pressure pulsation magnitude. The peak-to-peak value is obtained by subtracting minimum pressure value from the maximum pressure value. This was adapted by all the researchers after [28], [31], [32], [39], [47], [54].

Cortese [39] in her study, noticed that the pressure pulsation profile at an engine operation point exhibits repeating patterns. However, each pattern is not 100% exact. The peak-to-peak measurements can vary, sometimes reaching 10%. She also noted that this 10% variation may become very important when peak-to-peak value is used for a target value and the system is near this value.

Noise

Mizuno et al. [31] and Tariq and Tripathi [32] recorded the noise using microphones in their respective experiments. Mizuno et al. did a power spectrum analysis on the noise recorded and focused on the frequency range of 180 -300Hz, which is similar frequency range of a cabin noise. Tariq and Tripathi [32] compared the noise power spectrums of a baseline case and with optimized fuel rail design case to show 5dBA noise reduction.

In the simulation done by Chen and Yang [54], A-weighting relative response was used to quantify the noise. This is done by first taking the air pressure spectrum inside the vehicle compartment. Then A-weighting was employed in order to take into account of human hearing sensitivity adjustment. The A-weighted sound level spectrum, which is units of dBA, is further converted to the 1/3 octave bands. This lies in the normal human hearing range of 20-25k Hz. The simulation considered the acoustic energy being partially absorbed by the wall surface and furniture for better accuracy.

Williams et al. [22] proposed an interactive NVH simulator that can capture and understand opinions directly from the customers about vehicle sound quality in their research. Their focus have been on collecting inputs from customers (real customers, brand managers, marketing managers, NVH engineers and designers, engineering decision makers, etc.) via a virtual NVH simulator. The simulator has a complex evaluation system that creates subjective data regarding vehicle noise. This data is important during decision making process in order to deliver customer focused produces.

Other Parameters

Since noise is not the only issued caused by pressure pulsations, researchers also monitored other parameters. Cortese [39], Kim et al. [29], Heo et al. [57], Mizuno et al. [31], and Ogata et al. [47] in their respective studies all tested the pressure change period, which in turn showed the resonating frequency of the system. Ogata et al. [47] studied the factors affecting the system resonating frequency and proposed an alternate approach to reduce pressure pulsation: by tuning the system resonating frequency outside of the engine/injector-induced frequency. Heo et al. [57], through numerical simulation, looked into fuel rail wall thickness and fuel rail material and their effect on pressure change period. Cortese [39], and Kim et al. [29] noted that the temperature plays an important role in pressure pulsation. At low temperature, the

system is stiffer and fuel more viscous, causing even bigger magnitude in pressure pulsations. Cortese [39] kept track of the fuel injection parameters, which included the amount of fuel delivered, engine RPM, pulse width, and number of pulses. She went as far as collecting and measuring the weight of the fuel delivered by the injector on her system to obtain fuel maldistribution data. Tariq and Tripathi [32] pointed out that different types of the fuel system are inherently different when it comes to pressure pulsation. In general, pulsation noise found to be higher in returnless systems, due to its nature of the design.

Heo et al. [57], Mizuno et al. [31], and Ogata et al. [47] used the term "oil hammer" in their respective studies. The oil hammer technique, or oil hammer test, is to send a pulse signal to the system and to monitor how the pulse subsides. The resultant period is termed pressure change period, which by inversing yields a frequency. This frequency is the resonant frequency of the system. They observed when the injector frequency, controlled by the engine RPM, was close to the resonant frequency of the system, the pressure pulsation increased significantly. In fact, Ogata et al. [47] proposed to move the system's resonant frequency outside of the normal operating range of the engine RPM in order to achieve noise reduction/elimination. Table 2-2 below summarizes the parameters monitored by various researchers.

Table 2-2: Parameters Summary

Researcher and Year	Parameters Monitored	Further Comments
Chen and Yang 1998 [54]	pressure	Chen and Yang validated their model by comparing the pressure readings against the test data, under various parameter settings.
Izydorek and Maroney 2000 [24]	pressure	They recommended less than ±28.5kPa pressure pulsation magnitude performance target.
	noise	They recommended pulsation attenuation over a frequency bandwidth of the 10-200Hz range.
	temperature	They recommended the performance should be met over the range of -40 to +120 degree C.
Mizuno et al. 2002 [31]	pressure	Peak-to-peak value to quantify pressure pulsation.
	noise	They plot the noise data on power spectrum, with x-axis frequency and y-axis dBVr.
Ogata et al. 2003 [47]	pressure change period	They focused on parameters affecting the pressure change period.
Cortese 2004 [39]	pressure	Peak-to-peak value to quantify pressure pulsation.

Researcher and Year	Parameters Monitored	Further Comments
	injector fuel flow rate evaluation	She kept track of how much fuel each injector delivers at different settings (pulse width time, engine speeds) to quantify fuel maldistribution.
Roberts and Cui 2006 [28]	pressure	Peak-to-peak value to quantify pressure pulsation, which in turn indicates the pulse damper performance.
Orand and Rhote-Vaney 2009 [17]	pressure	Pressure analyzed both in real time and in frequency domain.
Kim et al. 2010 [29]	Individual cylinder equivalence ratio (actual air fuel ratio over stoichiometric air fuel ratio)	Their simulation estimated the equivalence ratio at each individual cylinder under different valve lift and injection duration conditions.
Spegar 2011 [58]	pressure	He used standard deviation of pressure to quantify pulsation
Heo et al. 2012 [57]	pressure	Peak-to-peak value to quantify pressure pulsation.
	pressure change period	They used "oil hammer" technique to obtain the pressure change period, which in turn yields the resonating frequency of the system.
Tariq and Tripathi 2013 [32]	pressure	Peak-to-peak value to quantify pressure pulsation.
	noise	Cabin noise (peak-to-peak) in dB(A) at engine idle RPM over the frequency range.

2.3.3 Instrumentation and Measurement Methods

Pressure

Neither Cortese [39], nor Mizuno et al. [31] provided detailed specs for the pressure measuring devices used in their studies but they detailed the locations of the pressure transducers. Mizuno et al. [31] located the pressure transducers at the intake port of the fuel rail when the pulsation damper was not used. When the pulsation damper was attached at the intake port of the fuel rail, the pressure transducer was located at the intake port of the pulsation damper. Tariq and Tripathi [32] located the pressure sensors at the same place as Mizuno et al. [31]. Cortese [39] used two pressure sensors to capture both the fuel rail inlet pressure as well as the pressure inside the fuel rail. She located one of the pressure sensors about

100mm from the fuel rail inlet line, and located the other pressure sensor inside the fuel rail directly above one of the injectors. The injector was the third out of the four injectors counting from the inlet of the fuel rail. Figure 2-3 below shows where Mizuno et al. [31] located the pressure sensors with and without the pressure pulsation damper attached.

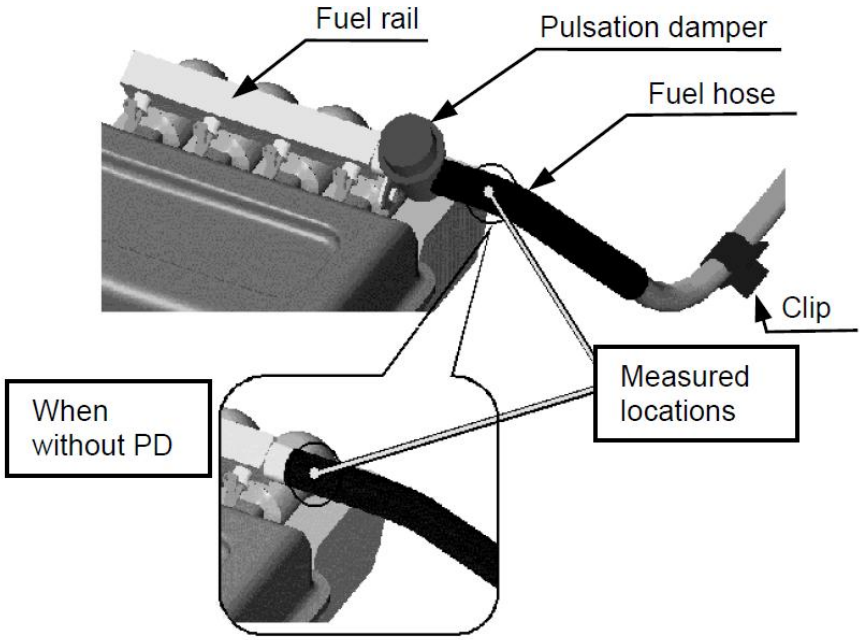

Figure 2-3: Pressure sensor location used by Mizuno et al. (reproduced from [31]**).**

Izydorek and Maroney [24] proposed a multiple transducer system to account for standing waves during measurement process. This system is able to obtain accurate dynamic pressure data at frequencies as low as 10Hz. They raised concern that the standing wave phenomenon inside the fuel line may adversely affect the accuracy of the dynamic pressure readings. If the pressure transducer is positioned at or near a node of the standing wave, it is possible that the readings were close to zero. They presented a six-transducer measurement system which, with properly curve fitting data from all six transducers, is capable of capturing an accurate estimate of the average dynamic pressure in line. The six-transducer method requires measurement of both upstream and downstream of the tested pulsation damper.

In application where detailed combustion analysis and combustion process monitoring is required, piezoelectric transducers are the most commonly used option [59]. If appropriate amplifiers and means of data acquisition are obtained, they can form a reliable and rugged system that is able to capture highly accurate and detailed pressure measurements. Because of this, piezoelectric transducers are by far the most widely used transducers for combustion measurement in engine research.

Noise

The information regarding the instrumentation for the noise recording was not provided in Mizuno et al.'s [31] nor Ogata et al.'s [47] respective studies. Mizuno et al. [31] briefly explained the location of the microphone which is used to capture the cabin noise. The microphone is roughly located at where the driver's head is inside the cabin. Tariq and Tripathi [32] positioned the microphone between the driver's and passenger's seat. Figure 2-4 below shows the microphone location in Mizuno et al.'s experiment.

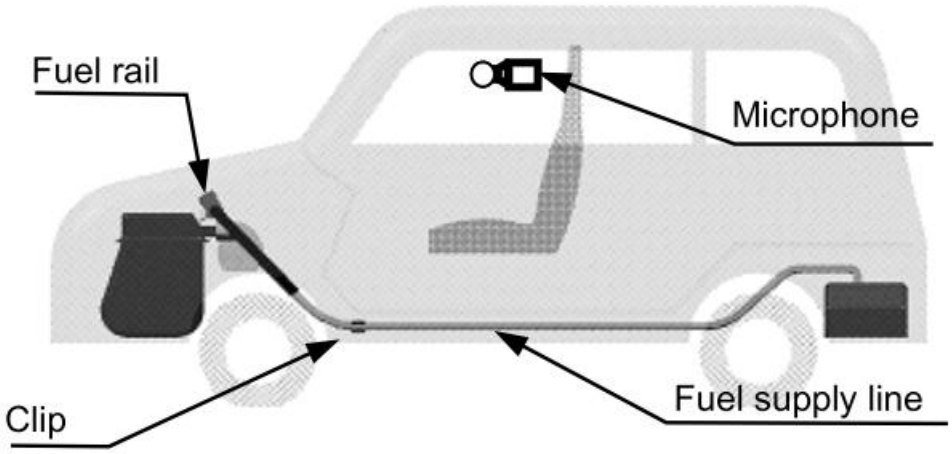

Figure 2-4: Microphone location in Mizuno et al.'s experiment (reproduced from [31])

Williams et al.'s simulator [22] is capable of re-create the NVH to almost "indistinguishable" compared with a real car. The simulator has a hierarchy data model which takes account of many different components for the vehicle noise. These components were synthesized, through a series of rules, in real time based on driver inputs. However, they did not present how this database was established.

Izydorek and Maroney [24] did not explain the methodology to capture/record the noise. However, they presented a quantitative relationship between the pressure pulsations and the noise level. A reduction in pulsation magnitude from ±52.5kPa to ±28.5kPa can lead to 5.3bB decrease in noise. They also provided some general guidelines on the conditions that should be met for the experimental setup for acoustical considerations.

- One-dimensional wave propagation assumption is true, which is satisfied if the diameters of the conduits are less than 25% of the highest frequency of interest.
- Viscous dissipation is negligible as long as the Reynolds Number is small.

- The amplitude of fluctuation in flow and pressure is small compared with mean flow and pressure.

The threshold values for the Reynolds Number or comparative percentage for the flow and pressure fluctuations were not specified. Table 2-3 below summarizes the methodology for different researchers who used experimental approach.

Table 2-3: Methodology Summary

Researcher and Year	Pressure	Noise
Izydorek and Maroney 2000 [24]	No recommendations on the pressure sensors, but provided guideline for pressure measurement. Proposed two pulsation damper evaluation methods: transmission loss, and insertion loss.	No recommendations on the noise sensors, but provided three considerations, however without clear threshold.
Mizuno et al. 2002 [31]	Sensor information was not provided, but the location of the sensors was shown.	Sensor information was not provided, but the location of the sensors was shown.
Cortese 2004 [39]	Sensor information was not provided, but the location of the sensors was shown.	Was not measured.
Tariq and Tripathi 2013 [32]	Sensor information was not provided, but the location of the sensors was shown.	Sensor information was not provided, but the location of the sensors was shown.

2.3.4 Pressure Pulsation Attenuation

System Resonant Frequencies

In her study, Cortese [39] setup a fixed design four cylinder fuel rail, where 6 different types of injectors were used. Through a wide range of engine RPMs and injector pulse width time, 3D topographic maps were created, by combining the collected data of peak-to-peak values. The results suggested that the injector designs did not have a real effect on the engine resonant frequency over the operation range. Rather, the fuel delivery system itself, including its geometric features, material, and other critical characteristics, played the vital role of the resonant frequency.

Heo et al. [57], Mizuno et al. [31], and Ogata et al. [47] in their respective studies confirmed that when the engine RPM generates a frequency that is close to the system's resonant frequency, the pressure

pulsation effect amplifies significantly. Thus, Ogata et al. [47] proposed a solution: instead of adding components such as pulsation damper to achieve pulsation attenuation, the effort was focused on shifting the system's resonant frequency.

Using numerical simulation, Ogata et al. [47] studied four parameters and how they affect the system's nature frequency: the sound speed inside fuel rail, the fuel rail length, the connect line length, and cross-section area ratio. The cross section area ratio is the area of the fuel rail to the area of the connect line. They concluded that in the opposed engine model case, the resonant frequency is inversely proportional to the sound of speed inside the fuel line, and proportional to the square root of the fuel rail length, the connect line length, and the cross-section area ratio, respectively. The same correlations were found in the in-line engine case for these four parameters.

Ogata et al. [47] further presented two cases where the system resonant frequency is within the normal range of engine RPM. One case the frequency corresponded to 960rpm, and the proposal was to shift this value down, thus moving outside of the normal engine RPM range. In the other case, the resonant frequency corresponded to 3060rpm. Thus, shifting this value up was a more viable solution.

Pulsation Damper

Pulsation dampers are used across many different industries. For example, they can be utilized to maintain flow coming from pumps in spray applications, or for decreasing pipeline vibrations and noise [60]. In automotive industry, pulsation dampers have been used for over 30 years to address the flow ripple problems in vehicle fuel systems. The pulse dampers can store and supply energy to meet the fuel system's flow demands, in the meantime attenuating the pressure pulsations [24].

Early pulsation dampers had mechanical spring diaphragms or air diaphragms to reduce pressure fluctuations. For instance, one type of pressure damper in this category is side-branched, spring-biased pulse damper. This in-line device can replace existing fuel connectors. Some of these designs even feature a diagnostic port [24]. However, the diaphragms in these dampers were susceptible to damage, raising concerns for potentially fuel leakage or fuel line blockage [28].

More recently, a new type of pulsation dampers with merely a specific geometric shape to attenuate the pressure waves has been introduced. It is commonly referred to as "Hockey Puck" damper because of its visual likeness of a hockey puck. Roberts and Cui [28] summarized that there are three factors that have been identified to influence the dampening characteristics: the angle between inlet and outlet, height-to-diameter aspect ratios, and varying inlet-to-outlet offsets. The reasons for these correlations were yet to be fully understood. Currently, the parameters offer the apparent optimum dampening effects

are determined through trial and error. This was studied both experimentally [61] and through numerical simulation [28]. Although they did not show a specific illustration of a hockey puck damper, the same design was included in Figure 2-1 which was presented by Mizuno et al. [31].

Fuel Rail Geometry

Mizuno et al. [31] tried to develop a fuel rail that has integrated pulsation dampening effect so that a pressure pulsation damper was not needed. They studied three geometric characteristics of the fuel rail: volume, cross-section, and width-to-height aspect ratio. They concluded that increasing the volume of the fuel rail to bring down the pulsation magnitude was not effective. As shown from the experimental results, a 90% increase in volume only reduced the pulsation by 30%. With volume constant, a circular-shaped fuel rail caused largest pressure pulsation, followed by square-shaped design, then rectangular-shaped design. They further looked into the aspect ratio effect within rectangular-shaped design and concluded that a width-to-height ratio of 2-3 could create the best pulsation reduction effect.

More recently, Tariq and Tripathi [32] did similar work. They used Robust Engineering Methodology to come up with an optimum fuel rail design that can reduce the pressure pulsation by 28% compared with baseline scenario, and was able to reduce the overall peak-to-peak acoustic noise level by 5 dB(A). This new design incorporates changing fuel rail material, increase in fuel rail length by 15%, doubling the fuel rail volume, and increasing fuel inlet radius by 79%.

Small Diameter Orifice

Another popular means of reducing pressure pulsation level in the fuel rail is to install a small-diameter orifice between the high pressure supply line and the fuel rail. The placing of the orifice prevents the high-frequency, pump-induced pulsations entering the fuel rail, prohibiting it from propagating effectively into the fuel rail [58].

Material and Wall Thickness of the Fuel Rail

The commonly used fuel rail materials are low-carbon steel, stainless steel, aluminum, or plastic. However, plastic has become obsolete in recent years due to concern of fuel permeation [31], [57].

There was no quantitative experimental data regarding how material of the fuel rail affects the pressure pulsations. Some experimental observations suggested that the softer material can better absorb and abates the energy and thus creates smaller pressure variations [31], [39]. With decrease in wall thickness, the fuel rail exerted a better pressure pulsation attenuation effect [57].

On the simulation side, finite element method can calculate the bulk moduli of the fuel rail wall. This was done by taking account of the material. Heo et al. [57] compared a fuel rail made of 0.7mm thick low-carbon steel and of aluminum with four different kinds of thickness: 0.5mm, 0.7mm, 0.9mm, and 1.0mm. The results showed that decreasing wall thickness reduced pressure pulsations. Aluminum has a better pressure attenuation effect compared to low-carbon steel, due to its superior elasticity.

Table 2-4 below summarizes all the pressure pulsation attenuation methods used by different researchers in chronological order:

Table 2-4: Pressure pulsation attenuation summary

Researcher and Year	Pressure Attenuation Methods	Further Comments
Izydorek and Maroney 2000 [24]	mechanical spring based pulse dampers	They did not perform experiments, but mentioned a commonly used pressure pulsation attenuation solution
Mizuno et al. 2002 [31]	fuel rail volume	They found increasing volume could bring down the pressure pulsation, however, this was not very effective. (90% increase in volume brought 30% reduction in pressure pulsation)
	fuel rail cross section	Circular shape resulted in largest pressure pulsation, followed by square shape and rectangular shape.
	fuel rail width-to-height aspect ratio	The flatter the shape, the better pressure pulsation reduction effect. Added with practical considerations, they recommended an optimum width-to-height ratio of 2-3.
Ogata et al. 2003 [47]	sound speed in fuel rail	They focused on the system pressure change period (resonant frequency) shifting as a means to reduce pressure pulsation. Pressure change period is inversely proportional to the square root of sound of speed in fuel rail.
	fuel rail length	Pressure change period is proportional to the square root of fuel rail length.
	supply line length (in-line engine design) or connection line length (opposed engine design)	Pressure change period is proportional to the supply line length or connection line length.
	cross section area ratio (fuel rail area over supply line area)	Pressure change period is proportional to the cross section area ratio.

Researcher and Year	Pressure Attenuation Methods	Further Comments
Cortese 2004 [39]	fuel delivery system features (geometry, material, etc.)	She did not study pressure attenuation methods; however, her findings indicated that the system's resonant frequency is more dependent on the fuel delivery system features rather than injector type.
Roberts and Cui 2006 [28]	angle between entrance and exit	Roberts and Cui studied how these three parameters affect the pulsation attenuation performance of a typical "Hockey Puck" pulse damper. They explained that there was no clear pattern between the correlations and the optimum design was relying on trial and error.
	height-to-diameter ratio	
	inlet-to-outlet offset	
Spegar 2011 [58]	small-diameter orifice between high pressure supply line and fuel rail	Spegar did not test pressure pulsation attenuation devices; however, he mentioned that adding small-diameter orifice is a common solution for pulsation attenuation in high pressure fuel supply line.
Heo et al. 2012 [57]	aspect ratio of fuel rail cross-section	Pressure pulsation is reduced by as much as 63.3% (peak-to-peak) with flatter fuel rail.
	wall thickness of fuel rail	Decreased wall thickness caused reduction in pressure pulsation up to 77%.
	material of fuel rail	Aluminum fuel rail can produce less pulsation compared with low-carbon steel.
	injector injection period	higher injection period increases pressure pulsation
Tariq and Tripathi 2013 [32]	fuel rail material	The optimum fuel rail design reduced the pressure pulsation by 28%. This new design has changed fuel rail material, increased fuel rail length by 15%, doubled fuel rail volume, and increased fuel inlet radius by 79%.
	fuel rail length	
	fuel rail volume	
	fuel inlet radius	

2.4 Summary and Conclusions

There is very little information available regarding the noise issue caused by pressure pulsation inside vehicle EVAP system. But studies have been done concerning pressure pulsation phenomenon inside the liquid fuel line. This thesis thus reviewed those studies and tried to extract useful knowledge that can be applied into the current pressure pulsation/noise issue. Through surveying other resources, porous material can reduce flow pressure pulsation when flow permeates through it.

All of the studies focused on the pressure pulsations in the fuel delivery system with some also recorded noise. And the pressure pulsation attenuation is the key to address the noise issue, along with other issues caused by pressure pulsations. However, the information regarding the measuring equipment

or methodology was very limited. No researches provided the sensor specs, some showed the location for the sensors.

As Tariq and Tripathi [32] summarized in their work, noise reduction can happen:

- At the source, in the case of fuel delivery system, the source can be pressure pump, fuel injector, fuel rail, etc.
- On the transmission path, through clamps or vehicle body.
- At receiver end-that is inside the cabin.

These above mentioned are also three main possible places where the noise issue can be addressed. From current researches, most solutions have been focusing on the pressure pulsation wave propagation path. Pulsation damper and fuel rail geometry are the most common approaches [24], [28], [31]. Within fuel rail geometry, volume, cross section, and width-to-height ratio were the most studied parameters, while wall thickness of the fuel rail, material of the fuel rail, and supply line length were also looked into [31], [47]. In high-pressure pump system, a small-diameter orifice is used to limit pressure pulsation from entering the fuel rail [58].

Using similar thought process, possible solutions to the noise issue inside the current EVAP system in this research are:

- At the pressure pulsation source-CPV. Modifications on CPV to reduce the pressure pulsation magnitude.
- On the pulsation transmission path-EVAP line. Using pulsation dampers, changing line geometry, adding small-diameter orifice, and porous material.
- At the noise source-FLVV. Modifications on FLVV to reduce its sensitivity on the pressure pulsation, thus making it less susceptible to be excited.

Because the OEM only provided the EVAP system, thus the noise propagation path and the receiver end are off the scope of this project. From previous researches, it is possible to add vibration-isolation clips, or other mechanical means to block the noise propagation, achieving noise reduction effect [31].

Chapter 3
Methodology

This research consists of two main parts: to build an experimental setup for noise studies; and to investigate several potential approaches to minimize/eliminate the noise. These two parts are very closely related. Many aspects of the investigation have to be taken into consideration before designing the experimental setup so that it can allow further studies.

This chapter breaks up each vital components of the experimental setup and explains how each of them affects the second part of this study. On top of the main experimental setup, this chapter also includes a detailed description of preliminary testing setup. The preliminary test setup used only critical parts to simulate the noise, eliminating most of the pipes from the system.

3.1 Preliminary Test Setup

Before a full experimental setup that integrates all the OEM parts, equipment, and sensors together, a preliminary test was carried out utilizing only critical parts to mimic the condition when noise occur. The parts included for the preliminary test were:

- Vacuum pump, for providing negative pressure needed for the system to run;
- manifold/CPV, for creating the pressure pulsation needed to excite the valve inside the fuel tank;
- piping, for transmission path; and
- FLVV/GVV, the excitation of the valve creates tapping noise.

Aside from the list of the parts provided by OEM, shown in Table 1-1, two sets of separate FLVV/GVV valve system were also provided. This enabled the test to be carried out without using the fuel tank. A bucket filled with water was used to simulate the fuel level inside the fuel tank and the FLVV/GVV valve system was partially submerged to imitate different fuel level and grade/orientation. Figure 3-1 shows the schematic of the preliminary test setup.

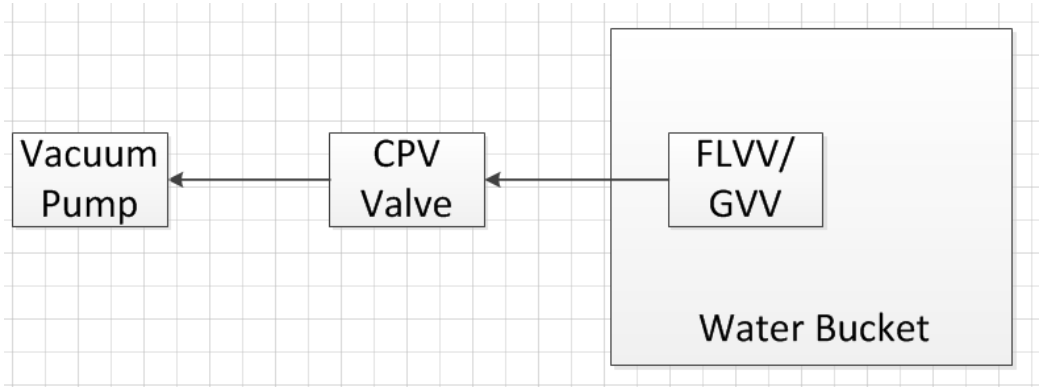

Figure 3-1: Preliminary test setup schematics

3.2 Experimental Setup Overview

The experimental setup consisted of all the OEM parts provided, other equipment/sensors purchased including a vacuum pump, two pressure transducers, an AD converter, mass flowmeter, and a computer for data collection and post-processing. There were in total five locations where the OEM parts were altered to have ¼ inch NPT female connection. They allowed attachments of pressure transducers and other components as part of the experiments. Figure 3-2 shows an overview of the experimental setup, including the locations of the ¼ inch NPT female connections, which are represented by the circled numbers. This schematic does not depict the computer and pressure transducers. The pressure transducer and data acquisition system (DAQ) will be discussed in more details in Section 3.3 that follows. A test rig was built to support the fuel tank, canister and major portion of the lines. The test rig is not shown in the overview schematics. It is covered in Section 3.6. There are in total 4 holes drilled on top of the fuel tank, two close to FLVV and two close to the GVV. The double-hole configuration was to accommodate both inspection camera head as well as extra lighting for better image/video quality. Section 3.4 has more details regarding the inspection camera. Figure 3-3 through Figure 3-5 show the actual setup in three components.

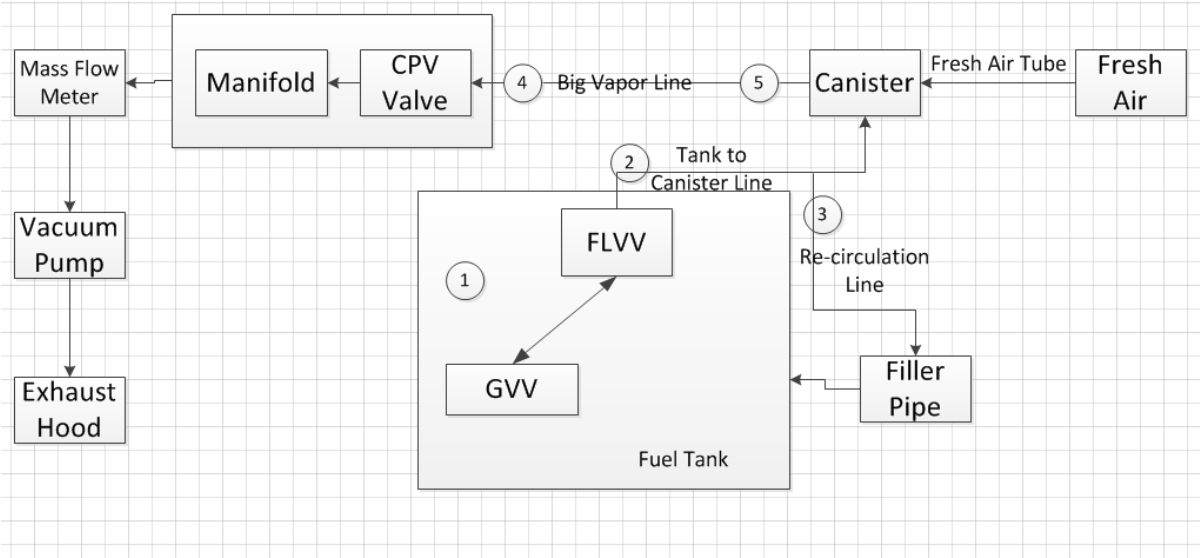

Figure 3-2: Experimental Setup Overview Schematic

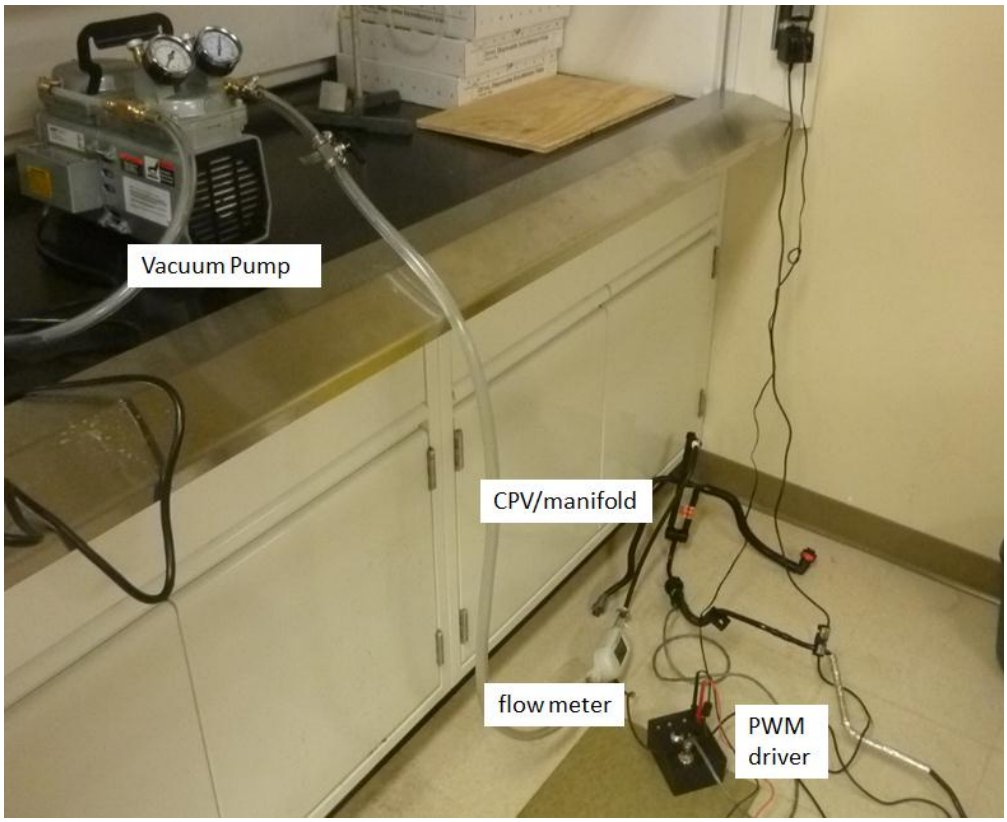

Figure 3-3: Experimental setup, vacuum pump to CPV/manifold

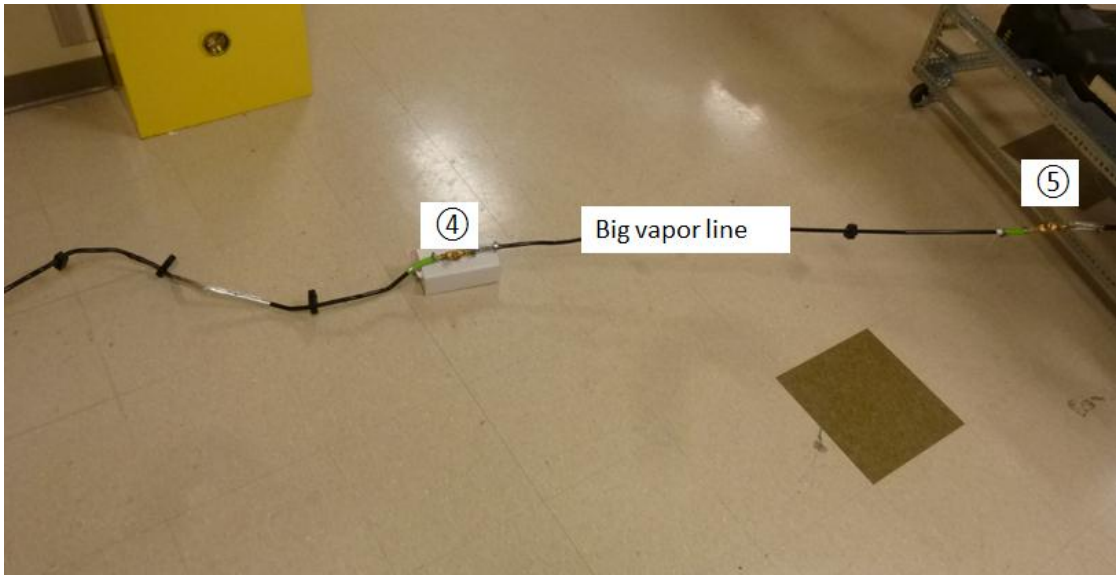

Figure 3-4: Experimental setup-big vapor line

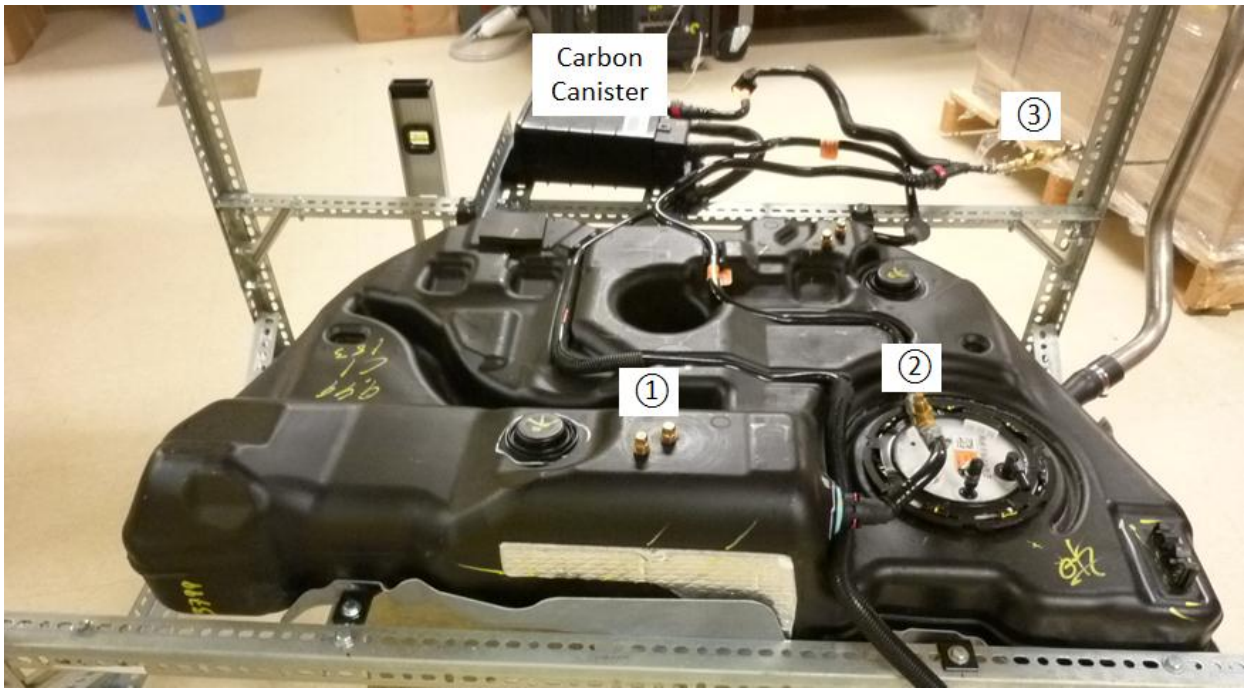

Figure 3-5: Experimental setup-fuel tank and canister

3.3 Sensors and Data Acquisition System

Pressure transducers

There are two pressure transducers used for this project, which can be mounted on any of the five locations in the system. These two pressure transducers are Omega PX209-30V15G5V. They have a full range of -1 to +1 bar (100kPa) with 2ms typical response time (500Hz). The natural frequency for this pressure transducer is more than 35kHz for 100 psi range. According to the calibration report provided by the supplier, the combined accuracy specification for the pressure transducers is ±0.25% of full scale, making the combined accuracy spec to be 500Pa, which is roughly 2 inches of water column. The two pressure transducers are arbitrarily assigned as Pressure Transducer #1-PT #1 (S/N 103898) and Pressure Transducer #2-PT#2 (S/N 103914). Figure 3-6 below shows the DAQ system schematic.

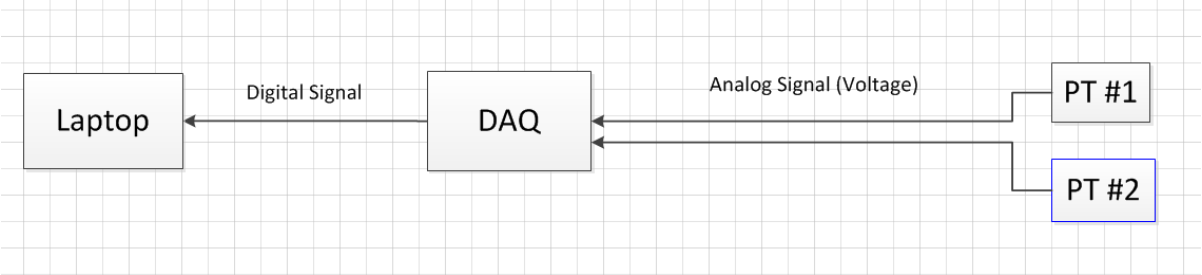

Figure 3-6: DAQ system schematic

Acquisition of pressure signals

The data acquisition system converts the analog signal coming from the pressure transducers into digital signal which is then fed into the computer for storage and post processing. One important factor to consider when selecting DAQ is the sample speed and bit rate. This determines how much information the DAQ can take in a given period of time (usually measured in one second). The unit used for this application is NI USB-6210 which is a basic DAQ model NI offers, it has 16 bit rate with 250kS/s (250 thousands samples per second). Given that only two channels are being utilized, the maximum sampling rate each channel has for each pressure transducer is 125kS/s. For the actual experiment, the sampling frequency and sampling rate is set to be 200Hz and 200S/s. These relatively small values are set to reduce the data size for post-processing. In Chapter 5, pressure readings were taken at 300Hz and 300S/s, and the results were compared with the benchmark scenario, which was also taken at the same sampling frequency and sampling rate.

There are two aspects considered in order to determine if the 200S/s sampling rate, which is the smaller of the two sampling rate used in this study with the other being 300S/s, is acceptable. First, this sampling rate should be at least twice compared to the maximum frequency that is of interest. In this experiment, the CPV frequency is running at 20Hz at normal condition, and the maximum frequency that can be achieved is no more than 35Hz. The set sampling rate is at least 6 times higher than 35Hz. Second, it is also important to understand the scan interval, which corresponds to the inverse of the maximum data acquisition rate per channel. In this case, the scan interval can be calculated out to be approximately 8 microseconds. The physical meaning of scan interval is the time for one cycle of data acquisition from one transducer to the other.

Processing of pressure signals

A Pentium-1.20 GHz laptop and LabVIEW 2012 software were used to acquire data from transducers. Also a Pentium Dual-Core- 2.7 GHz desktop with Matlab 2012 and MS Excel 2010 were employed to analyze the data. The pressure readings were stored into LVM format on the laptop. The readings were then transferred to the desktop for analysis. MS Excel can open the LVM format directly. It can calculate the mean, standard deviation, as well as perform Fast Fourier Transform (FFT). Matlab 2012 also has the capability of performing the above mentioned operations for a very large quantity of data. However, only MS Excel was used to perform FFT because the sample size for each measurement is small. The pressure pulsation was quantified by peak-to-peak value.

The pressure readings were taken using LabVIEW. They were taken in an interval of 5 seconds, which are 1500 samples in total. The FFT function requires a data size of powers of two, thus, it is chosen 1024 samples to be used. Under this arrangement, the frequency the FFT covers is 150Hz, which is more than 4 times of the maximum frequency of 35Hz the system can achieve.

Microphone

There are three different microphones used for this project. During noise generation phase, a handheld mobile phone (Samsung Galaxy Note II) was used to record the noise utilizing its built-in sound recorder functionality. A piezoelectric guitar pickup (Dean Markley Transducer Acoustic Pick Up) was later explored as an alternative, utilizing its working principle and ability to filter out the background noise. However, it was determined that the vibration signal generated by woodpecker noise was too small, making it difficult for the piezoelectric pickup to collect any meaningful data. Thus, a simple PC microphone was purchased for noise recording (NexxTech Omni-directional PC microphone, 2616448). The microphone can be directly connected to computer through the microphone jack. Due to limited

access to facility and equipment, the noise files recorded by the microphone were not further analyzed. The noise was subjectively evaluated as audible noise or non-audible noise.

One dimensional wave propagation assumption

According to Izydorek and Maroney's [24] recommended standard testing methods, the diameters of the EVAP line must be less than one fourth of the wavelength of the highest frequency of interest. Conversely, since the main fuel vapor line has a diameter of 0.31" (7.874mm), the maximum frequency that still satisfies this assumption is about 172kHz, assuming the speed of sound in gasoline vapor/air mixture is 340m/s [24].

Viscous dissipation

The CPV is rated to allow maximum of 85lpm flow to go through the fuel vapor line with 0.31" in diameter. The kinematic viscosity of the fuel vapor/air mixture is assumed to be 15.68×10^{-6} m^2/s, which is the viscosity of the gasoline. The Reynolds Number is 14610. Since Izydorek and Maroney [24] did not provide a threshold value for the critical Reynolds Number, in this thesis, it is assumed that the viscous dissipation effect is negligible.

Fluctuation in flow and pressure compared to mean flow and pressure

Due to equipment limitation, the fluctuation in the flow cannot be detected. While the maximum pressure fluctuation was measured to be 21kPa peak-to-peak. The system running condition is -40KPa gauge. Izydorek and Maroney [24] did not provide quantified requirement. However, this 21kPa peak-to-peak occurred at extreme case while most running conditions had fluctuations less than 10kPa. Thus, this effect is not considered in the final data analysis.

3.4 Inspection Camera

A DeWalt inspection camera (DeWalt DCT 410S1) was purchased for this project. The camera kit comes with a 17mm diameter camera head. An addition 9mm replacement camera head was purchased. The ¼ inch NPT hole on top of the tank (four in total) is big enough for the camera head to go in. Both of the camera heads are water proof and flexible. The inspecting screen is wireless and can be separated from the main unit. This camera is capable of taking both images and videos. A 16 GB micro SD memory card was purchased for storing all the images and videos, which could be later ported onto the computer.

3.5 Method of Processing and Analyzing Data

The pressure readings stored in the laptop were voltage readings. When they were ported into Excel or Matlab, they were firstly converted into pressure using simple mathematical relation: pressure values [kPa]=(voltage values[volts]-2.5)×40. This information was provided from the manufacture user manual for the pressure transducers. The pressure readings were presented using Excel scatter plot (lines) with mean and peak-to-peak value presented. The presented data was taken within 1 second; both x-axis and y-axis were fixed into one scale, except for some special cases, for easier comparison purposes. Fast Fourier Transform(FFT) was also performed on selected pressure readings. Both Excel and Matlab have the capability to do FFT on the data readings. Thus the data was analyzed in both time and frequency domain.

Initially, the recorded audio files were analyzed using Audacity. This audio software is free and readily available on the internet. It is capable of performing the FFT plot spectrum, amplifying the sound, cancelling the noise, and many other functions. However, because the microphones used to capture the noise were very low end products, plus the lacking of appropriate experimental environment (anechoic chamber), Audacity was not utilized.

3.6 Test Rig

A test rig was built using perforated steel and mounted on 4 wheels for easy mobility. The base dimension of the rig is 48 inches by 30 inches; this dimension was chosen in order to fit the fuel tank into the rig easily. The design of this rig is simple box-shaped structure, with some small pieces added for securing parts of the fuel tank/vapor line system. There was another “level” added to the rig in order to support more items. Figure 3-7 shows the rig with fuel tank mounted, and other parts on the second level.

Figure 3-7: Test Rig with fuel tank mounted

3.7 System Operation

During the experimental run, there were many factors that needed to be either controlled or closely monitored in order to ensure authenticity of the data collected. Among these factors, there were several identified as vital parameters: liquid level (water), test rig grade/orientation, CPV PWM (pulse width modulation) frequency and DC (duty cycle), vacuum level and flow rate. These factors were not considered as parameters to help decrease or eliminate the noise issue.

Water Level

Due to safety concern, water was used instead of gasoline. The water level was one of the most important factor to make noise occur (the other being nose-down angle). The FLVV design has a float, with a small "satellite" disc on top. This disc shuts off when the fuel level reaches certain height. When the fuel (water) level is at a height that the float is almost at its top position, in other words, when there is a small gap for the float/satellite disc to move, the pressure pulsation can excite the float/satellite disc to

move up and down, causing noise. The water level was controlled by how much gallon of water added into the tank, which in turn was monitored by a water flow meter (Cole Parmer RK-05611-22) and lab-use beaker (Pyrex 600ml). First, water was added into the tank through a hose connected to the water tap, monitored by the water flow meter. Then, beaker was used to "fine-tune" the volume inside the tank.

Test Rig Grade/Orientation

Another important factor for noise generation was the nose-down angle, which was realized by lifting one side (the back side) of the rig using car jacks. It was observed that by tilting the tank even at a small angle (1 or 2 degrees), the noise would occur. However, if the tank stood on a level position the noise would not occur. A level (Johnson Level) was used to monitor if the fuel tank was level. It was also used to measure the lift distance of the car jacks, which in turn indicating the angle of tilting. Figure 3-8 illustrates that: on the left, the level being used to determine if the rig/fuel tank system is level; on the right, the car jack and level being used to measure the lift distance, which in turn indicating the tilting angle.

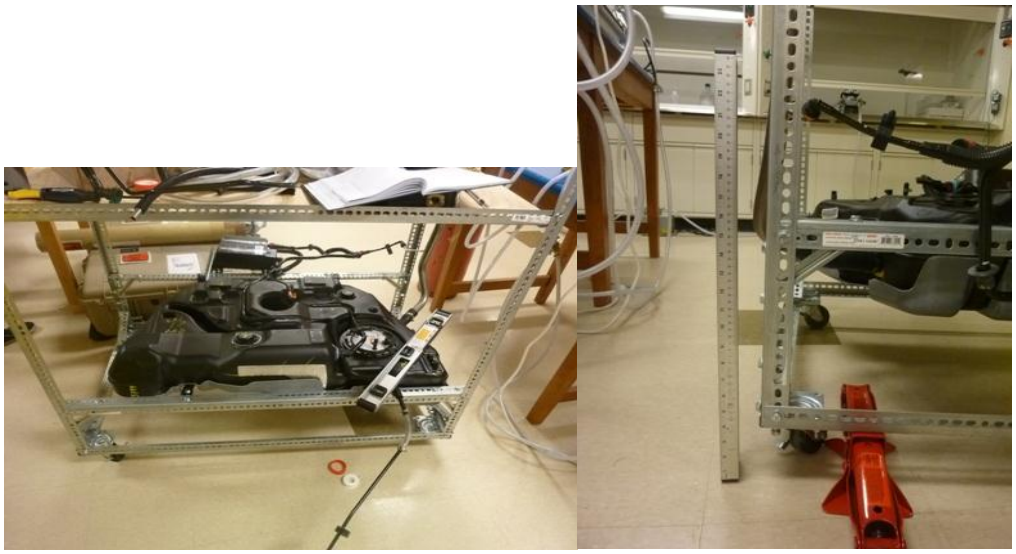

Figure 3-8: level positioned on the fuel tank; Right: car jack and level used to determine lift distance, which in term tells the tilt angle

Vacuum Level/Flow Rate

The pump used for this project is a vacuum/pressure diaphragm pump (Cole Parmer RK-070661-60). It has gauges, regulators, and relief valve. This pump is dual/parallel head design with a 2.2 CFM (62.3 LPM-liters per minute) free-air capacity, and uses 115VAC power. This pump is ULC approved.

The flow rate was monitored by mass flow meter (TSI 3630). The flow meter is in-line design. In the experimental setup, it was connected immediately before the vacuum pump. This flow meter could only measure flow rate without changing it. The CPV is designed to control the flow rate by a prescribed running frequency and duty cycle under a certain vacuum level.

From Section 5.2.3 on, the flow rate was determined on a simplified testing setup, instead of integrating the entire system. This test setup was to minimize factors that may affect the flow instead of the subject of interest. More detailed descriptions are cover in that section.

CPV Frequency/Duty Cycle

The CPV valve was powered by PWM driver which is capable of adjusting frequency and duty cycle. The frequency is indicated by voltage output, which was measured by a multimeter (ABRA 903-105). The PWM driver used in this project was custom built by UW Technical Services as per specs provided by the OEM. The voltage output for the PWM driver is 14V, which is enough to power the CPV. This driver has two dials that can change both the frequency and the duty cycle. The frequency range it can provide is from 8.7Hz to 32.7Hz, and it can provide 0 to 100% duty cycle. In Cortese's study [39], the fuel injectors inside the engine were also controlled by a PWM driver inputs. The PWM driver determines the pulse time, which controls the injector flow rate. She discovered that the injector flow rate almost solely depended on the pulse width time regardless of the RPM of the engine.

The vacuum pump does not have the capacity to support the full range of 100 percent duty cycle, the maximum duty cycle it can support while maintaining the desired vacuum level is 65 percent DC with roughly 34-36 LPM flow rate at 0.4 bar vacuum (12"Hg vacuum). Table 3-1 below shows the duty cycle and flow rate readings from the mass flow meter (at 0.4 bar vacuum):

Table 3-1: PWM driver Duty Cycle and corresponding flow rate at 0.4 bar vacuum

Duty Cycle (%)	Flow rate (LPM)
10	2.7-2.8
20	9.9-10.2
30	14.8-15.8
40	20.2-21.8
50	25.5-26.8
60	31.6-32.2
65	36.5-37.5

3.8 Baseline Scenario

It is important to have benchmark or baseline scenario so that any modification data (pressure readings) could be compared with the baseline to show improvements, if any. It was observed that at the range of 15.4 to 15.8 gallons water, the rig could produce the "best quality" noise. Within this range, 15.5 gallon was chosen to be used as the baseline scenario. Repeated tests confirmed that when the tank was filled with 15.5 gallons of water (94% of 16.5 capacity), as measured by the water flow meter (discussed in Section 3.7), and the nose-down angle of 4.5 degrees, the tank/valve system would make noise. The pressure readings were taken at location 2-tank-to-canister line, 4-big vapor line, close to CPV side; and 5-big vapor line, close to the tank side (shown in Figure 3-2). These pressure readings were analyzed in both time and frequency domain.

In Chapter 5, all the proposals were tested under the baseline scenario, which is 15.5 gallons water at 4.5 degree nose-down angle. The pressure readings at location 2, 4, and 5 were collected and analyzed in both time and frequency domains. The results were subsequently compared with the baseline results to show reductions in pressure pulsation attenuation, if any. The readings at location 4 and 5 were given special attention, because most of the pressure attenuation components were added between these two locations. This testing methodology is based on the insertion loss proposed by Izydorek and Maroney [24]. However, as discussed previously, due to limited resources the noise reduction could not be quantified. It could be only qualitatively identified as "noise" and "no noise" subjectively.

Chapter 4
Results and Discussion - Noise Re-creation

The first step of this research was to build an experimental setup that could re-create the situation where the tapping noise occurs. This was realized by imitating the running parameters as close as they are in actual running vehicle (full details have been discussed in Methodology). After the noise could be re-created, further observations and analysis were carried out to understand the noise phenomena.

This chapter presents the findings regarding the nature of the tapping noise. There are several key findings discussed, including how pressure fluctuations/pulsations are related to the CPV frequency, the FLVV design and the pressure balance across FLVV, the role GVV plays in the noise mechanism, the recirculation line, and a different kind of noise, which was arbitrarily named "satellite disc noise". The tapping noise was subsequently named as "woodpecker noise". The inspection camera enabled some visualization inside the fuel tank and it is discussed in corresponding sub-section.

4.1 Pressure Readings

During this phase of the test, the tank inside and tank-to-canister line locations were used for pressure measurements the most for collecting pressure readings. Pressure readings were recorded when there was noise. The pressure readings when there was no noise were also recorded for comparison purposes. The location of the pressure transducers were chosen to be: PT #1 at the tank inside (① in Figure 3-2 and PT #2 (② in Figure 3-2) at the tank-to-canister line. Figure 4-1 shows the locations of the two pressure transducers mounted on the system:

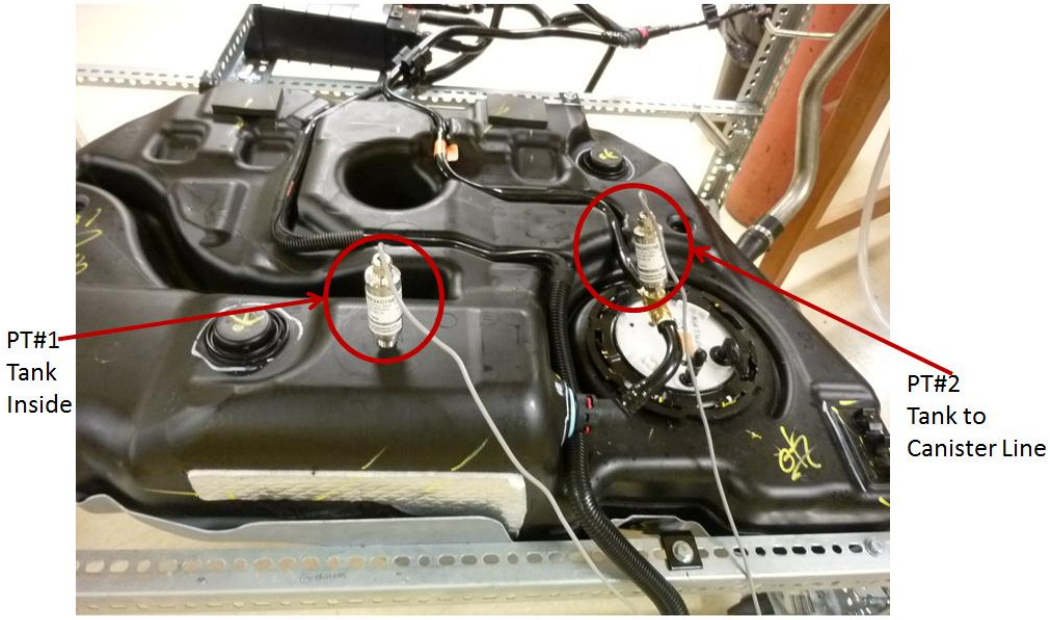

Figure 4-1: Pressure transducers locations

Time Domain

Pressure readings from PT#1-tank inside and PT#2-tank-to-canister line were simultaneously taken and recorded. The readings were then plotted using MS Excel in the time domain. For easier comparison purposes, the scales on x and y axis were set to be equal. Averages of the pressure readings, as well as the peak-to-peak values were presented. The peak-to-peak value was used to show the pressure pulsation magnitude. Figure 4-2 and Figure 4-3 illustrate how the pressure readings were presented. The first figure shows when the tank was level and there was no noise, and the second shows when tank was at 5 degree nose-down angle and there was woodpecker noise. Other conditions at the moment when the pressure readings were taken were: 15.8 gallon water level - 95.8% of 16.5 gallon full capacity; CPV running at 50% duty cycle, and 20Hz.

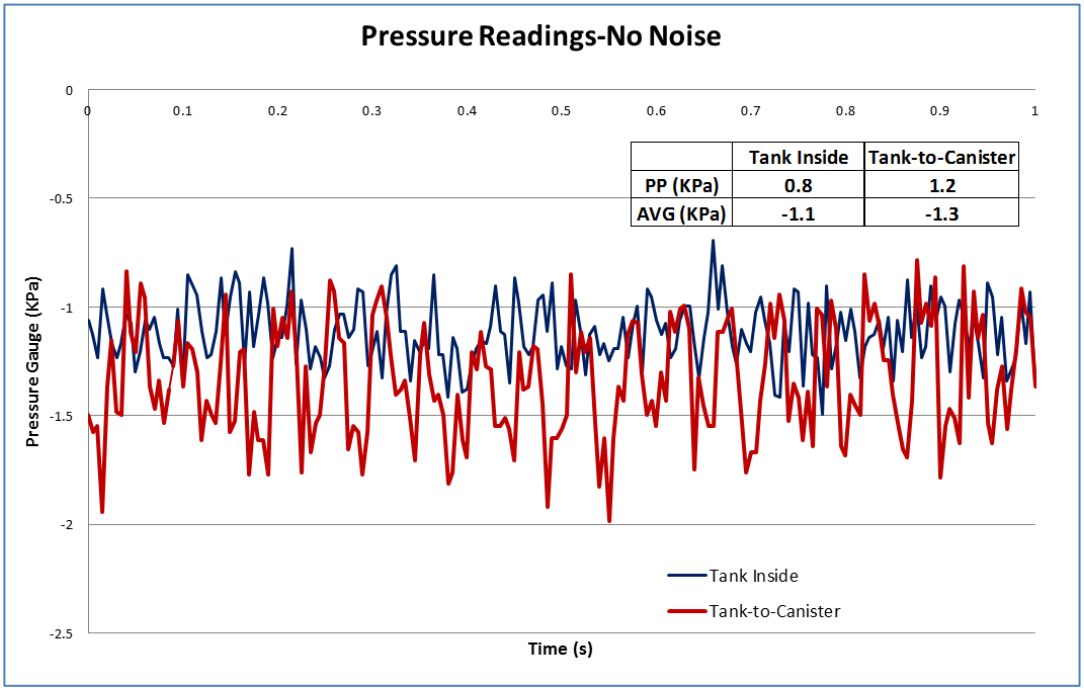

Figure 4-2: PT#1-tank inside and PT #2-tank-to-canister line readings-no noise

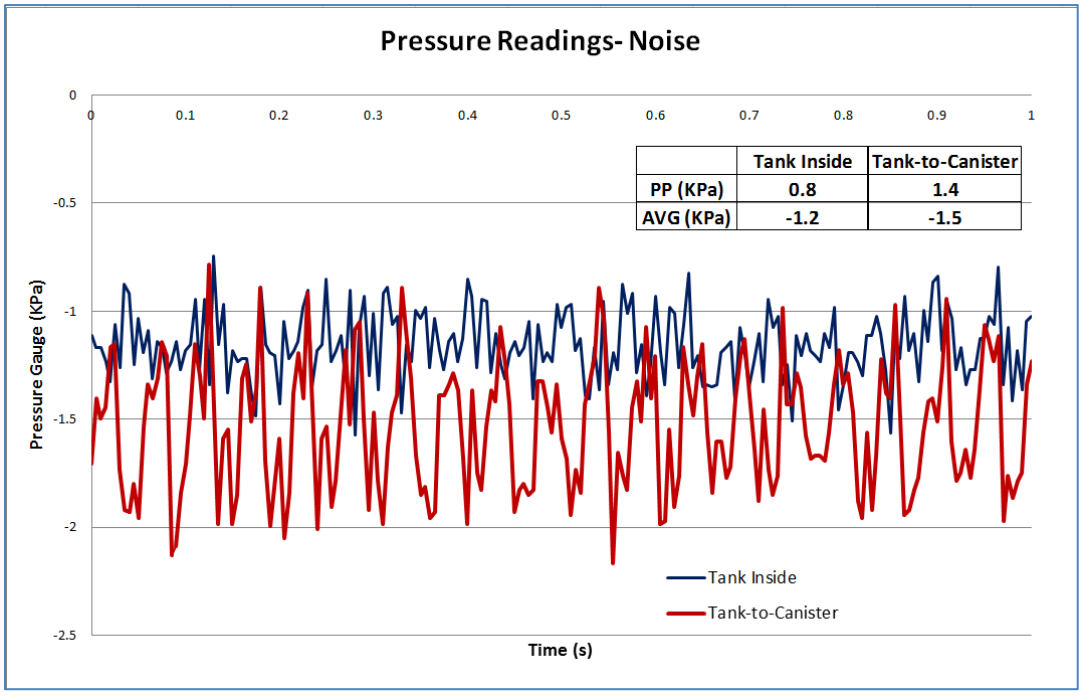

Figure 4-3: PT#1-tank inside and PT #2-tank-to-canister line - noise

From the two figures above, it can be seen that the both the averages and the peak-to-peak of the pressure inside the tank and on the tank-to-canister line were different when there was woodpecker noise and when there was no noise. The one thing that stood out is the peak-to-peak of the PT#2-tank-to-canister line pressure which increased about 13% compared to when there was no noise.

Frequency Domain

The sampling frequency was 200Hz and sampling rate was 200S/s. The sample size must be a power of 2 for FFT. In this case, the sample size was chosen to be 512, which covered roughly 2.5 seconds of data readings. These values changed to 300 S/s in Chapter 5, to bring a wider range of frequency coverage in FFT plots.

Using the same pressure readings as in Figure 4-2, Figure 4-3 through Figure 4-7 show the pressure readings in frequency domain. The PT#1 readings-tank inside do not have very clear pattern. The PT #2 readings tank-to-canister lines show very clearly a spike at 20Hz frequency, which is the CPV operating frequency. This pattern is very clear that the tank-to-canister line pressure pulsation is driven by CPV. There are smaller peaks in PT#2 readings when it was not making noise and when there was noise. The peaks occurred at the multiples of the driving CPV frequency was evident, but was not noted by other researchers in their publications.

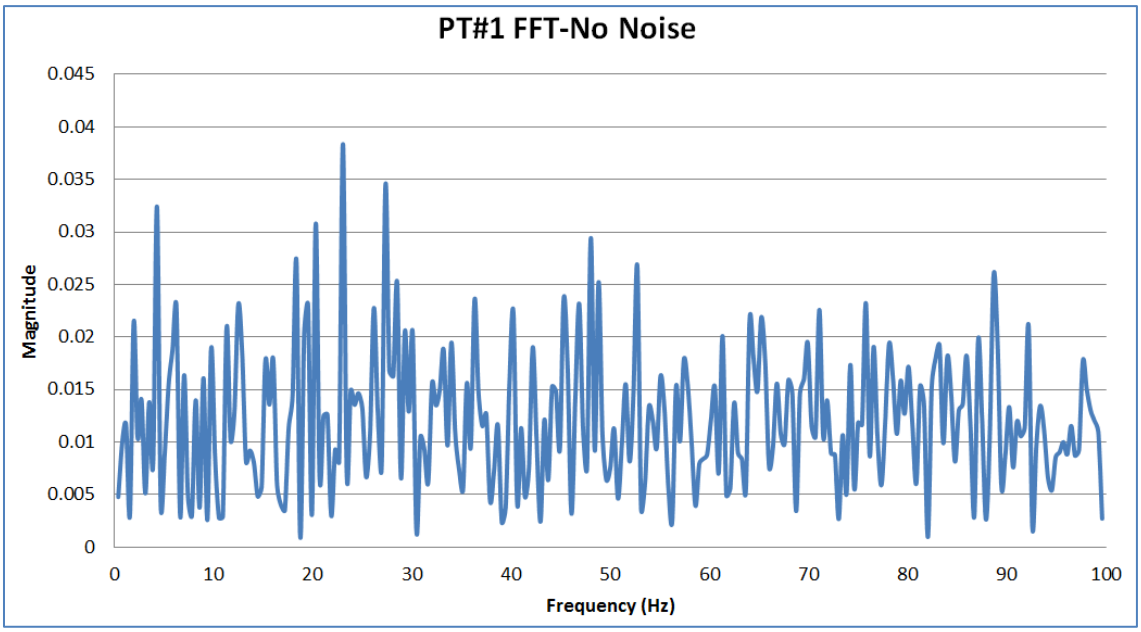

Figure 4-4: PT#1- Tank inside FFT, no noise

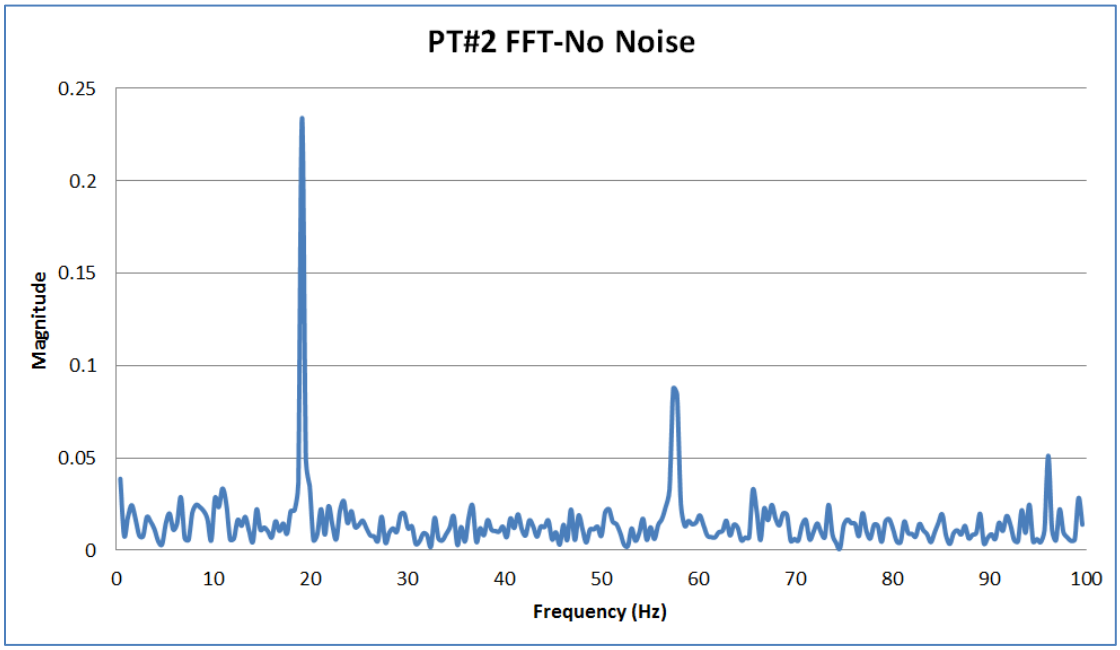

Figure 4-5: PT#2 tank-to-canister line, no noise

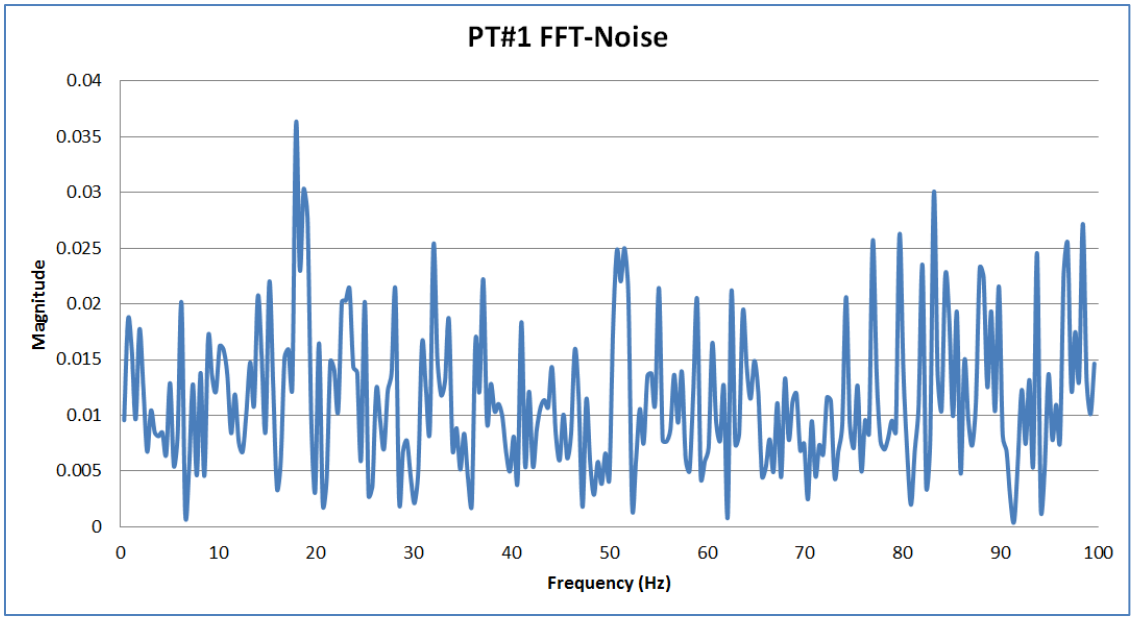

Figure 4-6: PT#1-tank inside, noise

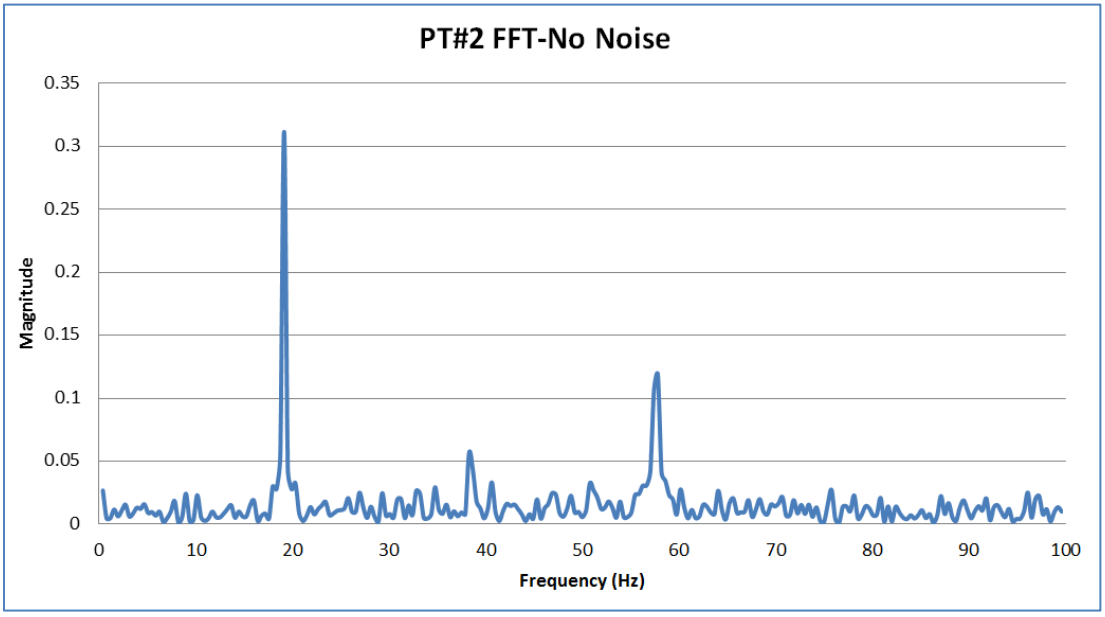

Figure 4-7: PT#2 tank-to-canister line, noise

4.1.1 Harmonics on Pressure Readings FFT Plots

The FFT plots presented in the previous section can show that aside from the dominant peak frequency occurring at 20Hz, there are smaller peaks at 60Hz in both cases where there was noise and there was no noise. When noise occurred, it was noticed that there was a smaller peak at 40Hz. These smaller peaks, which occur at multiples, or harmonics, of the dominating CPV frequency 20Hz, reoccurred in all of the pressure readings obtained throughout the experiments.

These harmonic peaks were also observed in the pressure readings measured at other locations in the system. The two pressure transducers were mounted on location 4-CPV side and 5-fuel tank side, which were on the big vapor line, for testing the pressure pulsation attenuation effect in Chapter 5. The FFT plots for the pressure readings can better illustrate this phenomenon. First, it is because that the pressure on the big vapor line has bigger fluctuations as they are closer to the pressure pulsation source – CPV. Second, the readings were taken at a higher sampling rate (300S/s as opposed to 200S/s), while bigger sized samples (1024 samples as opposed to 512 samples) were used for FFT. This enabled the FFT to cover a wider frequency spectrum: from 100Hz to 150Hz. Figure 4-8 and Figure 4-9 show that the harmonics not only occurred at the CPV frequency of 20Hz, they were also present at other CPV frequencies. The data collected throughout this project all exhibited this phenomenon.

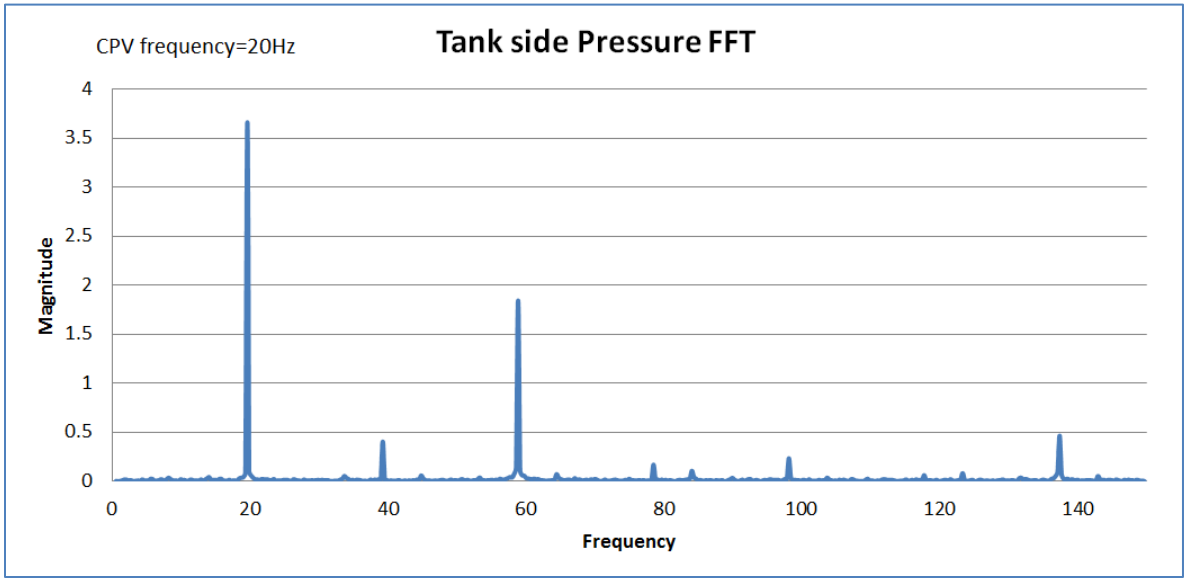

Figure 4-8: Tank side Pressure FFT-20Hz

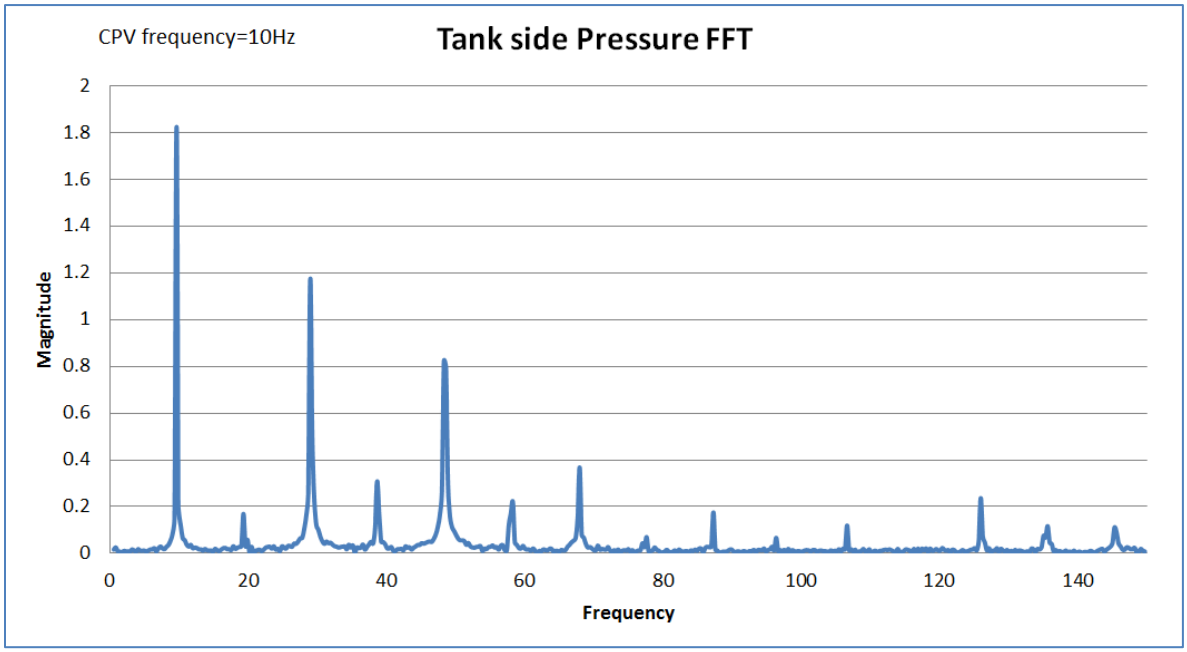

Figure 4-9: Tank side Pressure FFT- 10Hz

The two figures shown above seem to suggest that there is a pattern in these harmonic peaks: that the odd-numbered harmonics (1^{st}, 3^{rd}, 5^{th}, etc.) exhibited smaller peaks, while the even-numbered harmonics

(2^{nd}, 4^{th}, 6^{th}, etc.) showed bigger harmonics. The magnitudes all show descending trend which is intuitively expected.

In Mizuno et al.'s work [31], the phenomenon that harmonic peaks occurring at multiples of the driving frequency was evident in the data. However, they did not note this in their discussions. In the pressure reading power spectrum, the data suggests that there are multiple peaks occurring at frequencies that is multiple of roughly 23Hz. This is the driving frequency induced by the 4 cylinder engine running at 700rpm. Figure 4-10 below showed Mizuno et al.'s work where peaks occurring at multiples are evident.

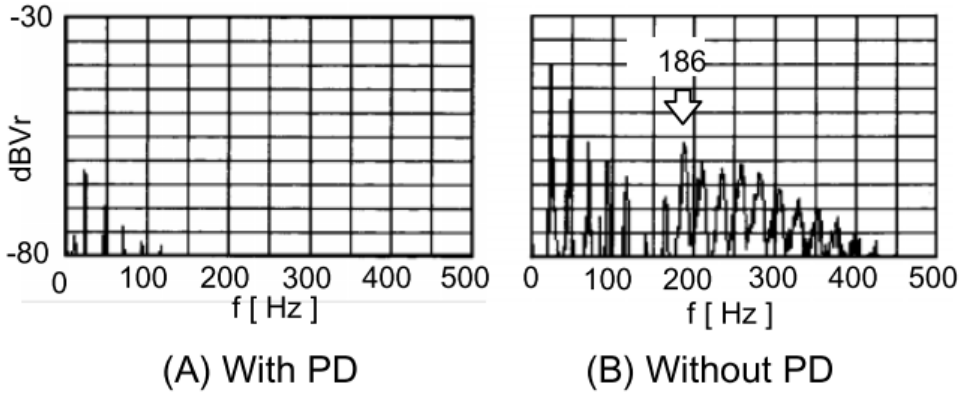

Figure 4-10: Mizuno et al.'s pressure readings in frequency domain (reproduced from [31])

Due to lack of theoretical background, this phenomenon could not be explained fully. Similar patterns were not found in other people's work. This is mainly due to the fact that the pressure readings were not analyzed in the frequency domain in their work. The focus on pressure analysis was to use peak-to-peak value to quantify the pulsation and pressure change period to identify the resonant frequency where the pressure pulsation was at its peak.

4.1.2 Causality

It is very important to understand the causality in this case in order to determine which scenario is a more accurate depiction of the noise generation mechanism. Was the noise causing the pressure fluctuation, or the pressure fluctuation causing the woodpecker noise? It is also possible that they work both ways. The answer to this question can help to pinpoint the cause of the noise, and thus providing insights about how to solve the noise issue.

From the system overview in Figure 3-2, the pressure pulsation path can be seen. The pressure pulsation travels from CPV, which is the source of pressure pulsation, through the big vapor line to the carbon canister, then split into two paths. One of the paths was to the ambient atmosphere through the fresh air tube while the other was to the fuel tank through the tank-to-canister line. This was further confirmed by the pressure readings taken, which showed that the pressure readings closer to the CPV was constantly more negative. This is the exact opposite direction of the air flow, which traveled from fuel tank through canister, big vapor line, CPV, to the vacuum pump and finally discharged into the exhaust hood. The PT#2 readings are pressure on tank-to-canister line (location ② in Figure 3-2) while PT#1 readings are pressure inside the fuel tank (location ① in Figure 3-2). It is clear that PT#2 was on the upstream of the pressure pulsation traveling path, with both FLVV and PT#1 downstream. Figure 4-11 below illustrates this concept with only relevant components shown.

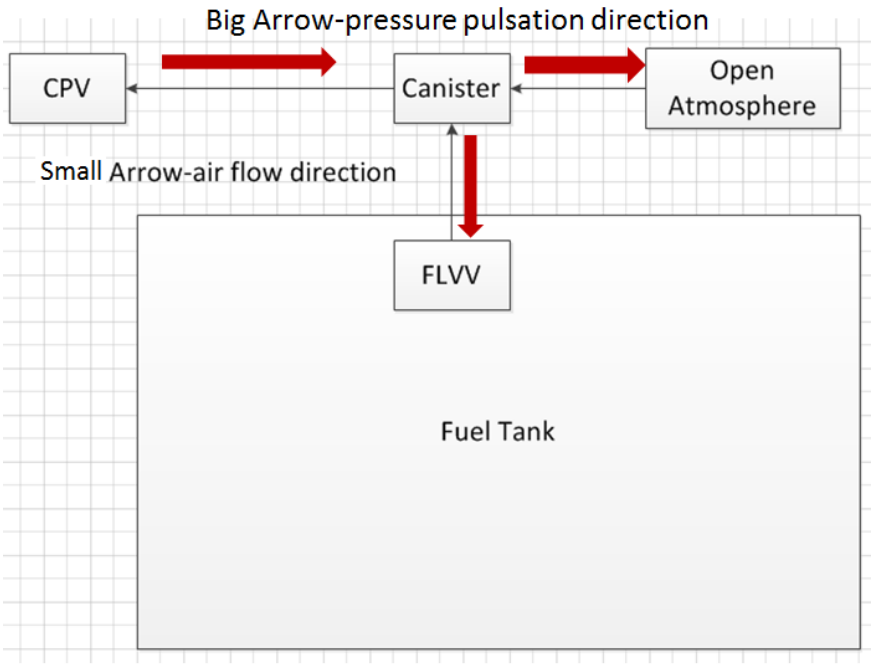

Figure 4-11: Air flow direction and pressure pulsation direction

It is likely that the changing of pressure in tank-to-canister line is a necessary but not sufficient condition for noise to occur. First of all, location ② pressure change should not be the "cause" but the "result" of the woodpecker noise. According to the pressure pulsation travel direction shown above, location ② pressure is mostly affected by CPV under normal condition. The noise caused disturbance which makes pressure at ② behave differently. However, it was observed that when CPV was bypassed,

the fuel tank system would not make noise. In other words, if there was no pressure pulsation present, the woodpecker noise would not occur. The pressure pulsation is caused by CPV due to its nature of operation. Based on this theory, it is important to identify other necessary conditions that may initiate the FLVV excitation. More details are covered in Section 4.3.

4.1.3 Pressure Balance across FLVV

Pressure plays a vital role in the noise generation, and it was worthwhile to look into the pressure balance across FLVV, which seemed to be the noise source. In order to understand the pressure balance, it is necessary to understand the FLVV/fuel tank/line structure layout. Figure 4-12 below shows an overall schematic of the system.

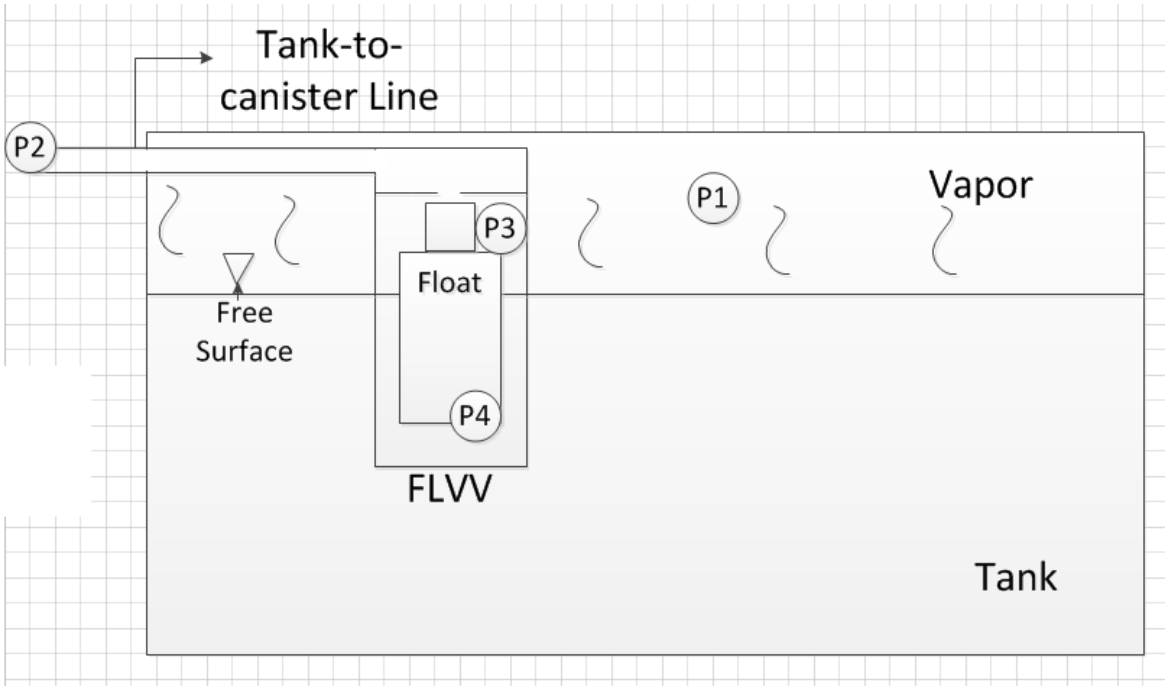

Figure 4-12: FLVV/fuel tank/line layout schematic

In this schematic, there are 4 pressures at different locations. P1 is the pressure inside the fuel tank; P2 is the pressure in the tank-to-canister line; P3 is the pressure inside the FLVV; and P4 is the liquid pressure acting on the bottom of the float. The relation between these 4 pressures, in other words, the force acting on the FLVV float/satellite disc, will determine the motion of the float/satellite disc.

Currently, there is "communication" between P1 and P3. This is due to the design of FLVV: a pin inside the FLVV is lifted when the float position is high, opening a small port to connect the tank inside

and FLVV inside. There is also "communication" between P2 and P3. This is very clear as shown in Figure 4-12. However, there is no real communication between P1 and P2. Thus, one potential solution approach is to establish this communication. Figure 4-13 below illustrates this concept.

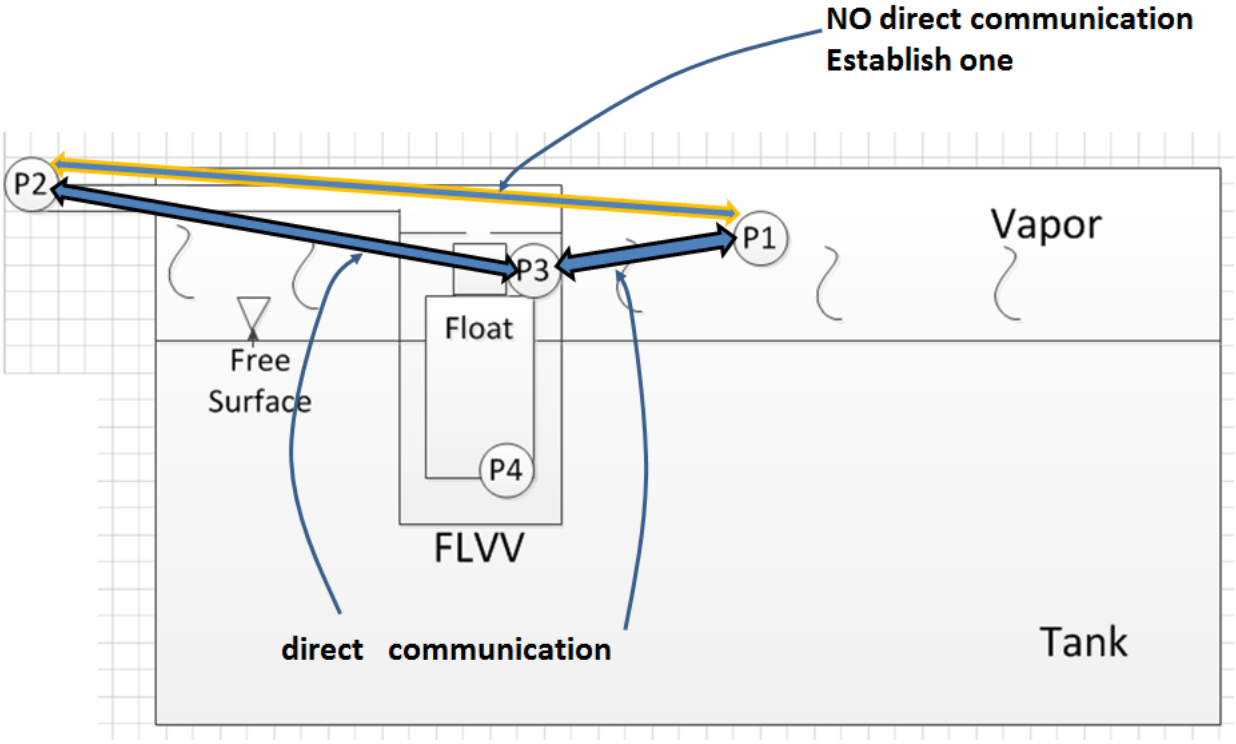

Figure 4-13: Communication between P1, P2, and P3

Based on this thought, a connecting tube was used to connect the tank inside and the tank-to-canister line. The previously mentioned ¼ inch NPT female ends (① and ②in Figure 3-2) were utilized for this purpose. Two barbs were installed and the tube was connected on both ends. It was observed that the connecting tube ID (inner diameter) played an important role. When 3/8 inch ID tube was used, the woodpecker noise was effectively eliminated under all circumstances: across the full range of CPV frequency and duty cycle the testing system could provide. The frequency is limited by PWM driver: 8.7-32.7 Hz. The duty cycle is limited by vacuum pump capacity, which is at 0.4kPa vacuum. It can provide up to 36.5 lpm flow rate, corresponding to roughly 60-65% CPV duty cycle. When smaller ID tubes were used (3/16 inches, and 1/8 inches), the woodpecker noise still persisted. Figure 4-14 is the picture of the tube connecting tank inside (①) and tank-to-canister line (②).

Figure 4-14: Connecting tube- tank inside and tank-to-canister line

Two T-outs were added on the connecting tube to take pressure readings shown in Figure 4-15 below. One of the T-outs was close to the tank inside location (① in Figure 3-2) and the other was close to the tank-to-canister line location (② in Figure 3-2). PT#1 and PT#2 were mounted on location ① and ② respectively. This is similar to the mounting position shown in Figure 4-1.

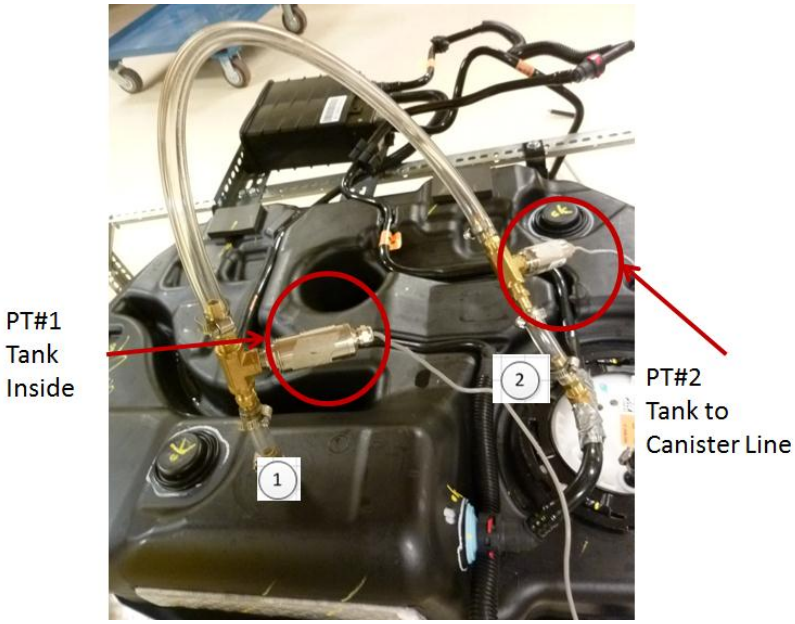

Figure 4-15: Pressure transducers on connecting tube

Pressure readings from PT#1 and PT#2 were taken when the fuel tank/rig was on level ground and there was no noise. Then fuel tank/rig was lifted to 5 degrees nose-down angle to take more readings. This 5 degree nose-down angle was found to have woodpecker noise when there was no connecting tube. When the connecting tube created communication between the tank inside and tank-to-canister line (as illustrated in Figure 4-13), it was observed that the woodpecker noise went away. At this angle, pressure readings were taken at different CPV frequencies and duty cycles. There was no noise observed. Figure 4-16 and Figure 4-17 below show the PT#1 and PT#2 FFTs at 20Hz.

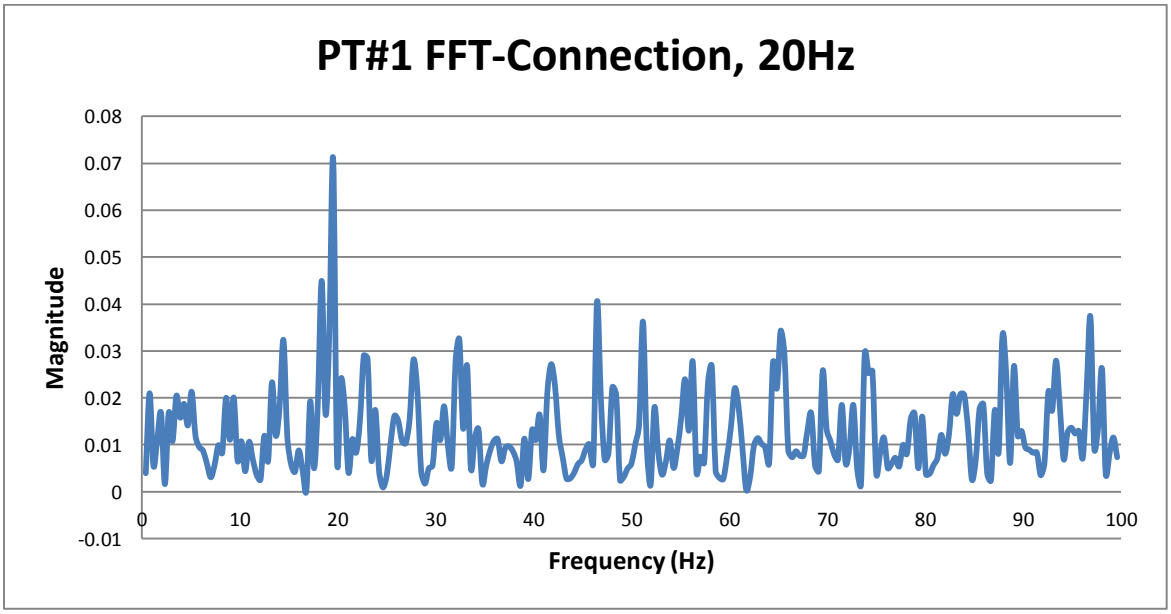

Figure 4-16: PT#1 FFT, connection, CPV frequency 20Hz

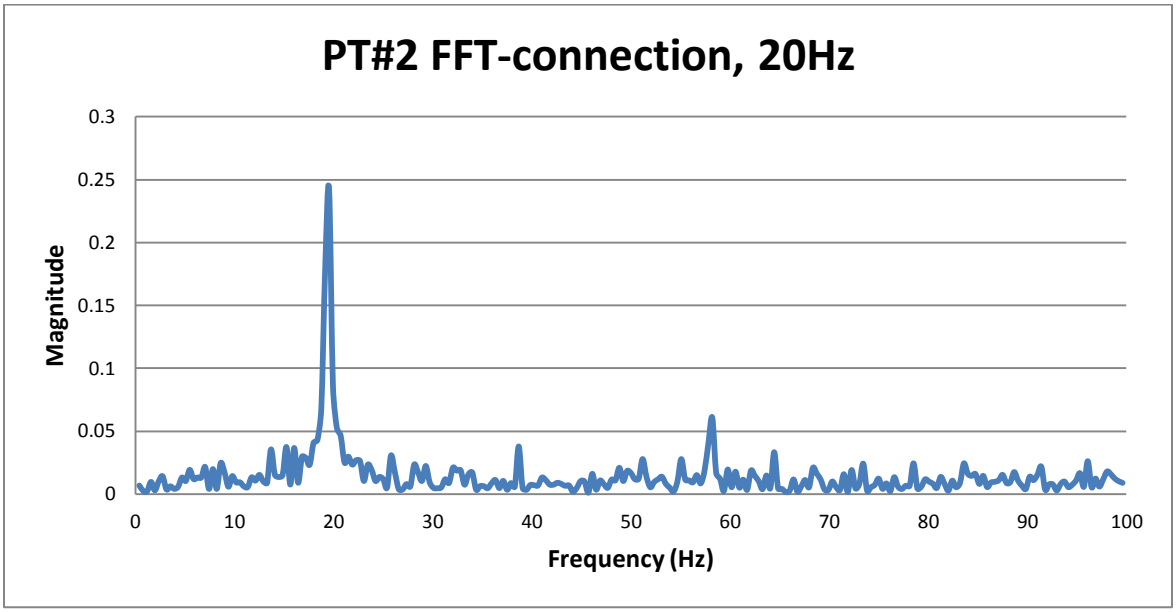

Figure 4-17: PT#2 FFT, connection, CPV frequency 20Hz

4.1.4 CPV Frequency and Noise

CPV frequency is an important factor in the system operation (details discussed in Section 3.7) as the CPV frequency determines the frequency of the pressure pulsation in the vapor line. Thus, it is worthwhile to investigate if CPV frequency may affect the noise generation. According to vehicle calibration specs, the CPV frequency is set to be 20Hz (or 17Hz depending on the vehicle specs) and this value does not change. This is because changing CPV frequency has significant impact on the entire vehicle calibration.

A simple controlled experiment was designed: under 20Hz normal CPV operating frequency, appropriate amount of water was added and the fuel tank/rig was lifted to the right nose-down angle such that the woodpecker noise was generated. CPV frequency then changes from 8.7-32.7Hz, which is the full range of input frequency the PWM driver can provide. It was observed that the noise persisted through the entire range with small changes in noise character. It was observed that the woodpecker noise did decrease in intensity as the CPV frequency decreases, under certain water level and nose-down angle, the noise completely disappeared at 8.7Hz. This deviation from OEM's finding, which indicates that noise completely disappears at 14Hz, may be due to the use of water instead of gasoline or other differences in the experimental design.

Pressure readings and noise at different frequencies were recorded. Pressure sensors were mounted at locations ①-tank inside and ②-tank-to-canister line (Figure 3-2). The pressure transducer locations are the same as shown in Figure 4-1. Noise was observed at different CPV frequencies.

Pressure readings were analyzed in the frequency domain. It was observed that there was no clear pattern in PT#1-tank inside pressure FFT plots under different frequencies. However, there is one clear pattern in PT#2-tank-to-canister line pressure FFT plots: one dominant spike exists at the frequency that is equal to the CPV frequency. It is clear that the tank-to-canister line pressures are not different when there is no noise and when there is woodpecker noise. Despite being different in the time domain, the tank-to-canister line pressure readings did not have significant changes in the frequency domain. However, no conclusions can be drawn based on the PT#1-tank inside pressure readings in neither time domain nor frequency domain. Thus, only selected FFT plots for PT#2-tank-to-canister line are included in this report. Figure 4-18, Figure 4-19, Figure 4-20 are the FFT plots for PT#2 tank-to-canister line pressure at 10Hz, 25Hz, and 32.7Hz CPV frequency respectively.

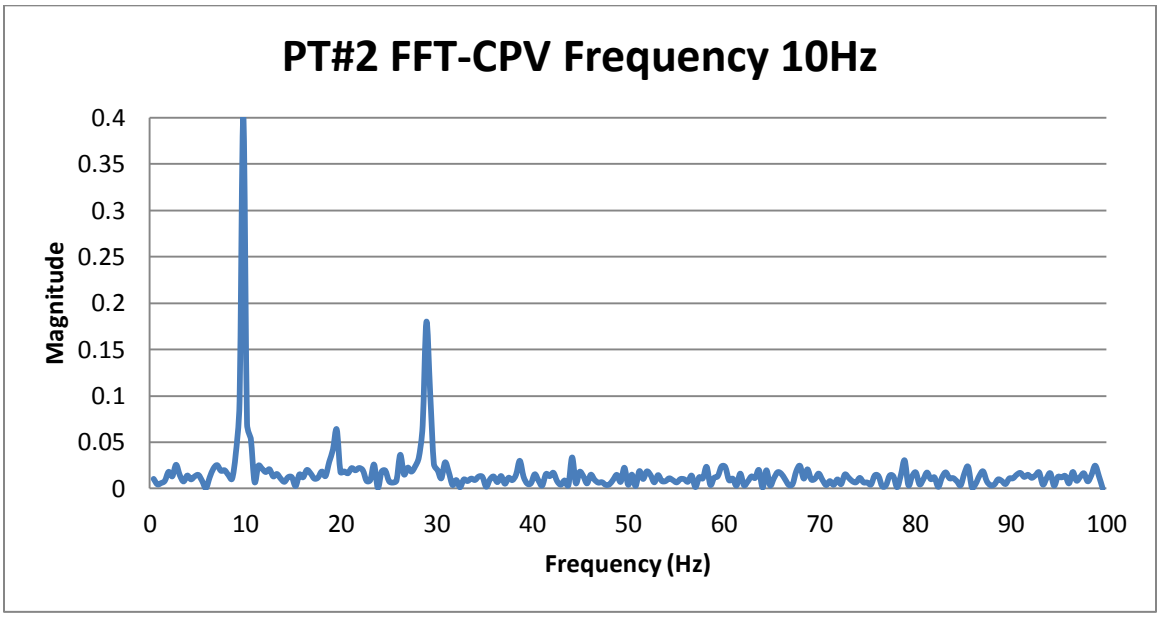

Figure 4-18: PT#2 FFT-CPV frequency 10Hz

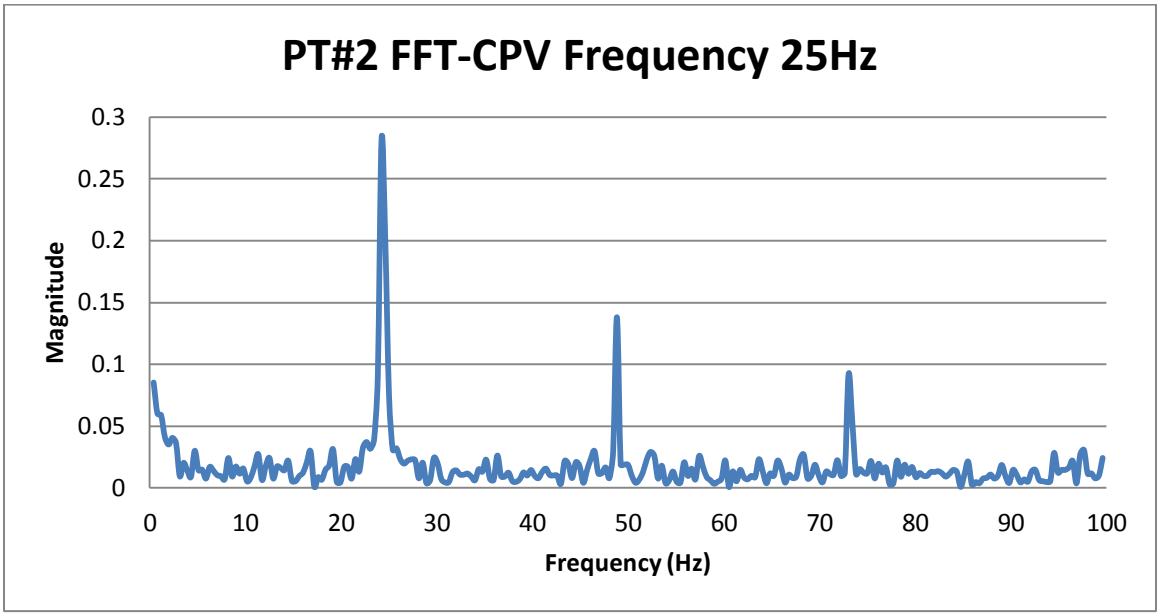

Figure 4-19: PT#2 FFT-CPV frequency 25Hz

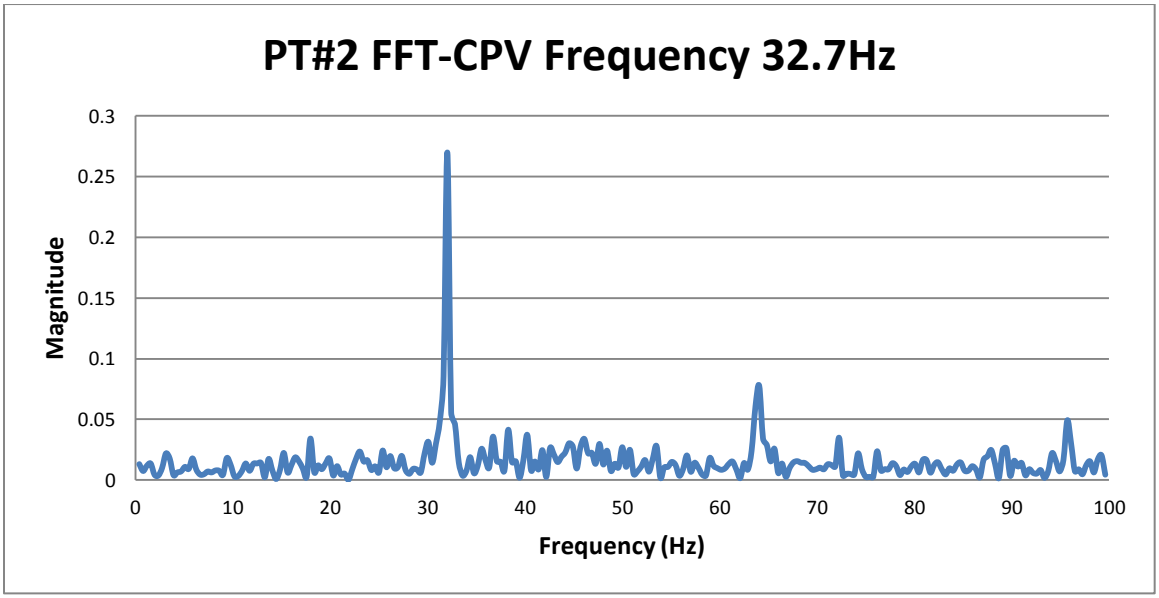

Figure 4-20: PT#2 FFT-CPV frequency 32.7Hz

4.1.5 The Role of Re-circulation Line

The re-circulation line is the line that is connected to tank-to-canister line and connects back into the filler pipe (shown in Figure 3-2). The main design function for this re-circulation line is for some of the

vapor created during re-fuelling process to re-enter the filler pipe and then condense back into fuel droplets, thus reducing amount of fuel vapor generated and stored into the carbon canister.

One theory for noise generation mechanism is that when pressure pulsation reaches the tank-to-canister line/re-circulation line/filler pipe system, there is not enough space or buffer to absorb the pressure pulsation. Thus, if there can be more space in the re-circulation line, e.g. adding a bigger diameter pipe, it might be able to help reduce the pressure pulsation which in turn reduces/eliminates the noise.

Based on this belief, a quick test was devised by simulating an extreme case: open the re-circulation to atmosphere pressure. Modification was done on the re-circulation line to add a T-joint. A pressure transducer was attached on tank-to-canister line to study the pressure pulsation change. Figure 4-21 below shows the experimental setup. The experiment was at benchmark case, which had 15.5 liter water, 50% duty cycle, and 20Hz CPV frequency. In order to produce woodpecker noise, the tank was lifted to a nose-down angle of 4.5 degrees.

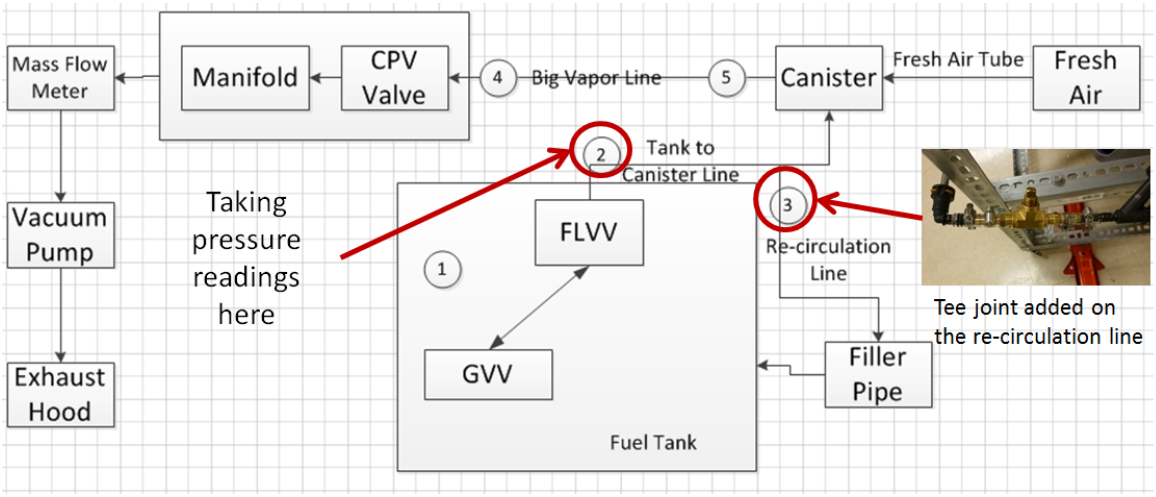

Figure 4-21: Re-circulation modified

It was observed when the tap on the T-joint was taken out, there were no noticeable changes on the woodpecker noise subjectively. The pressure readings on location 2 in both cases were taken: baseline, when there was no modification; and re-circulation line open, when the tee joint tap was removed. Figure 4-22 and Figure 4-23 below show both the readings in time domain and frequency domain. In frequency domain, the changes are not significant enough. In time domain, it is clear that both the average pressure level and the peak-to-peak pressure fluctuations are close.

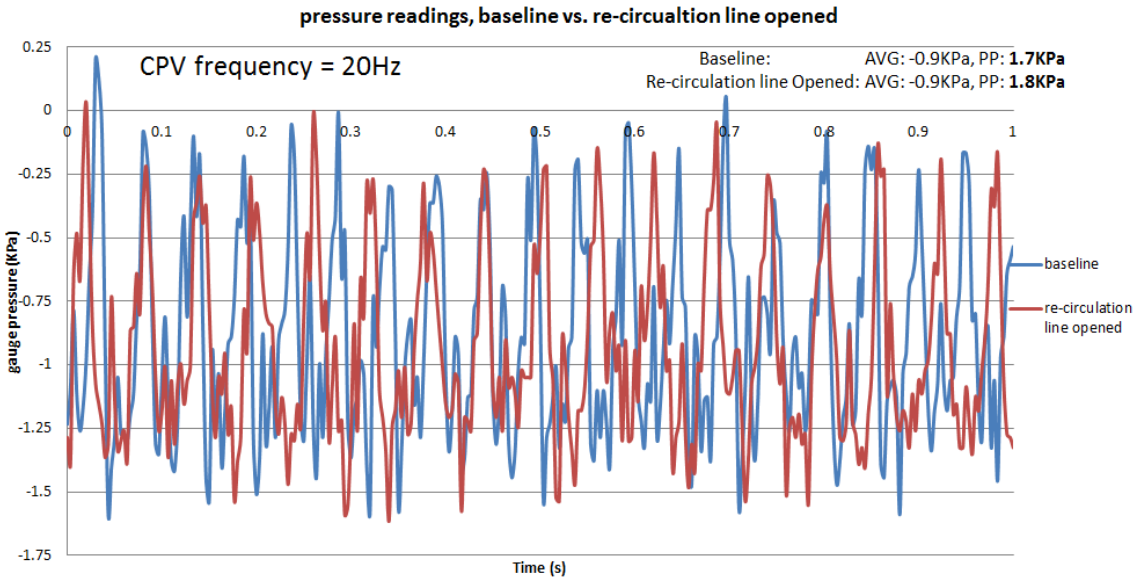

Figure 4-22: Pressure readings, baseline vs. re-circulation line opened, time domain

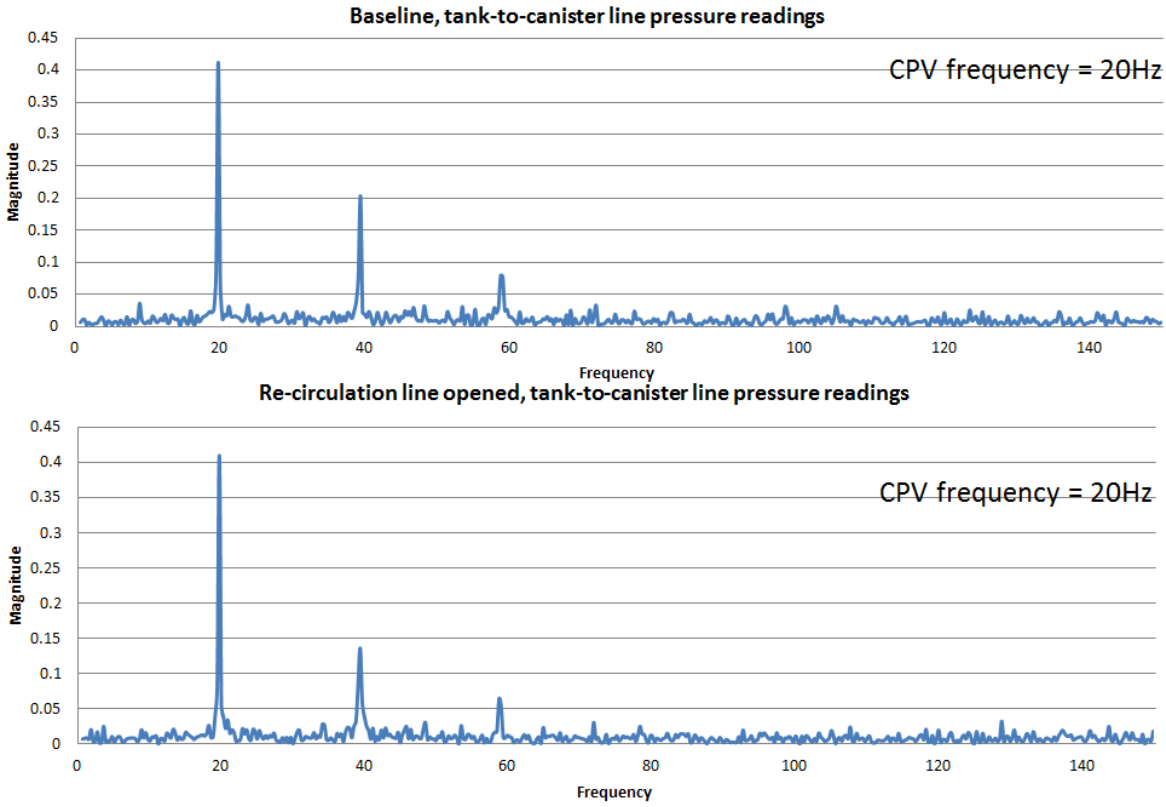

Figure 4-23: Pressure readings, baseline vs. re-circulation line opened, frequency domain

In addition to this observation, attempts were made to connect the re-circulation line to different locations to ensure pressure balance, in hope that it could help reduce/eliminate the woodpecker noise. The theory was based on what has been discussed in Section 4.1.3. Connection between re-circulation line, and tank-to-canister line, and the tank inside respectively (connecting ①&③, and ③& ② as shown in Figure 4-21) but neither produced noticeable changes on the woodpecker noise.

Possible Explanation

Because this system is subject under vacuum pressure, opening re-circulation line to ambient atmospheric pressure technically does not provide extra space for the pressure pulsation to escape but rather for more air to be drawn into the system. However, from the pressure readings in both time domain and frequency domain, it can be shown that this change of system does affect the pressure pulsation to some degree without affecting the noise too much.

4.2 "Woodpecker" Noise and "Satellite Disc" Noise

Inside the FLVV, satellite disc sits on top of the float. When the float is at its top position, there is still small clearance for the satellite disc to move up and down. In other words, the satellite disc can be affected by the pressure pulsation coming from the CPV end. Due to its light mass, the satellite can be easily driven up and down, and sideways. Figure 4-24 below shows the satellite disc on top of the float. The blue piece is the float, and the small white piece is the satellite disc.

Figure 4-24: FLVV float assembly, white-satellite disc, blue-float,

The OEM previously provided several audio files for the woodpecker noise. The woodpecker noise was identified, based on this information, under different operating conditions. However, there was a

different type of noise that was observed and it was arbitrarily named as “satellite disc” noise. This noise is much quieter compared to the woodpecker noise. Woodpecker noise happens when the FLVV float/satellite disc are excited by the pressure pulsation caused by CPV. The satellite disc noise may be caused by satellite disc alone being excited. Figure 4-25 below illustrates this concept.

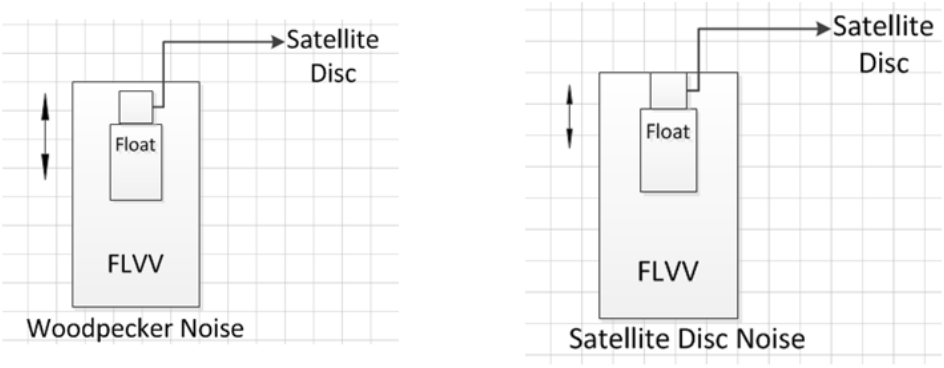

Figure 4-25: Woodpecker noise and satellite disc noise

From the experiment, it was observed that the satellite disc noise comes “after” the woodpecker noise. When the fuel tank is at level position (0 degree nose-down), there was no noise. The test rig/fuel tank was then lifted up by two car jacks, as the nose-down angle increased, the woodpecker noise would appear first (given the appropriate conditions). If the nose-down angle kept increasing, the woodpecker noise would turn into satellite disc noise. The satellite disc noise ceased when the nose-down angle was high enough. By experimental observations, there was one to two nose-down degrees zone for the system to make woodpecker noise. It took additional one to two nose-down degrees for the satellite disc noise to occur. There was no noise when the rig/fuel tank was tilted further.

4.3 Noise Initialization

When the test rig was on level ground, woodpecker noise could not be re-created, regardless of the running conditions it was under. However, at the appropriate water level (roughly 90-99 percent of 16.5 gallon full tank capacity), the woodpecker noise occurred by increasing the nose-down angle. In other words, noise only occurred when the rig was tilted to an angle. This observation invoked the speculation that there was an initialization or excitation mechanism that caused the woodpecker noise to occur given the appropriate conditions. In this case, the conditions may include, but not limited to, water level, nose-down tilt angle, and CPV duty cycle.

4.3.1 Sloshing Liquid Frequency and Pressure Pulsation Frequency Lock-in

When the tank is on a tilted angle, the liquid inside the tank will slosh. This sloshing effect may excite the FLVV float/satellite disc system, causing it to move up and down due to changing buoyancy force (P4 in Figure 4-12) acting on the bottom of float/satellite disc. At the same time, the suction force due to vacuum pressure acting on top of the float/satellite disc pulses, varying in magnitude (P3 in Figure 4-12). This pressure pulsation is driven by CPV frequency, while the sloshing liquid inside the tank has its own frequency. If there is interaction between these two frequencies and a lock-in effect takes place, it may cause the float/satellite disc to move up and down inside FLVV, hitting the structure and making woodpecker noise. Figure 4-26 below illustrates this concept.

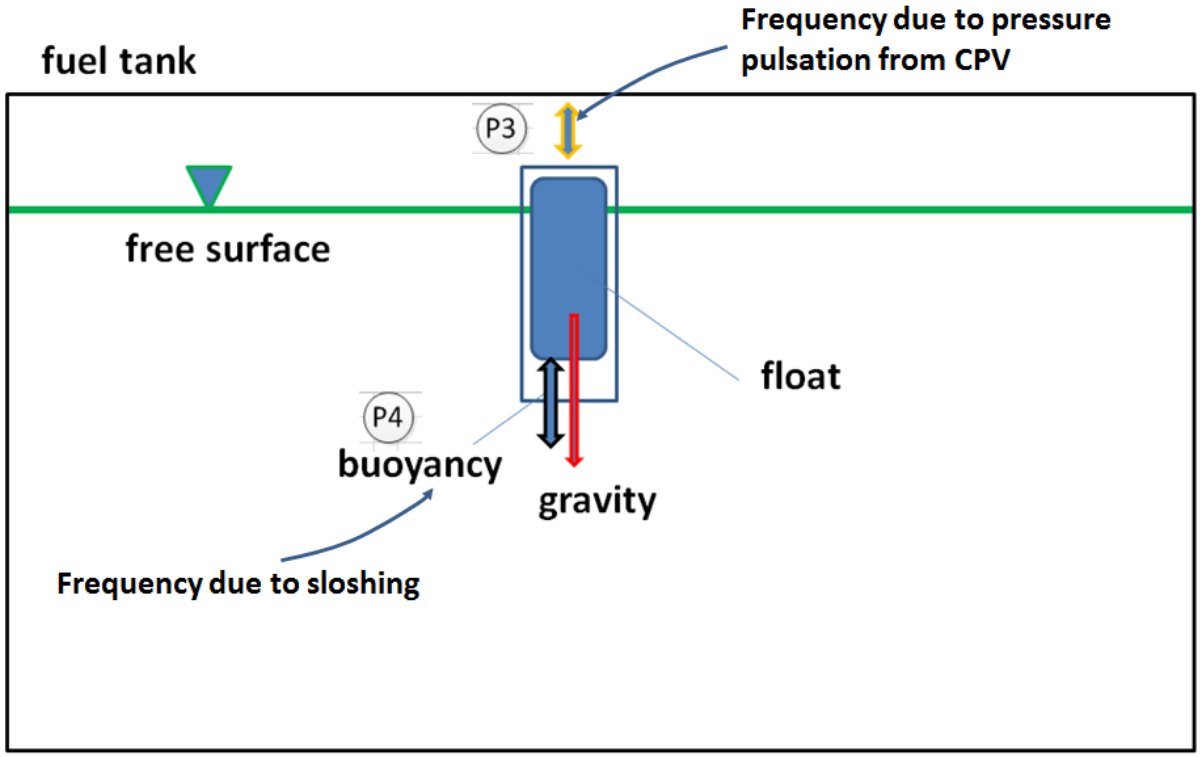

Figure 4-26: Sloshing liquid frequency and pressure pulsation frequency

4.3.2 Satellite Disc Excites Float

A test was done when the tank was at the appropriate conditions (liquid level, nose-down angle, CPV duty cycle and frequency, etc.) and was making woodpecker noise, the power of the vacuum pump was

cut. It was observed that the woodpecker noise would immediately disappear. After at least 5 minutes had passed to ensure the liquid inside the tank sit still, the power of the vacuum pump was turned on. Then a small sound could be heard. This sound would become louder and louder and eventually turn into woodpecker noise. This process could take as long as 2 minutes and as short as several seconds. This small sound may be the result of the satellite disc alone being excited by the pressure pulsation and moving up and down initially, hitting the FLVV structure and the float. Because the satellite disc sits on top of the float, the up-and-down motion hits the float, building up momentum which eventually gets big enough to cause the float to move up and down with the satellite disc.

4.4 The Role of GVV

FWD (Front Wheel Drive) design has two valves inside the fuel tank: FLVV and GVV. The FLVV and GVV are connected in such way that the vapor going through GVV will goes through FLVV first before exiting the fuel tank to tank-to-canister line (see Figure 3-2). On the vertical level, the FLVV is higher than GVV. For the woodpecker noise test, the water inside the tank was usually filled to 15.4 gallons and over, that is over 93% of the 16.5 tank rated capacity.

The GVV is head valve design: a small ball with certain mass sits on a port. This port is normally closed due to the ball's mass. GVV will pop open if the pressure differential across the port becomes greater than 3.5kPa. This value is per the design specs, which was provide by the OEM. There is a 0.5mm bleed notch on the port, leaving small room for the vapor to vent out when the port is closed. Figure 4-27 shows a brief sketch of the GVV design and the bleed notch.

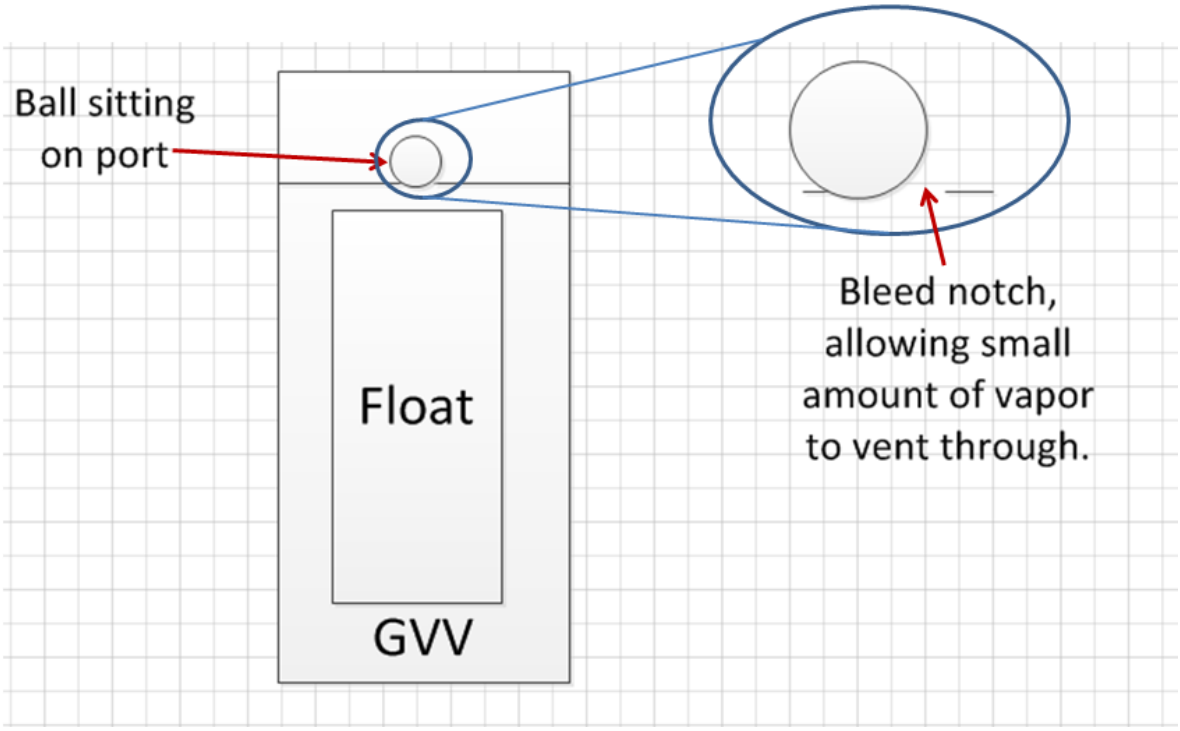

Figure 4-27: GVV head valve and bleed notch design

It is necessary to look into the pressure balance for the fuel tank/FLVV/GVV system in order to understand the role GVV is playing in noise generation. Because the FLVV and GVV are connected, the pressure imbalance in FLVV affects the pressure balance in GVV. Inside the FLVV, the float/satellite disc moves up and down. Figure 4-28 shows the fuel tank/FLVV/GVV system with pressure at different locations, this illustration compliments Figure 4-12 as GVV is added.

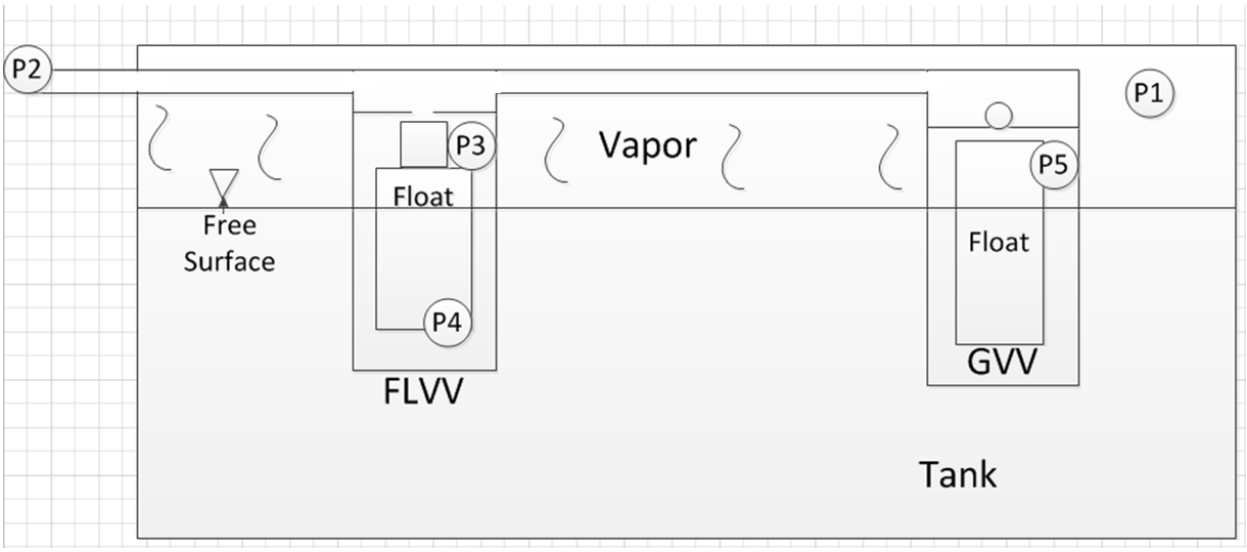

Figure 4-28: Fuel tank/FLVV/GVV system overview

When FLVV float/satellite disc is at the top position, the vapor flow path through FLVV is severely restricted, forcing the head valve open inside GVV. The opening of GVV head valve reduces the pressure on the FLVV side, causing the FLVV float/satellite disc to move down, opening up the FLVV path for the vapor flow. This decreases the pressure differential across the GVV head valve and the ball drops, closing the GVV port. This process repeats, making woodpecker noise. Figure 4-29 and Figure 4-30 illustrate this concept about possible interaction between FLVV and GVV.

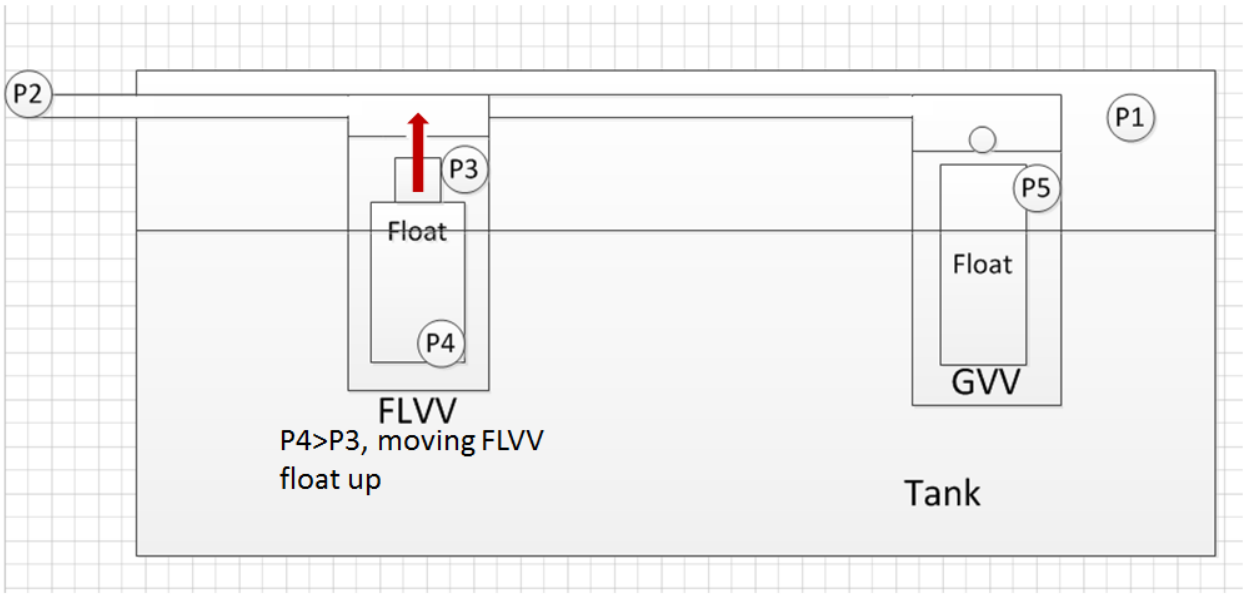

Figure 4-29: FLVV/GVV interaction-1

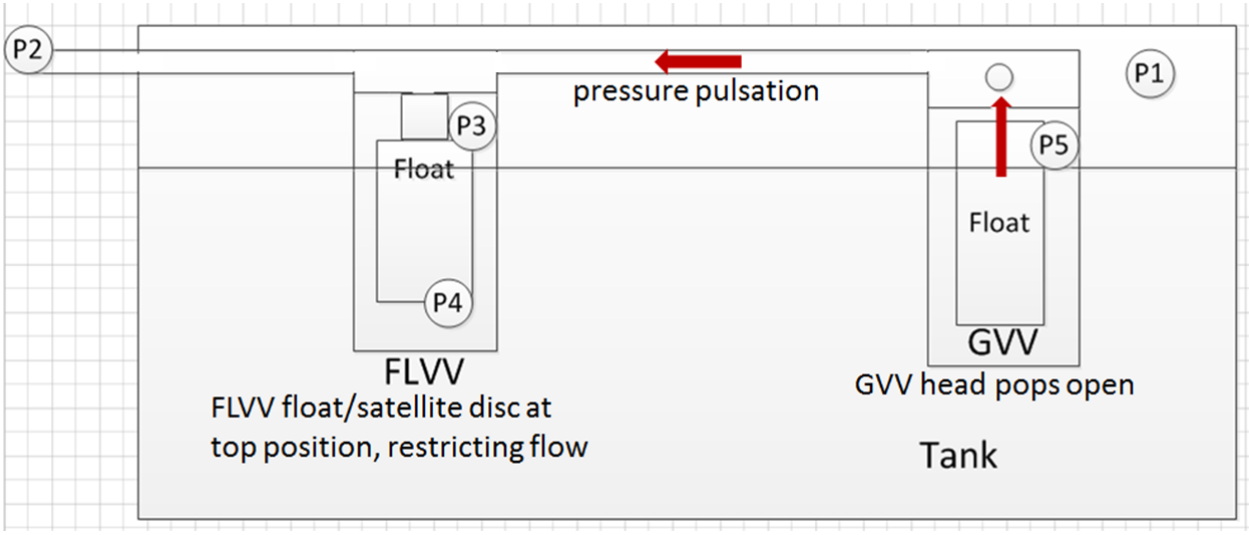

Figure 4-30: FLVV/GVV interaction-2

4.4.1 FLVV/GVV Interaction Tests

Empty Tank Test

A simple test was devised to test the FLVV/GVV interaction on the semi-realistic vacuum level going into FLVV. The fuel tank was drained and the FDM (fuel delivery module) port was open while all the

other components of the system were connected to simulate the normal running conditions. The open FDM port enabled manual control of the close/open state of both FLVV and GVV.

The procedure of this simple test was as follows: the FLVV float was manually lifted to almost close position, with the GVV float at its bottom position due to gravity. Then, the GVV float was held at its top position thus achieving GVV close state. FLVV float was manually lifted to the same almost closed position.

It was observed that:

- The FLVV float was not moving due to pressure pulsation;
- However, the satellite disc was caught by pressure pulsation and hitting the valve structure, making "satellite disc" noise;
- The close/open state of GVV did not affect the disturbance of FLVV satellite disc.

Test on Separate Unit in Preliminary Test

Another simple test was performed on separate FLVV/GVV unit in preliminary test setup. The detailed description of the test setup is covered in Section 3.1. The OEM provided two sets of FLVV/GVV: conventional design and next generation design, which has different mounting mechanism. Both of these two sets were tested: FLVV was put into water at roughly equivalent to 95% water level with GVV either open or closed to investigate the woodpecker noise change. It was observed that FLVV valve would make woodpecker noise regardless of the open/closed state of GVV. Thus it was concluded that GVV does not play a vital role in causing the noise.

4.5 Visualization

The inspection camera was inserted into the fuel tank through the holes drilled, which is on top of the tank close to the FLVV. The camera's extension cord is flexible, thus enabling the inspection inside the fuel tank. The first trial gave two pieces of new information:

- The water level is was the bottom portion of the FLVV even at over 93% water level;
- The water close to the side port of FLVV was very disturbed when there was woodpecker noise, which may be an indicator that the float/satellite was moving up and down, disturbing the water inside FLVV.

4.5.1 Water Level and FLVV

The water level plays an important role in woodpecker noise. When the water inside the fuel tank is roughly at 15.8 gallon, which is about 96% of the full 16.5 gallon capacity, the water level just reaches the bottom portion of the FLVV. This was at level ground and the system was not making any noise. Car jacks were used to lift the fuel tank/rig to increase the nose-down angle, which in turn increased the local water level on FLVV. In the video captured by inspection camera, it showed that as the water level kept going up on FLVV and eventually reached the "side port" of the FLVV, woodpecker noise could be heard. This indicated that the up-and-down motion of the float/satellite disc caused water waves inside the FLVV, and the wave travelled outside through the side port of the FLVV. Figure 4-31 below shows the approximate water level on FLVV at the level ground and at 4 degree nose-down angle.

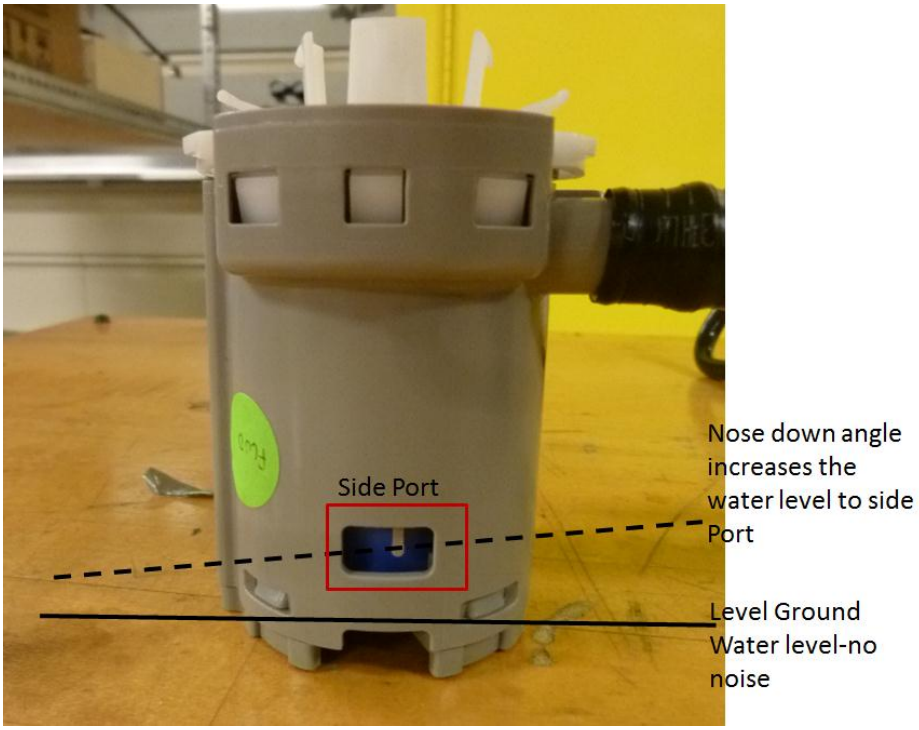

Figure 4-31: Water level and FLVV

4.5.2 Test on Separate FLVV/GVV System (Preliminary Test)

OEM initially only sent the parts for fuel tank/vapor system (details in Section 1.2). They later sent two separate FLVV/GVV systems. Even with the help of inspection camera, it was still difficult to observe the FLVV/GVV system inside the fuel tank. The location of GVV made it especially hard for the camera head to reach. Thus, some simple tests were done using the separate FLVV/GVV system.

The test setup did not include most of the EVAP lines and carbon canister, but the vacuum pump and CPV/manifold were included. This test could not fully imitate rig level conditions. On the rig level testing, there was carbon canister and filler pipe/re-circulation line which was not included in this simple test. The direct effect is the pressure: the pressure reaching FLVV (P2 in Figure 4-28); and the pressure FLVV/GVV subject under (P1 in Figure 4-28). A T joint was attached on the line connecting the CPV/manifold to the FLVV. This T-joint had an opening that was open to the atmosphere and the size of the opening could be controlled. This design was to attempt to indirectly control the vacuum level (P2) reaching the FLVV. Figure 4-32 below is the schematic of the test setup.

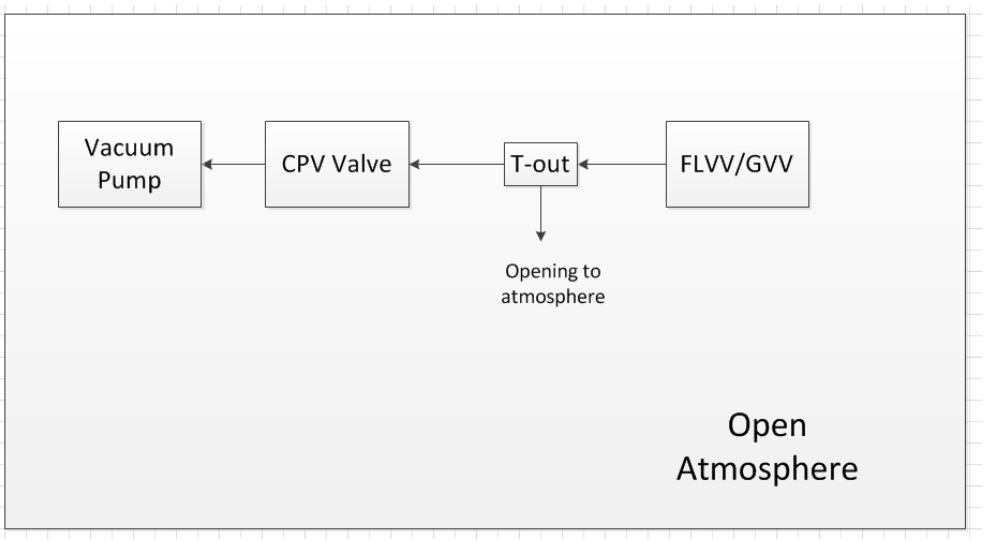

Figure 4-32: Separate FLVV/GVV test setup schematic

The same phenomenon could be observed: when the water was slightly over the bottom of the FLVV, there was no noise; when the water level reached about the side port of the FLVV, the FLVV float/satellite disc got excited, moving up and down. This up-and-down motion hit the FLVV structure and made noise. It also disturbs the water level, which could be observed through the side port of the FLVV.

4.5.3 Water Level and GVV

It was discussed in Section 4.4 about the role of GVV and the importance to understand the close/open state of FLVV and GVV inside the fuel tank. Thus, two holes were drilled close to the GVV location on top of the fuel tank. One hole was for the inspection camera head, while the other was for external lighting. The benchmark scenario (discussed in Section 3.8) was used to monitor the water level

of the GVV at different nose-down angles. It was observed that at level ground, the water level at GVV was very high, which pushed the GVV float to its top position. As the nose-down angle increased, the water line slowly receded, eventually opening up the GVV again. Figure 4-33 below shows the water level at GVV at level ground and at 7 degrees nose-down angle.

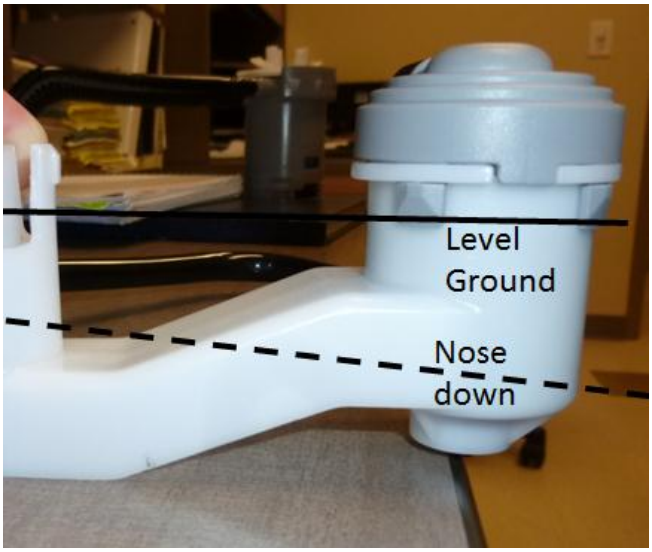

Figure 4-33: GVV water level

4.6 Applying Force on Tank Surface and Woodpecker Noise

It was observed that when there was woodpecker noise, by applying force on certain area of the tank surface, the woodpecker noise changed its "characteristics", to a point where the noise would completely disappear. This phenomenon would become more prominent as the CPV frequency increased. When the CPV frequency went higher than 25Hz, even by touching the fuel tank surface with hand would make the noise completely go away. Figure 4-34 below has two circled areas where when applying forces on these two areas, the changes in woodpecker noise were observed to be the greatest.

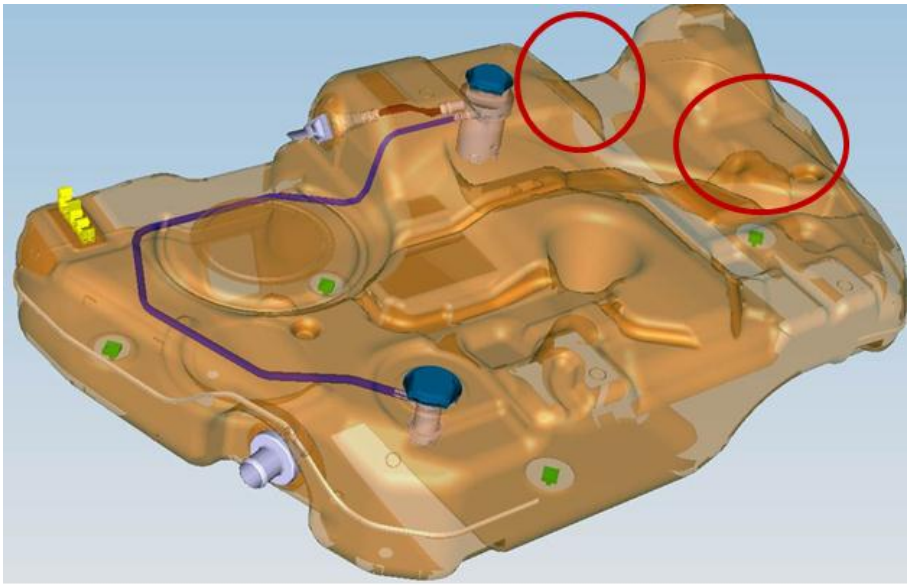

Figure 4-34: Applying force on tank surface

Chapter 5
Results and Discussion-Noise Reduction

One of the main objectives of this project is to investigate different methods/approaches to reduce or eliminate the noise. These methods/approaches can be called proposals, which is a commonly used term in the industry. Thus, this section includes all possible solutions for the woodpecker noise. Detailed descriptions of the proposal/method, and data collected to assess the effectiveness are covered.

The nature of the noise generation mechanism, as observed and discussed in Chapter 4, presented three main focuses where the noise issue may be addressed. The first is at the pressure pulsation source – CPV. If modifications can be made to the CPV so that the pressure pulsation would not be generated or reduced effectively, the noise issue can go away. The second is at the pressure pulsation transmission path – from the big vapor line all the way to the tank-to-canister line. If the pressure pulsation can be reduced or eliminated on its path before reaching FLVV, the FLVV may not get excited and create noise. And the third is at the noise source – FLVV. If the FLVV can change its behavior and become less susceptible to pressure pulsations, the noise would not occur. This was discussed in literature review summary as well.

Based on the information provided by the OEM, it was decided that the second approach, which is to focus on reducing or eliminating the pressure pulsation on its transmission path, is most feasible. This was done by process of elimination: both CPV and FLVV have intricate design specs that meet multiple design requirements. This makes changing their design extremely difficult and most likely very expensive.

Adding components on the pressure pulsation transmission path in order to reduce/eliminate the pressure pulsation is a common approach [28], [31], [32]. The pressure pulsation transmission path is through several pipes and components, giving many possible locations to add the components. However, due to configuration of the experimental setup, it was easier to add the components onto the big vapor line and to take pressure readings. The ideal place was between location 4 and 5 shown in Figure 3-2. Figure 5-1 and Figure 5-2 show the location where different components were added to test their effect on pressure pulsations.

All of the methods addressing the noise issue on the pressure pulsation transmission path had components or modifications added on the location pointed in Figure 5-1 below. The two pressure transducers were mounted at either side of the big vapor line. This configuration of the pressure

transducers enabled a direct pressure pulsation changes comparison between the upstream and the downstream.

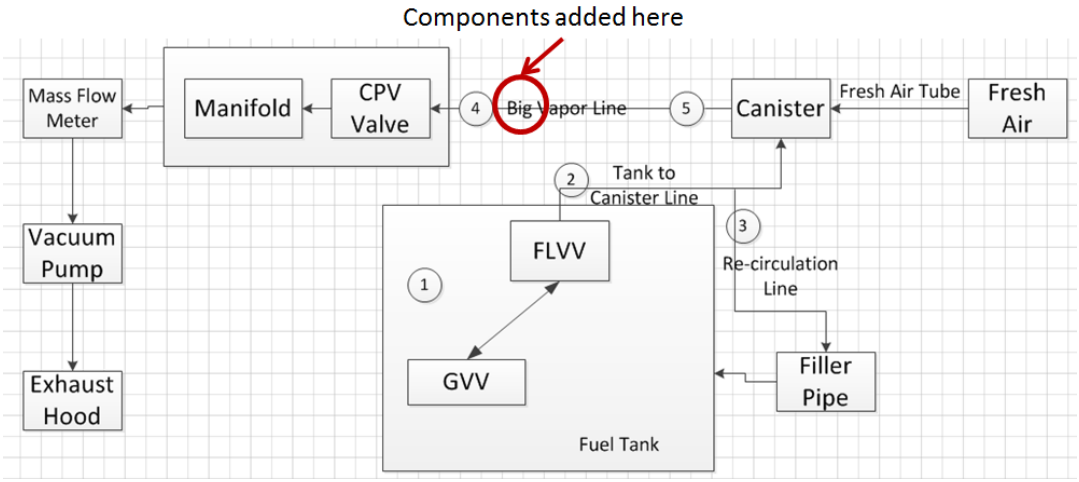

Figure 5-1: Components added on big vapor line between location 4 and 5-schematic

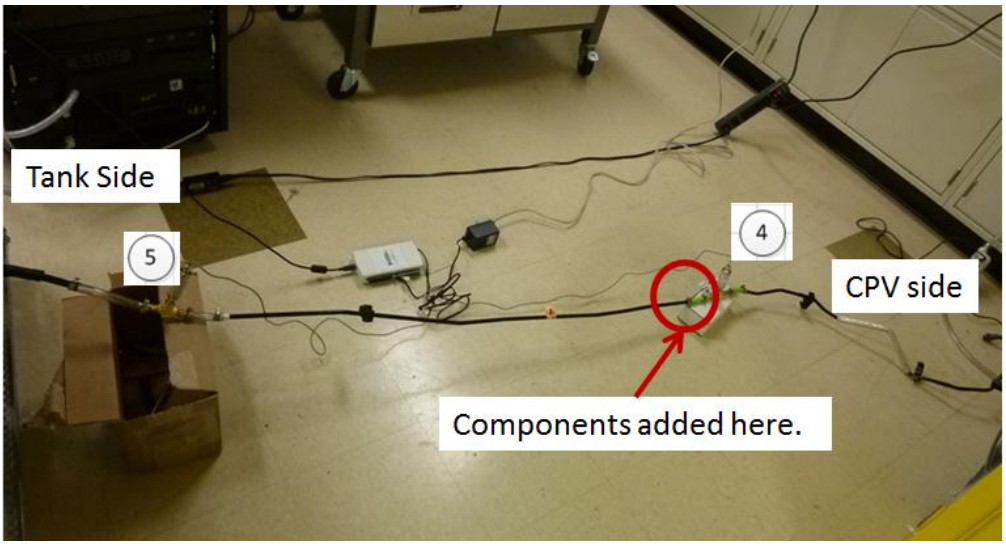

Figure 5-2: Components added on big vapor line between location 4 and 5

5.1 Method #1-Porous Material in Line

Porous material added in-line was proved to be able to reduce the pressure pulsations [40], which in term reducing/eliminating the woodpecker noise. In order to simulate porous material in the vapor line, regular steel wool was purchased and stuffed into tubing. There were in total three different configurations tried on the testing bench: 2-inch length of 3/8 inches ID tube with densely packed steel, 4-

inch length of 3/8 inches ID tube with densely packed steel, and 5-inch length, 5/8 inches ID tube with densely packed steel wool. All of these different configurations were added on the big vapor line between locations 4 and 5 as shown in Figure 5-1. Figure 5-3 below shows these three different configurations.

Figure 5-3: Left: 2-inch 3/8 ID tube; Middle: 4-inch 3/8 inch ID tube; Right: 5-inch 5/8 inches ID tube. All tubes are densely packed with steel wools

It was observed that all three configurations could effectively eliminate the woodpecker noise. Pressure readings were taken at location 5 and 4 to find the effect the porous material had on the pressure pulsations. Among the three different steel wool configurations, only the 2-inch 3/8 inch ID tube with densely packed steel wool case was studied due to time constrain. However, it is reasonable to assume that the other two cases would yield greater dampening effects on the pressure pulsations.

5.1.1 Flow Rate

It is very important to look at the flow restriction by adding the steel wool onto the big vapor line. The flow rate is crucial in terms of engine performance and severe restriction caused by the steel wool may render this option not feasible [29]. Figure 5-4 shows the flow rate at different duty cycles and compares the benchmark results with the steel wool piece added. From the figure, it shows no significant drop of the flow rate with the steel wool added. However, it should be noted that if porous material is added on the actual vehicle EVAP line, condensation may happen. This may pose other complications as the flow restriction will increase, causing variable flow rate at the same CPV duty cycle, which is highly undesirable in the vehicle design.

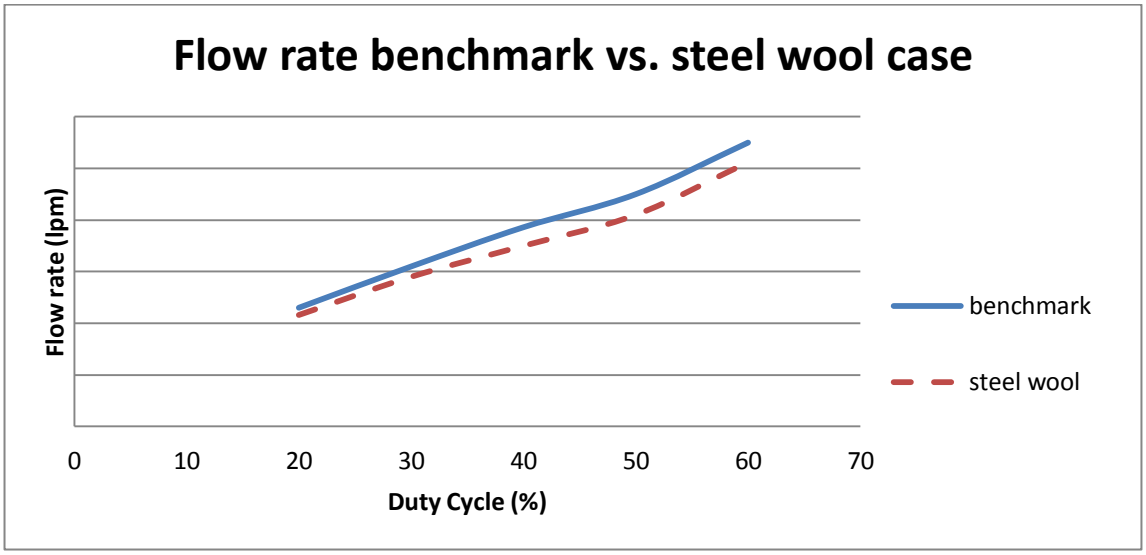

Figure 5-4: Flow rate, benchmark vs. steel wool case

5.1.2 Pressure Readings

It is important to look at the pressure readings on both time domain and frequency domain. Figure 5-5 and Figure 5-6 show the FFT plots of the pressure readings at location 4 and 5 (shown in Figure 3-2). It is clear that in frequency domain, adding steel wool virtually had no effect on the location 4 readings (Figure 5-5), which is close to CPV side. However, the steel wool greatly reduced the pulsation on location 5 (Figure 5-6), which is the side that connects to the canister and subsequently the fuel tank. Referring back to Figure 4-11, this is expected as the pressure pulsation travel direction is from location 4 to 5.

Figure 5-7 shows the pressure readings in the time domain for location 4-CPV side and 5-tank side, and compares the steel wool case readings with the readings obtained from baseline testing results. The averages and peak-to-peak values of each reading were also included in the plot. There are several observations can be made from the pressure readings in time domain:

- Adding steel wool increased the vacuum level at the CPV side (from -2.6 KPa to -4.93 KPa) while decreased the vacuum level at the tank side (from -1.45 KPa to -0.98 KPa);
- The pressure pulsation/fluctuation on CPV side did not have noticeable change (also shown in FFT plot Figure 5-5) while on tank side this decreased by about 50% in peak-to-peak fluctuation (shown in Figure 5-6 FFT plot as well).

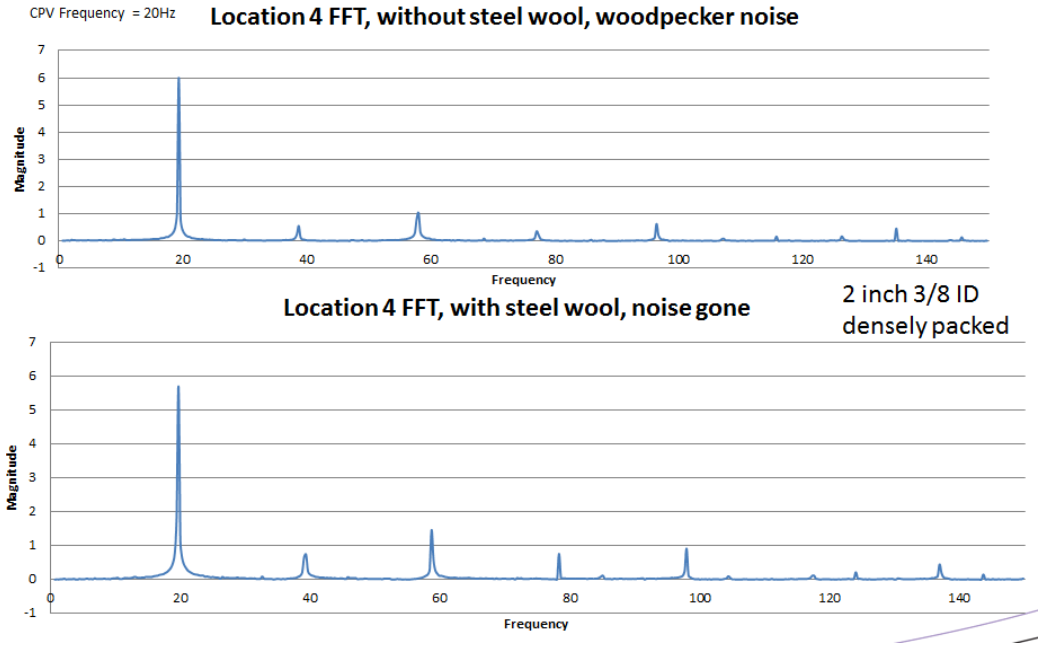

Figure 5-5: Location 4 FFT, benchmark results (top) vs. steel wool case (bottom)

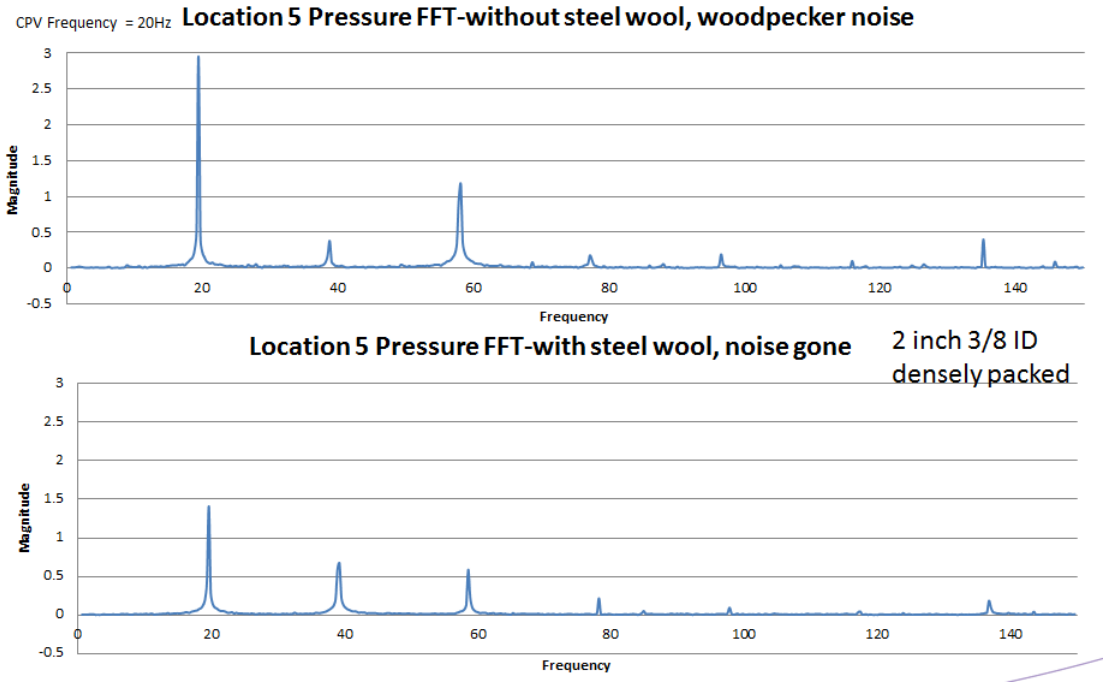

Figure 5-6: Location 5 FFT, benchmark results (top) vs. steel wool case (bottom)

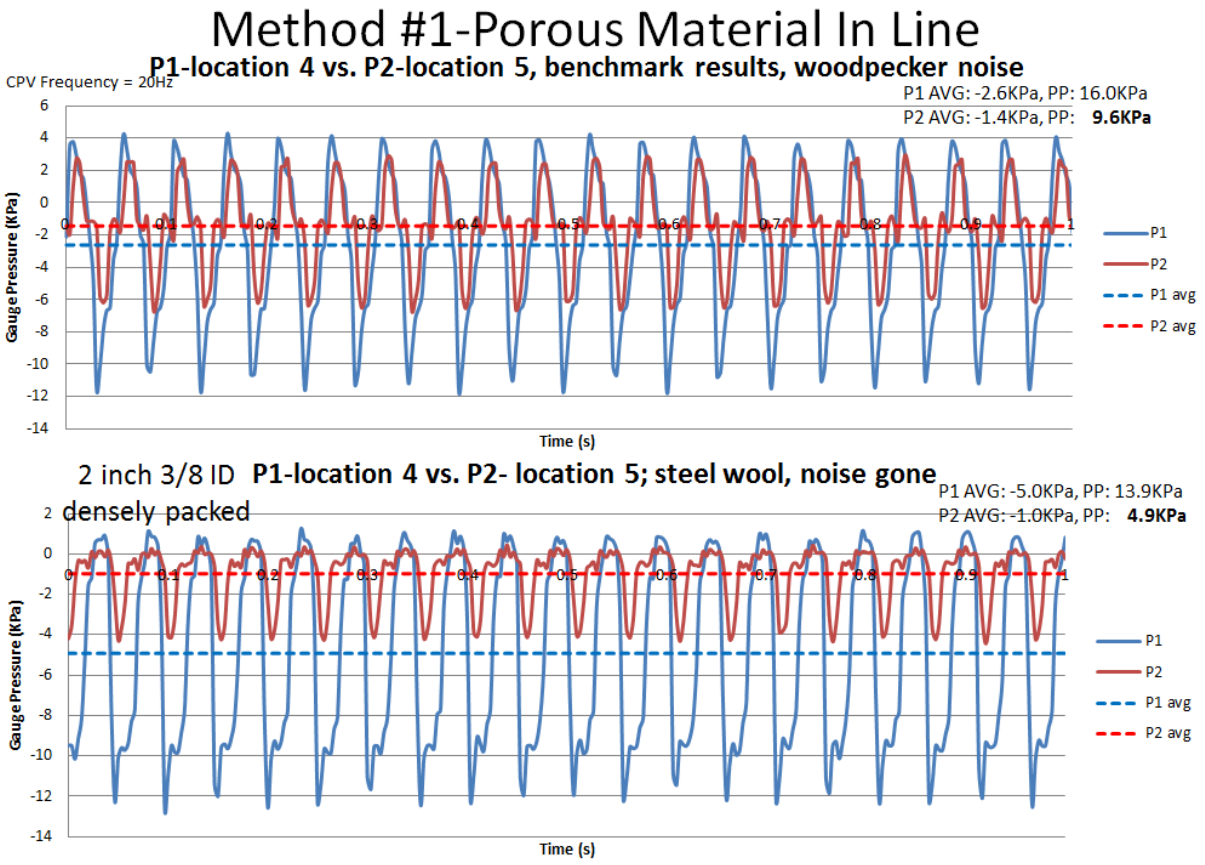

Figure 5-7: Time domain, benchmark results vs. steel wool case

5.2 Method #2-Nozzle/Orifice

Nozzle was added on the big vapor line to test if it could help reduce the pressure pulsations. The nozzle used in the preliminary test showed very promising results. The geometric dimension of the nozzle is shown in Figure 5-8. The nozzle was obtained from regular department store and was not standard parts. The theory was that restriction in the line caused by small orifice size limits sudden change in flow to pass through, effectively reduction pressure pulsations [58]. From the nozzle configuration, there were two possible orientations that this nozzle could be installed in the flow path: narrow channel (2.36mm diameter) pointing to CPV, or pointing to the tank side. Figure 5-9 shows this concept. Preliminary tests simulated both orientations and concluded that they had very similar results, thus, data from one orientation (small end pointing to the fuel tank in Figure 5-9) is presented in this report.

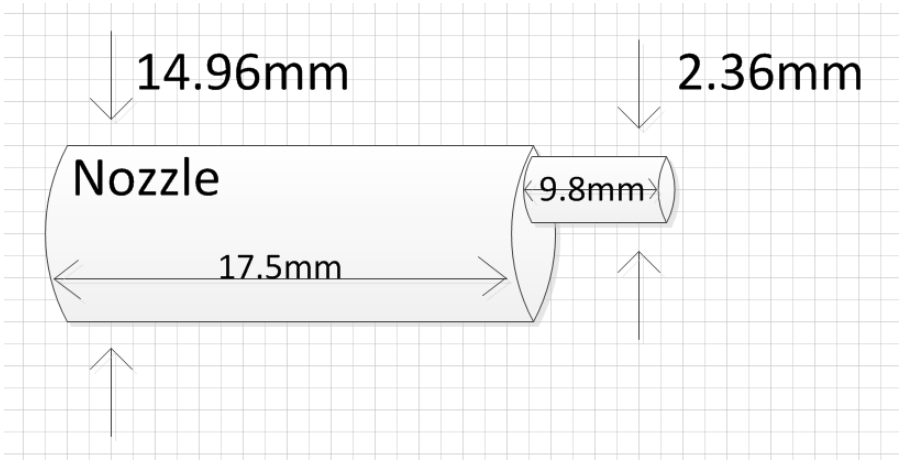

Figure 5-8: Proposal #2 Nozzle Dimension

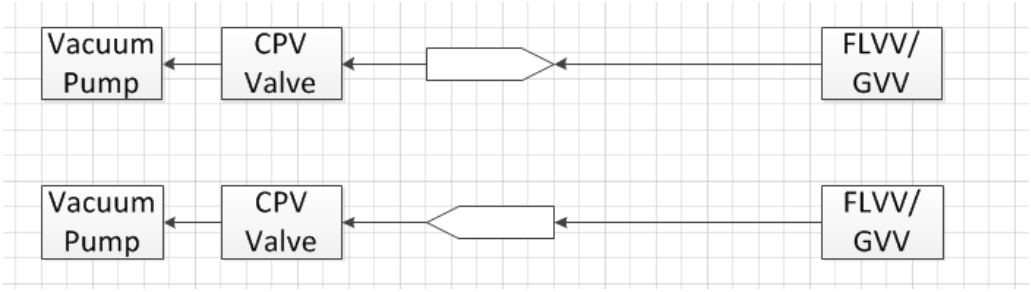

Figure 5-9: Nozzle orientation

5.2.1 Flow Rate

It was observed that adding nozzle exerted similar flow restriction effect as the steel wool (2 inch 3/8 inches ID) case. The overall reduction was about 10% of the benchmark results. The reduction percentage was calculated by averaging the reduction percentage at each duty cycle tested. Figure 5-10 shows the flow restriction with the nozzle added at different CPV duty cycle.

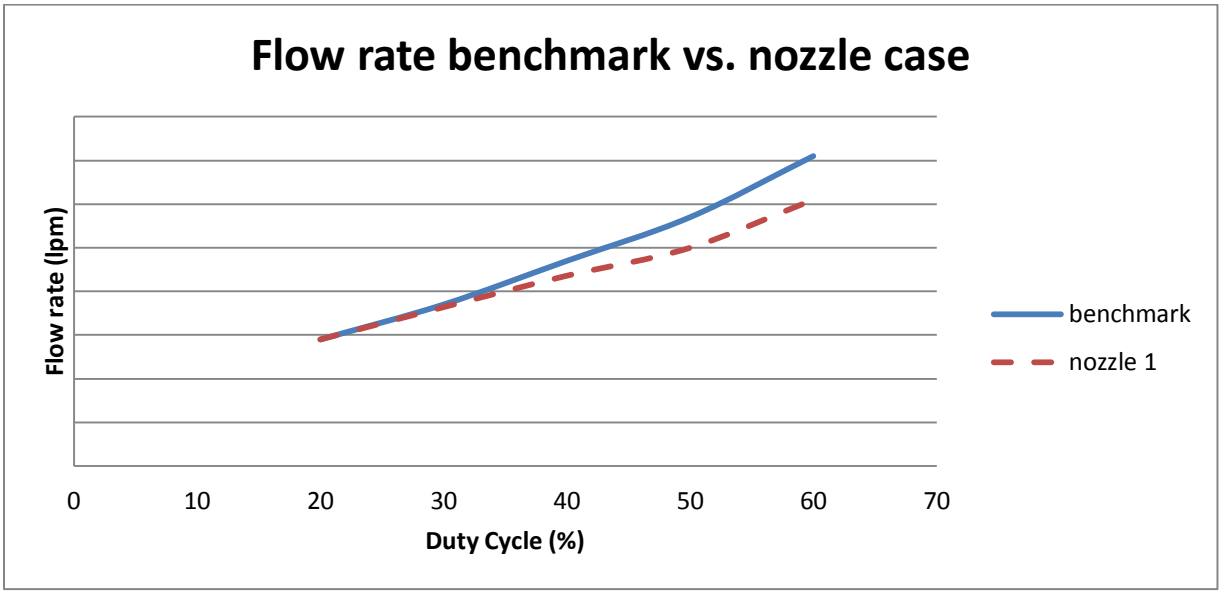

Figure 5-10: Flow rate restriction chart, nozzle case.

5.2.2 Pressure Readings

It was observed that in the frequency domain, adding nozzle in line virtually did not change the pressure on the CPV side. On the tank side, it was clear that the nozzle helped to reduce the pulsation by significant amount. This was expected, given the pressure pulsation transmission direction (details discussed in Section 4.1.2). In the time domain, the pressure readings showed that the nozzle changed both the vacuum level and fluctuation on location 4 (CPV side) and location 5 (tank side). Another observation was made: pressure readings on location 4 were reduced when nozzle was added. This change may be due to incorrect transducer response. However, it was clear that the vacuum level going to tank (location 5) was reduced. The peak-to-peak value for the pressure close to CPV did not change significantly. However, it is clear that the vacuum level on the CPV side increased by about 50% from -2.62KPa to -4.06KPa. Conversely, on the tank side, the pressure level did not change significant, with about 40% reduction in fluctuation. This reduction in vacuum level and fluctuation may contribute to the reduction/elimination of the woodpecker noise. Similar to Section 5.1, the pressure readings are presented in both frequency domain in FFT plots format (Figure 5-11 and Figure 5-12) and time domain (Figure 5-13). The benchmark results are presented in the same plots and at the same location as reference. From these figures, some observations can be made:

- At CPV side, nozzle did not change the pressure significantly in frequency domain, but the vacuum level increased, from -2.62KPa to -4.06KPa in timed average pressure reading.
- At tank side, however, the vacuum level did not have significant changes as shown in time domain.
- At tank side, adding nozzle significantly decreased the pressure fluctuation by about 40% in peak-to-peak value.

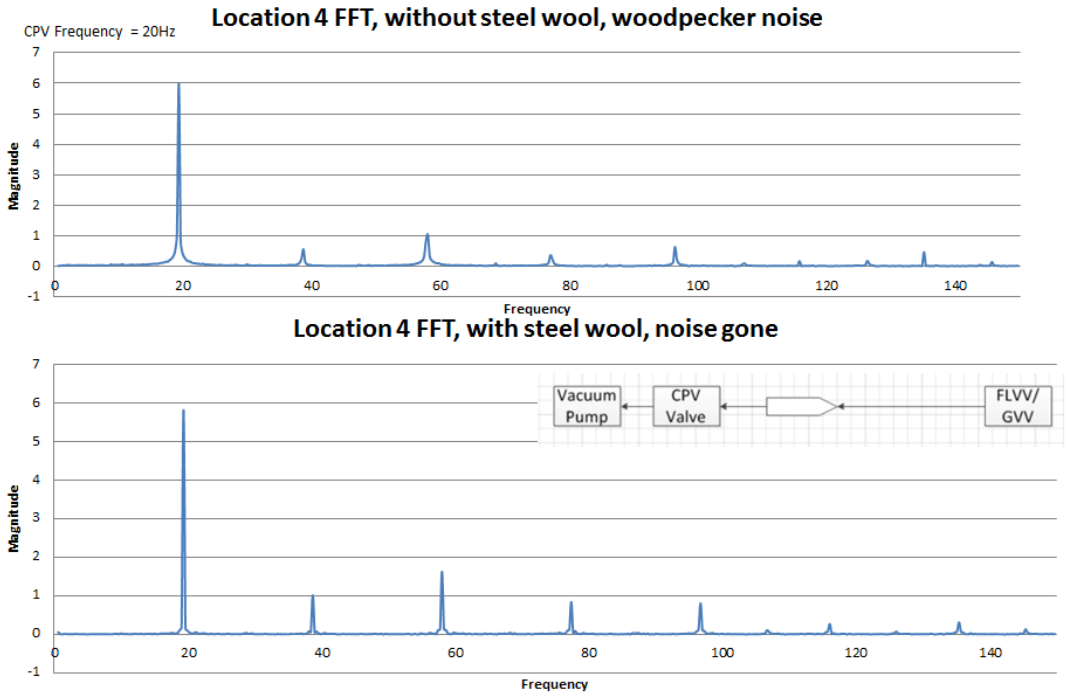

Figure 5-11: Location 4 FFT, benchmark results (top) vs. nozzle case (bottom)

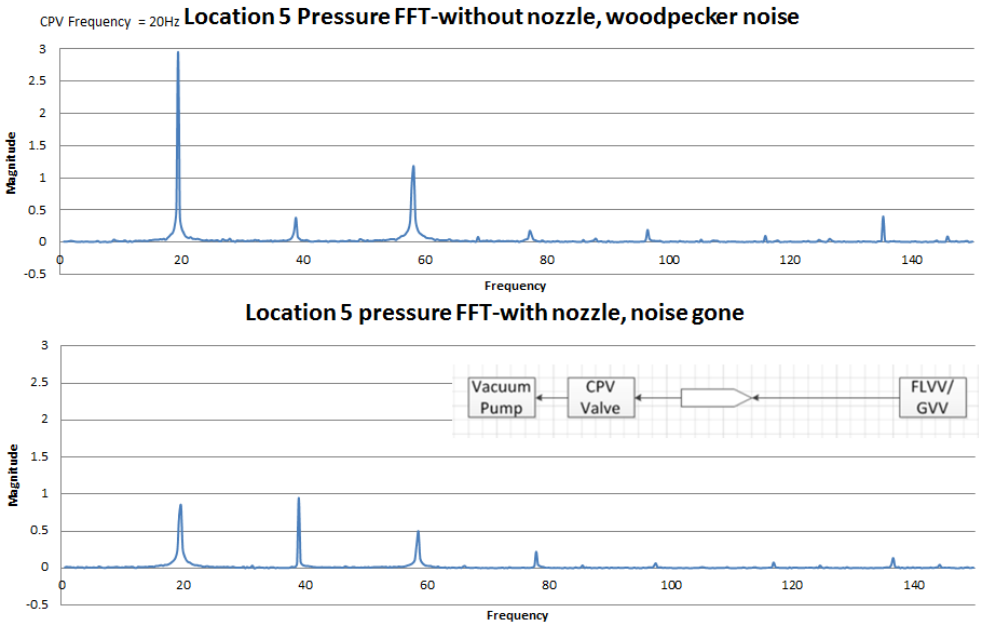

Figure 5-12: Location 5 FFT, benchmark results (top) vs. nozzle case (bottom)

Figure 5-13: Time domain, benchmark results (top) vs. nozzle case (bottom)

5.2.3 More Nozzle Testing

Since the test with non-standard-sized nozzle showed promising results, more tests were carried out using nozzles with different dimensions. There were in total 4 additional nozzles made by the student machine shop and their sizes were: 3/8 inches going into 5/16, 1/6, 3/16, and 1/8 inches. The nozzles were made from ½ inch diameter aluminum tubing. Due to the machining process that the drill bits are slightly tapered at the tips, the transition is thus slight tapered, as shown in Figure 5-14 below.

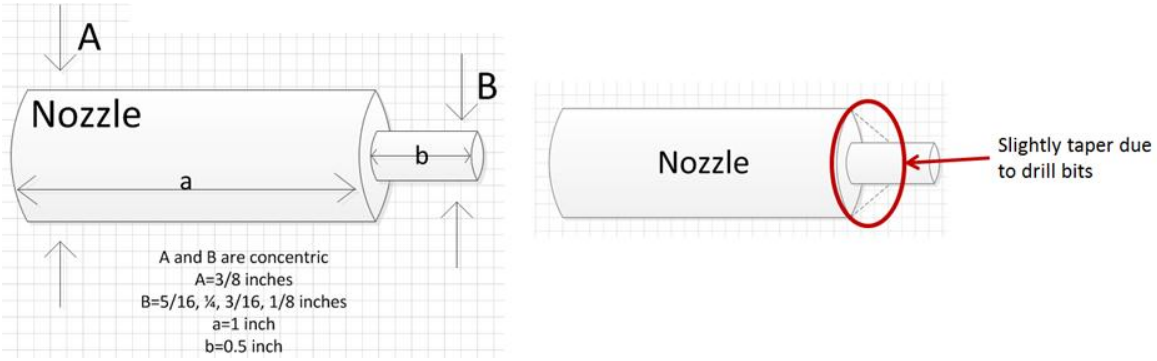

Figure 5-14: Nozzle dimensions

As with the initial test, the effect the nozzles had on the flow rate was at first investigated. At this point, a new testing methodology was devised for the flow rate. The entire testing setup included the vacuum pump connecting to CPV valve, which was driven by PWM driver, the nozzles were connected after the CPV valves and the other end directly opens to the atmosphere. Figure 5-15 below illustrates the flow rate testing setup schematics. It should be noted that the smaller end of the nozzle was pointing to the open atmosphere direction.

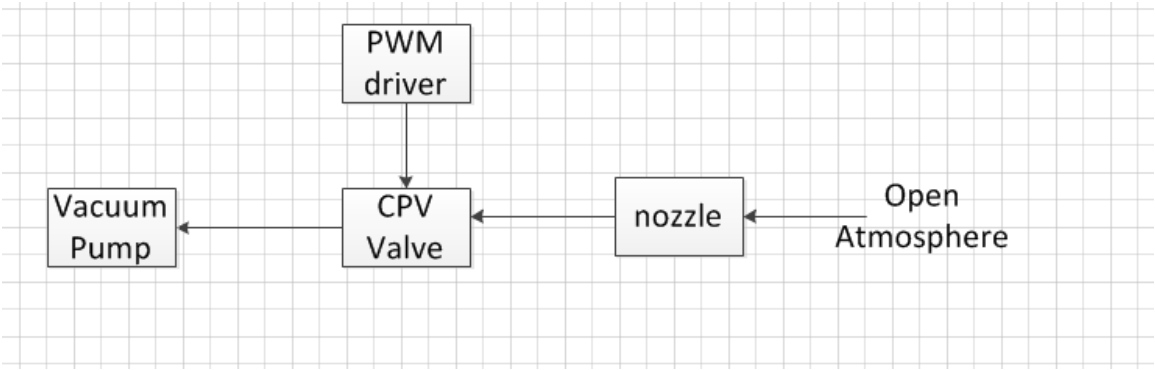

Figure 5-15: Nozzle flow rate testing setup

There were sets of tests: constant CPV frequency with changing duty cycles, and constant duty cycle with changing CPV frequencies. When CPV frequency was kept at 20Hz, the duty cycle was changed from 20 to 60 percent, which falls under the running conditions of the vacuum pump. When duty cycle was held constant at 50 percent, the CPV frequencies varied from 8.7Hz to 32.7Hz, which is the full range of frequency the PWM driver can provide. Figure 5-16 and Figure 5-17 below show the flow rate results for both cases. It is clear that the 1/8 inch nozzle had a much bigger effect on the flow rate in terms of

restrictions [58]. Based on the flow rate data, it was speculated that the 1/8 inch nozzle could better reduce the pressure pulsations.

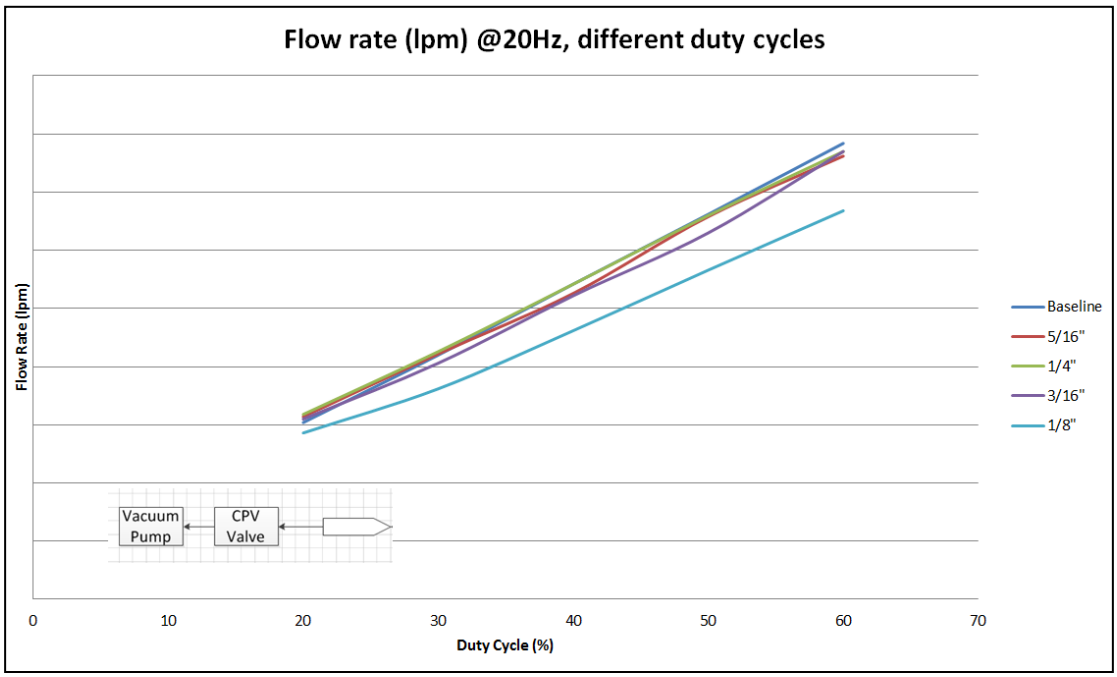

Figure 5-16: Nozzle flow rate at constant CPV frequency and changing duty cycles

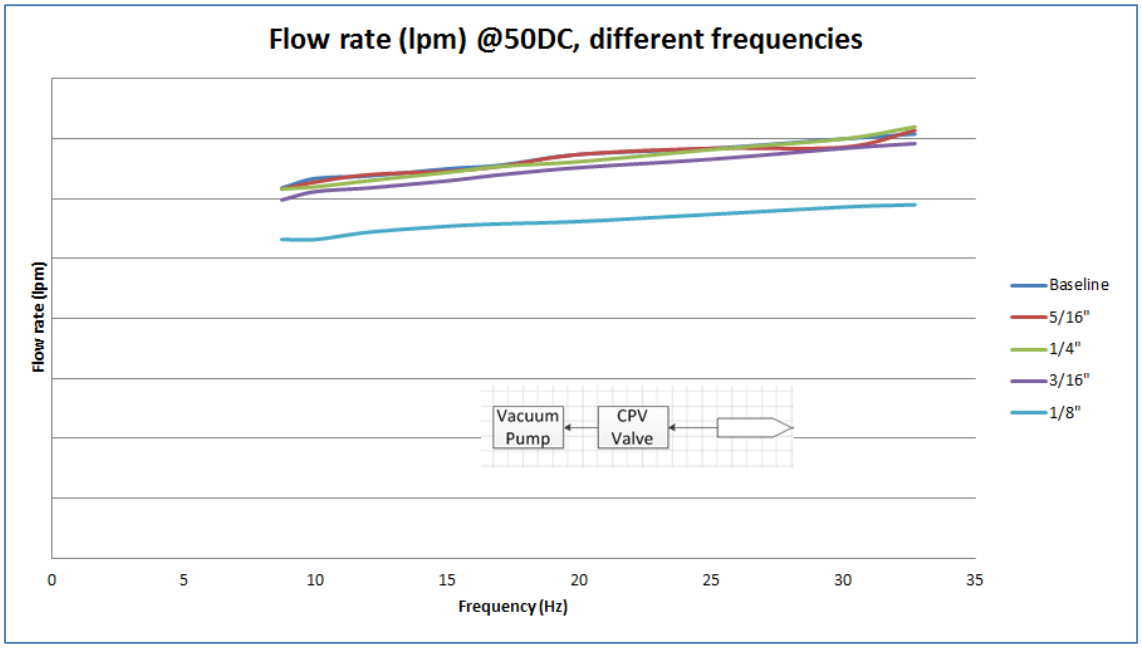

Figure 5-17: Nozzle flow rate at constant duty cycles with changing CPV frequencies

The nozzles were then installed in the system located immediately after location 4's T-joint as shown in Figure 5-1. Both configurations (illustrated in Figure 5-9) were tested for each nozzle. The results showed that only 1/8 inch nozzle was able to eliminate the woodpecker noise while all other three nozzles tested were not able to provide noticeable changes on the pressure pulsations, which in term did not help reduce the woodpecker noise. Figure 5-18 and Figure 5-19 show the pressure readings. It should be noted that the location of the pressure transducer was in the big vapor line that is close to the tank side, which is location ⑤ shown in Figure 3-2.

The observation was similar to that of the initial test using a non-standard size nozzle. The pressure change on the CPV side was not included. The pressure pulsation on the tank side was reduced by about 40% in terms of peak-to-peak value. The vacuum pressure itself was also reduced slightly from -1.772 kPa to -1.457kPa.

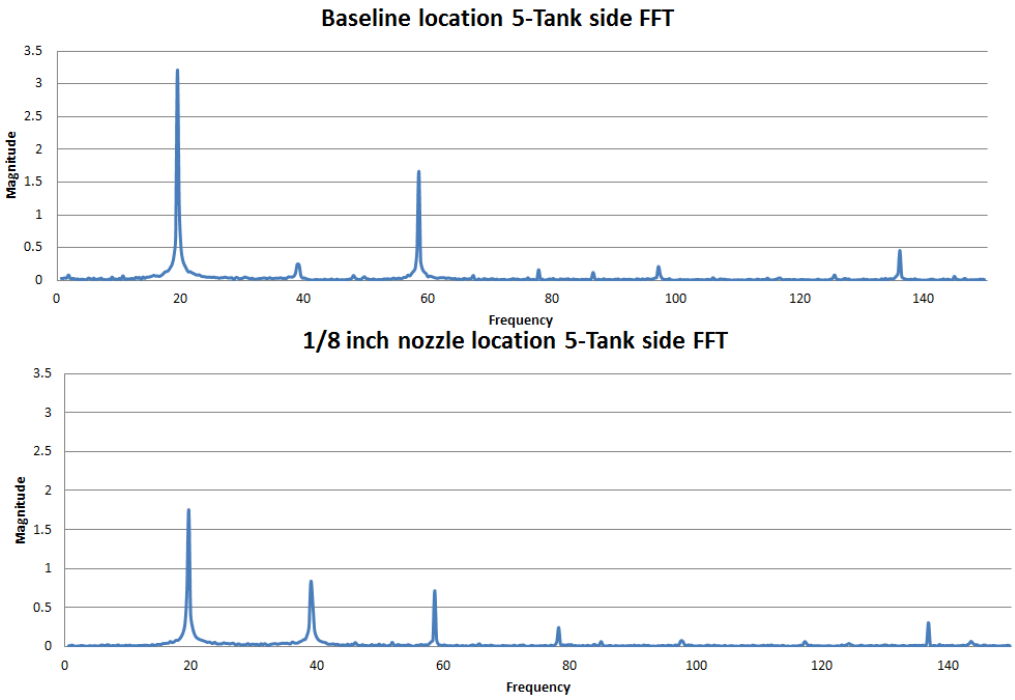

Figure 5-18: Pressure readings FFT, big vapor line close to tank side, baseline vs. 1/8 inch nozzle

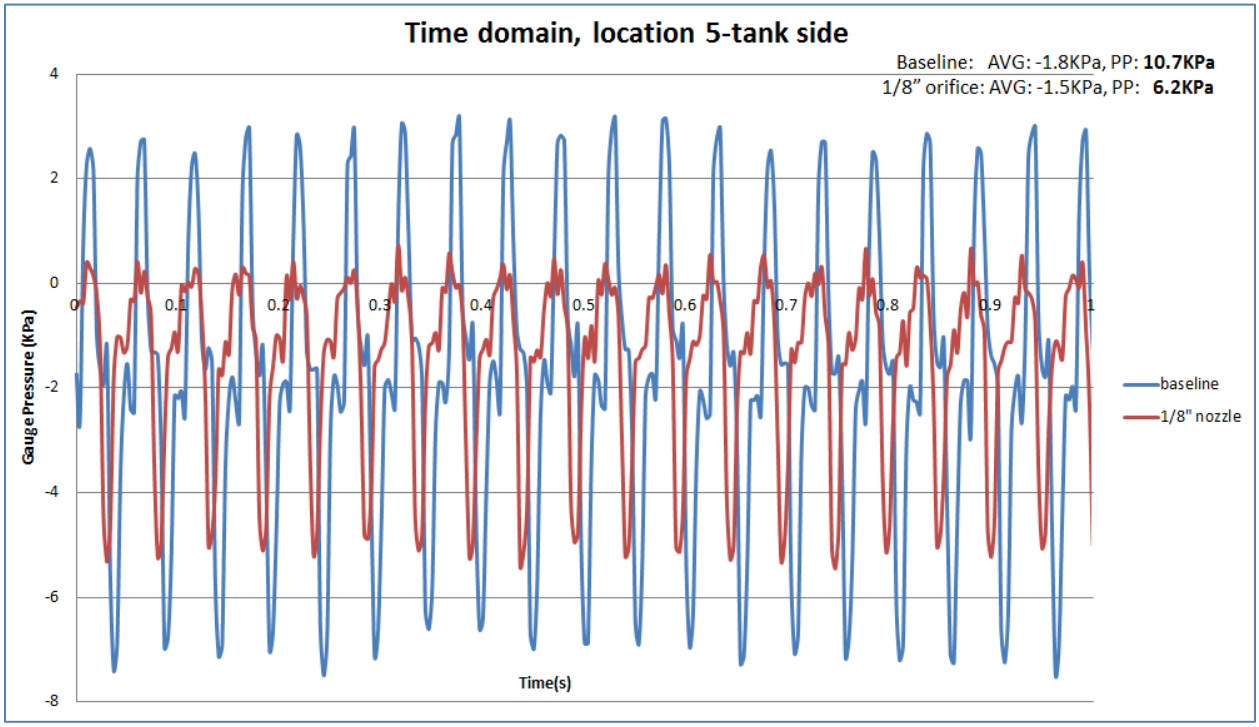

Figure 5-19: Time domain, location 5 pressure readings, baseline vs. 1/8 inch nozzle

5.3 Method #3-Changing Pipe Diameter

Mizuno et al. [31] attempted to increase the fuel rail's volume in order to achieve pulsation attenuation. Based on this, test was done to replace the big vapor line with roughly equal length pipe (7 feet) of various diameters to study the effect they had on the pressure pulsations. Three different diameter pipes were purchased, all from the same manufacture and same material (clear vinyl, manufactured by WATTS®), and their inner diameters are 5/8, 3/8, and 3/16 inches. Including the original/baseline pipe ID, the IDs from biggest to smallest are as follows: 5/8 (0.625)>3/8 (0.375)>baseline (0.31)>3/16 (0.1875).

5.3.1 Flow Rate

The flow rate was at first tested with different ID pipes attached. In order to avoid uncertainties caused by the system, the test was done with one end open to atmospheric pressure. This was discussed in details in Section 5.2.3. The results showed that different ID diameter transmitting pipe changed the flow rate considerably, with 3/16 inch ID causing flow rate drop and 3/8 and 5/8 inch ID causing flow rate to increase, as shown in Figure 5-20 below.

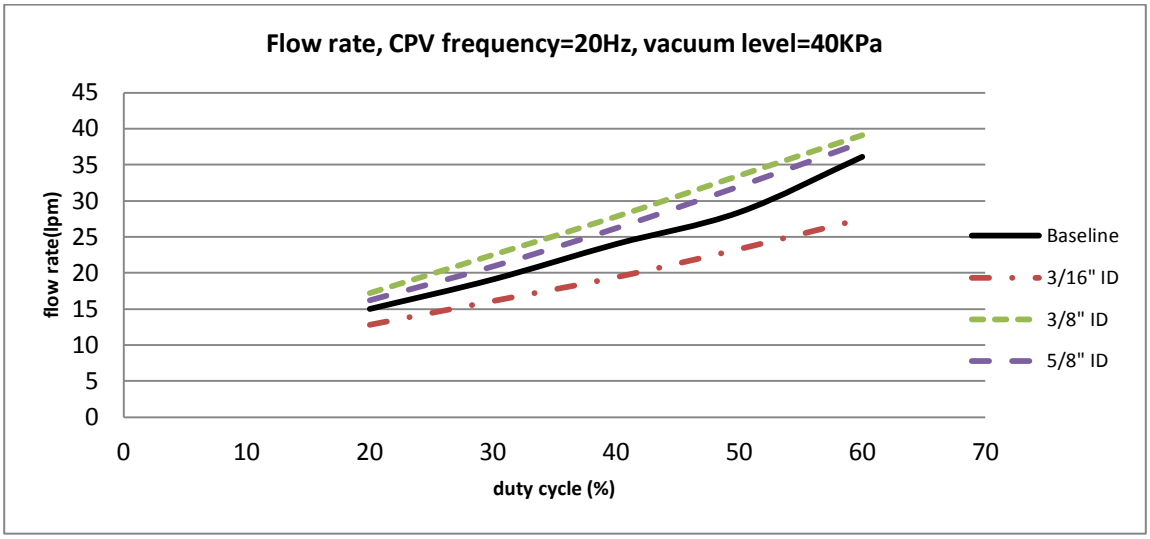

Figure 5-20: Flow rate with changing pipe IDs

5.3.2 Pressure Readings

In order to accommodate the full length of 7 feet of each testing pipe, the location ④ tee joint was moved immediately after CPV. Thus, the location ④ of the baseline was different compared with the location of varying diameter tubing. Figure 5-21 shows the experimental setup. The two pressure transducers were attached on location ④ and ⑤. Thus, it can be shown that not the entire big vapor line was replaced, only the portion between CPV and location ⑤ was replaced by different ID pipes. The flow rate was kept constant instead of duty cycle, making the comparison more accurate. Constant flow rate was achieved by adjusting CPV duty cycles. As a result, the pressure readings shown in this section were taken at the same volumetric flow rate with different CPV duty cycles.

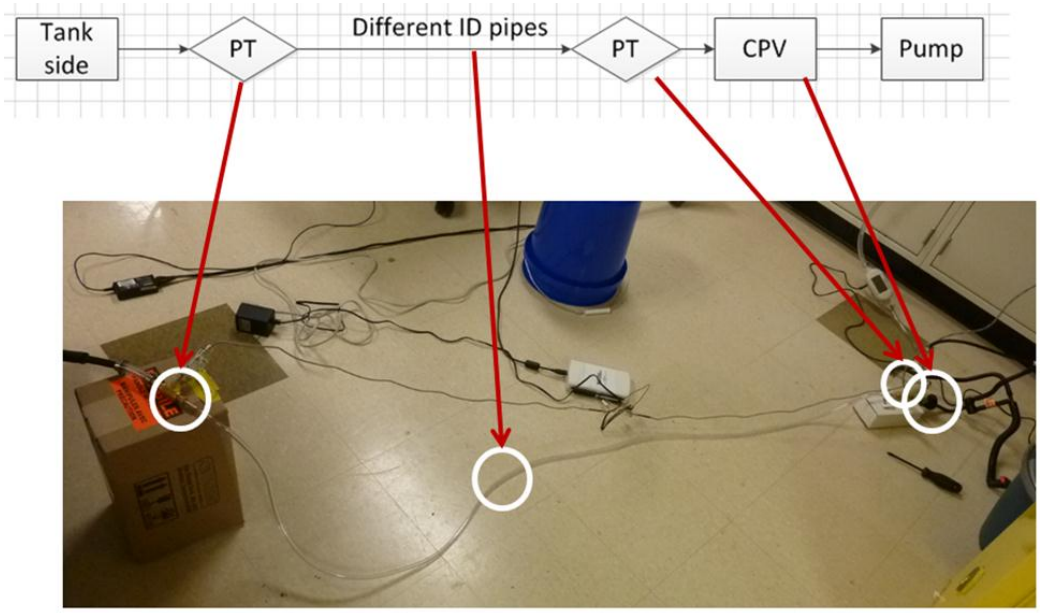

Figure 5-21: Different ID pipes connected onto the system

It was noticed that under the same conditions: 15.5 gallon water, CPV frequency 20Hz, same flow rate (15, 20, 25, 30 liters per minute), and 4.5 degree nose-down angle, baseline and 3/8 inch pipe would generate woodpecker noise, while 3/16 and 5/8 inch would not have woodpecker noise. This report only presents the time domain data in tabulated table formats shown in Table 5-1. Because it is the pressure going into the tank/FLVV that is the concern in this study, Figure 5-22 is also included. From this figure, it is clear to understand why 5/8 and 3/16 inch ID pipes can eliminate the woodpecker noise.

Table 5-1: Pressure reading averages and peak-to-peak values (PP) with varying ID pipes

5/8" 30lpm, no noise			**baseline 30lpm, woodpecker noise**		
	Tank Side	CPV Side		Tank Side	CPV Side
AVG(Kpa)	-1.6	-2.4	AVG(Kpa)	-1.6	-3.1
PP(Kpa)	**5.9**	7.9	PP(Kpa)	**10.5**	16.8
3/8" 30lpm, woodpecker noise			**3/16" 30lpm, no noise**		
	Tank Side	CPV Side		Tank Side	CPV Side
AVG(Kpa)	-1.7	-2.8	AVG(Kpa)	-1.3	-17.8
PP(Kpa)	**11.8**	17.2	PP(Kpa)	**3.6**	21.9

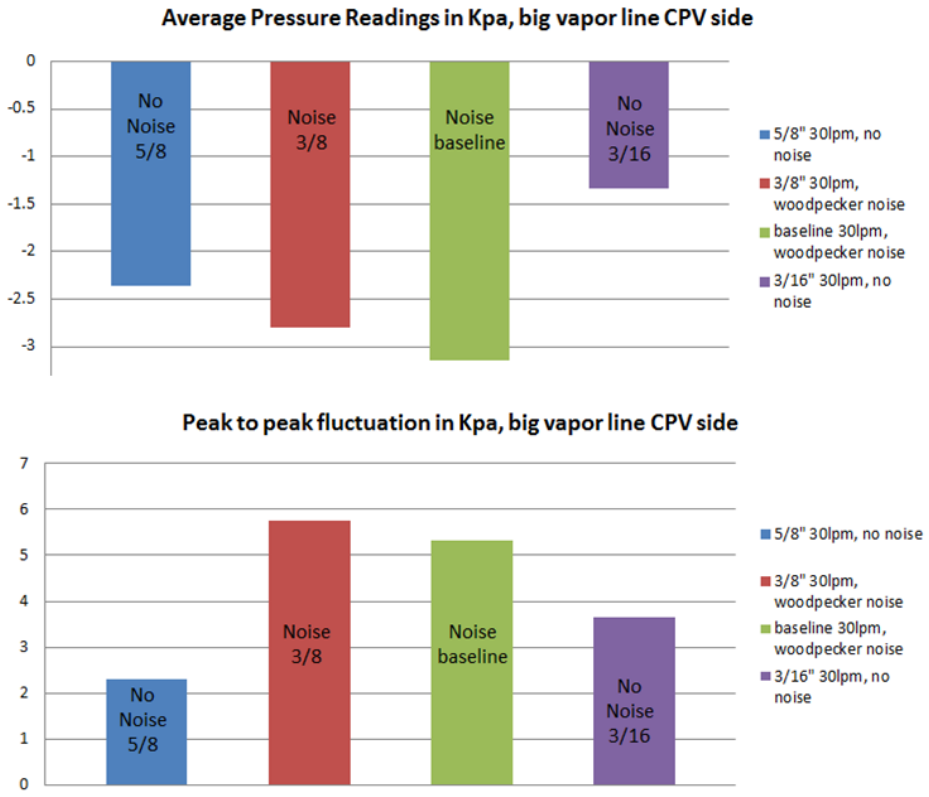

Figure 5-22: Pressure readings averages and peak-to-peak values, on the tank side

5.4 Method #4-Convolute Piping

A combination of increasing the volume and change of the aspect ratio may provide favorable results on pressure pulsation attenuation [31], [57]. Based on this belief, a quick test utilizing a corrugated discharge hose purchased from home hardware store was done. The dimension of the hose is 7 feet long and 5/8 inches ID. With the full length hose attached replacing the part of the big vapor pipe between location ④ and ⑤, the pressure pulsation was reduced significantly. Figure 5-23 below illustrates the corrugated hose was attached to replace part of the big vapor line. It was observed that the convolute pipe did not create flow rate restrictions. Similar to the 5/8" ID smooth pipe, the 5/8" ID convolute pipe provided higher flow rate. The hose not only decreased the pressure pulsation on the tank side, it decreased the pressure pulsation on the CPV side.

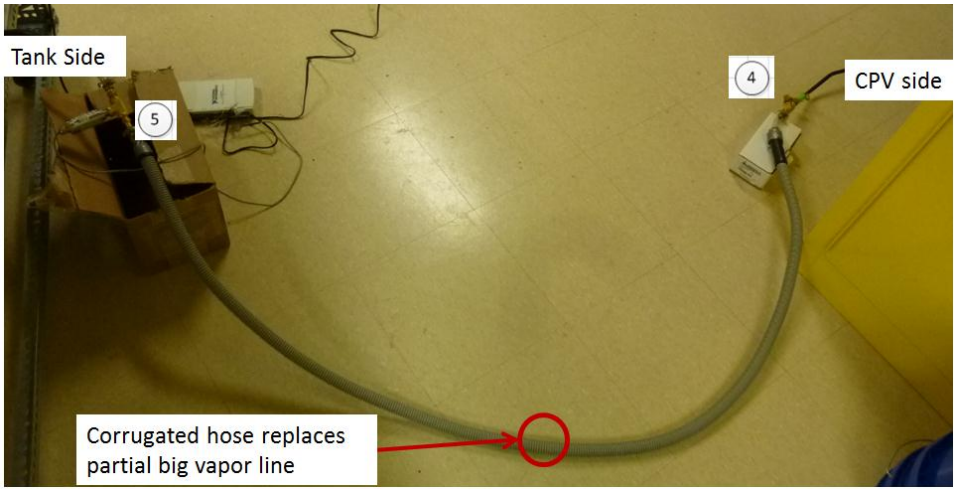

Figure 5-23: Corrugated hose attached to replace portion of the big vapor line

5.4.1 Pressure Readings

Figure 5-24 and Figure 5-25 show that the pressure FFT comparison between the convolute pipe and the baseline results. It is clear that the convolute pipe helped to equalize the pressure on both ends. Figure 5-26 presents data in time domain which can better illustrate the effect the convolute pipe had on the pressure. The pressure curve of CPV side and tank side were "brought" closer. Both the pressure averages and the peak-to-peak values were very similar when convolute pipe was attached. The peak-to-peak fluctuation decreased significantly at the CPV side, from 15.97kPa down to 5.126kPa.

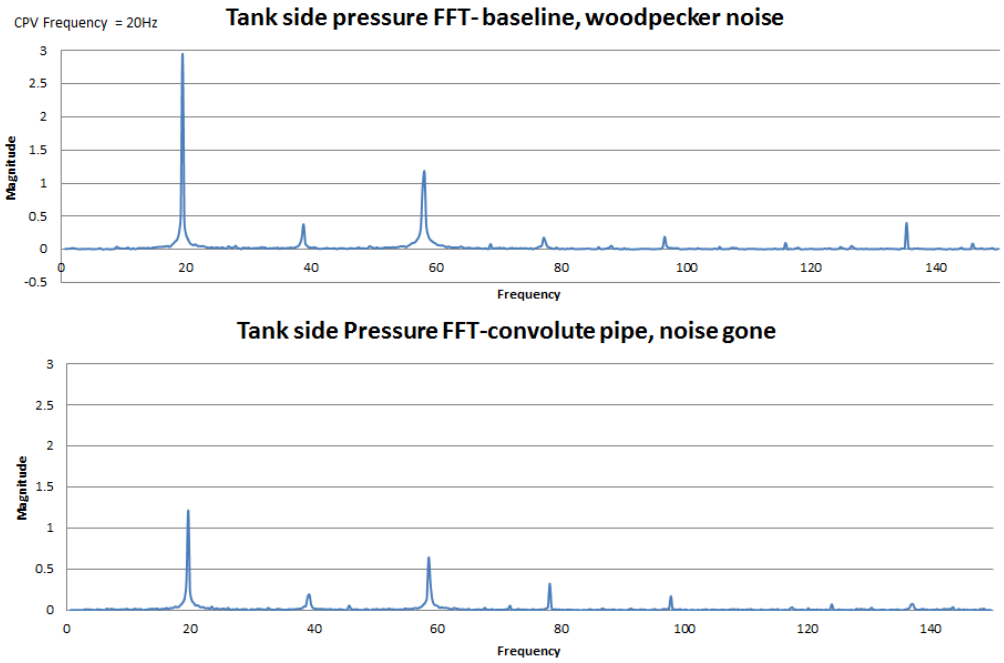

Figure 5-24: Pressure reading FFT, convolute pipe vs. baseline, big vapor line tank side

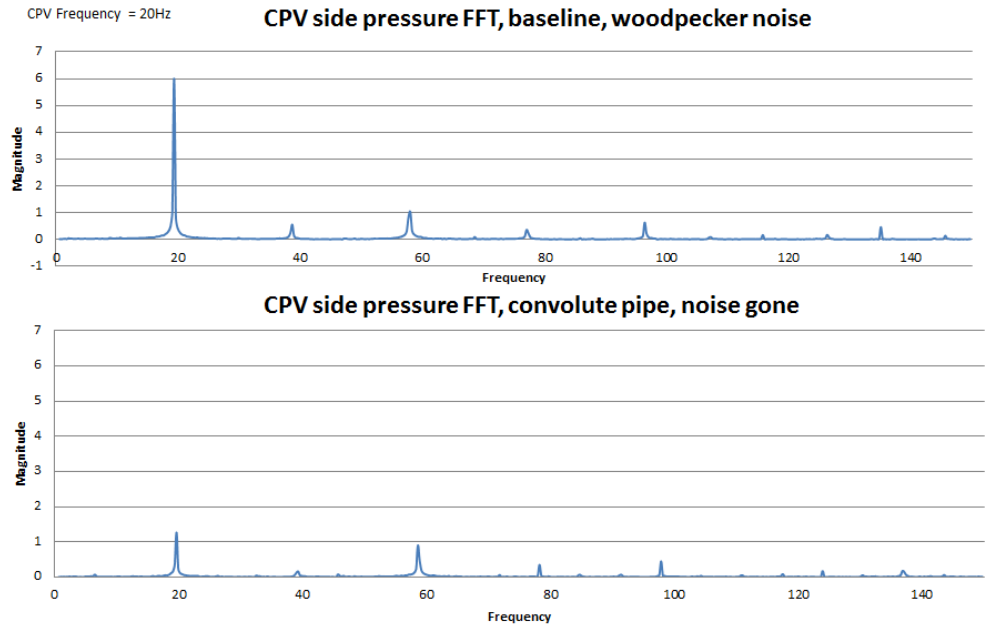

Figure 5-25: Pressure reading FFT, convolute pipe vs. baseline, big vapor line CPV side

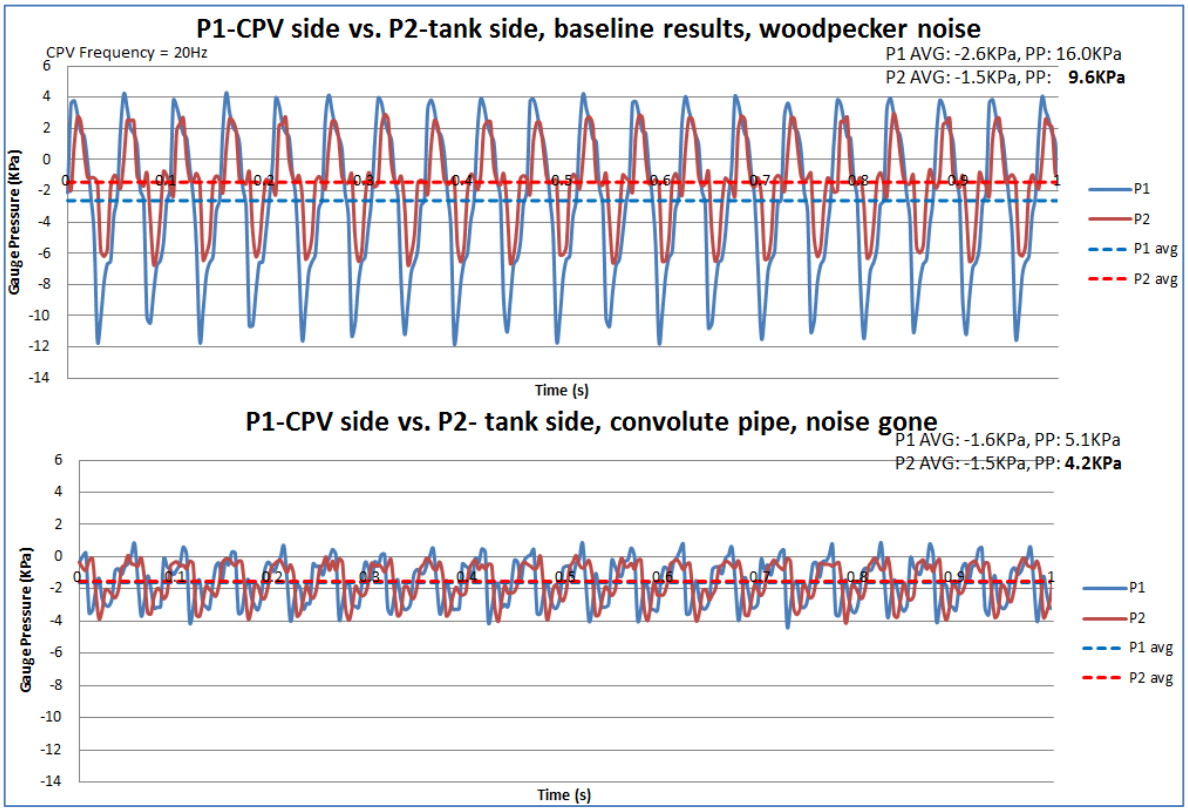

Figure 5-26: Pressure reading, time domain, convoluted pipe vs. baseline

The full 72 inches (6 feet) convolute pipe was cut into smaller pieces to test what was the minimum length for the pressure pulsation to be sufficiently reduced to eliminate the woodpecker noise. The convolute pipe was subsequently cut into 36, 18, 9, and two 4.5-inch pieces to be tested. The preliminary results showed that at 18-inch length, the convolute pipe would be able to dampen enough pressure pulsation to eliminate the woodpecker noise.

5.5 Method #5-Pulsation Damper (Empty Chamber)

The OEM provided a small chamber that was from a production vehicle assembly by a different OEM (Figure 5-27). This small chamber was tested on the test setup, adding the chamber onto the location specified in Figure 5-2. The test results showed that the woodpecker noise was completely eliminated. Another benefit of adding chamber was that it did not affect the flow rate.

Figure 5-27: Small chamber provided by OEM for testing

It was determined that the flow rate was not affected by adding the small chamber. Thus, the focus was shifted to the pressure reading analysis. Pressure readings were recorded on three different locations, shown in Figure 5-28. The pressure readings obtained showed that the pressure pulsation was greatly reduced, eliminating the woodpecker noise. Both flow orientations were tested (from A to B, or from B to A) to investigate if there was any difference in pressure reduction effect. It was noticed that both connection scheme would eliminate the noise completely with small difference in pressure pulsation attenuation.

5.5.1 Pressure Readings

Figure 5-29 and Figure 5-30 show that pressure reading FFTs at the big vapor line tank side location and tank-to-canister line (④ and ② respectively as shown in Figure 5-28 below). To make convention easier, Port A was named “short port” as it had a shorter piece of connection tube, while Port B was named “long port”. When the pressure pulsation reaches the tank side of the big vapor line, it is already reduced significantly. It was clearly shown that there were no noticeable differences in the FFT plots for the pressure readings on the tank-to-canister line when there was woodpecker noise and when the woodpecker noise was eliminated.

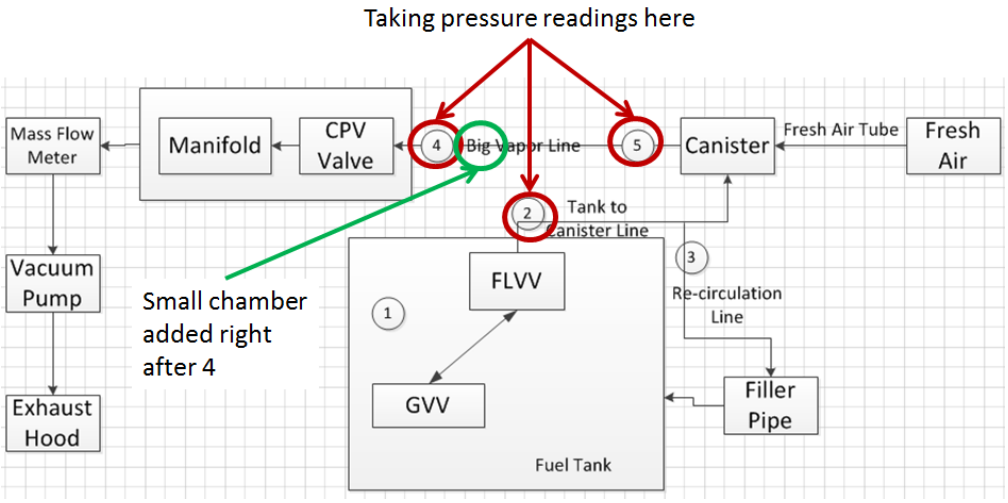

Figure 5-28: Small chamber testing setup

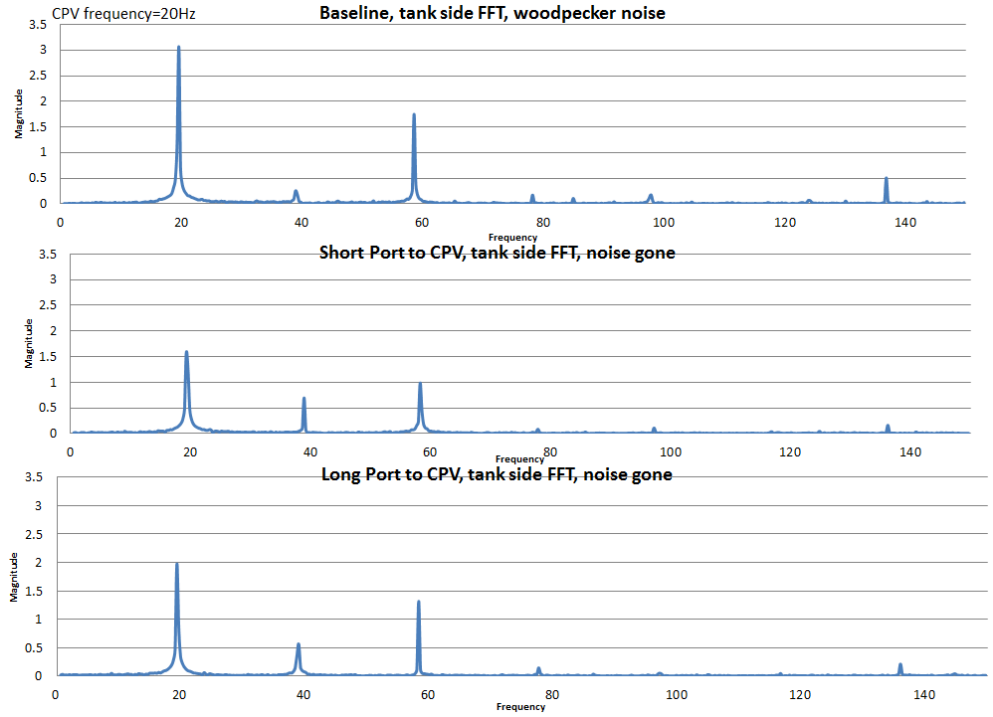

Figure 5-29: Pressure FFT, tank side, baseline vs. small chamber

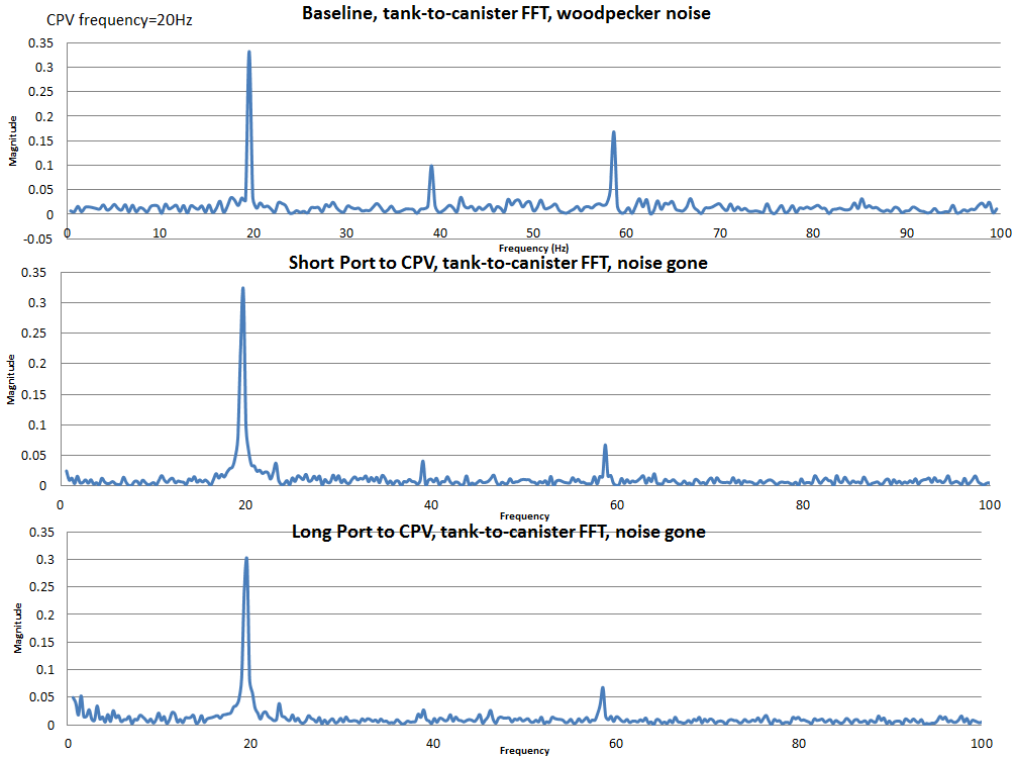

Figure 5-30: Pressure FFT, tank-to-canister line, baseline vs. small chamber

In the time domain, the pressure fluctuations were greatly reduced when chamber was attached in line compared with the baseline situation. Table 5-2 shows the pressure readings in the time domain. It was clear that the pressure damping effect was better when the short port connected to the CPV compared to the long port connected to the CPV. However, the design specs of this chamber and the science behind them were not fully understood at this point [28].

Table 5-2: Time domain pressure readings comparison

Baseline		
	Tank Side	CPV Side
PP(Kpa)	**10.3**	16.3
AVG(Kpa)	-1.6	-2.9
Short Port to CPV		
	Tank Side	CPV Side
PP(Kpa)	**6.7**	11.9
AVG(Kpa)	-1.4	-3.6
Long Port to CPV		
	Tank Side	CPV Side
PP(Kpa)	**7.2**	11.9
AVG(Kpa)	-1.5	-3.7

5.6 FLVV Casing Modifications

Two thoughts were proposed to modify the FLVV casing. First was to have small openings on the top portion of the FLVV case. This is based on the pressure balancing concept discussed in Section 4.1.3. Second approach was to extend the FLVV outside casing so that the water column beneath the float could provide damping effect, preventing FLVV float from moving up and down. The water level in FLVV was discussed in Section 4.5.1. The water level on FLVV is not very high but it can provide enough buoyancy force to lift the float at the position where it can be caught by the pressure pulsation, causing woodpecker noise. When the float is moving up and down, it hits the water beneath and the FLVV structure. The two approaches mentioned above both modify the FLVV so that this float excitation can be reduced or avoided.

Based on the first idea mentioned above, the separate FLVV (next generation design) was modified such that there are smaller holes on the side of the FLVV shell to allow flow to pass and also to create pressure balance across the FLVV float. Preliminary testing results showed that when four upper holes (7/64 inch diameter) were opened, the FLVV float would become effectively "immune" to the pressure pulsation and would not move up and down. It should be noted that this test was only carried on the individual valve level. Figure 5-31 below can show this concept more clearly.

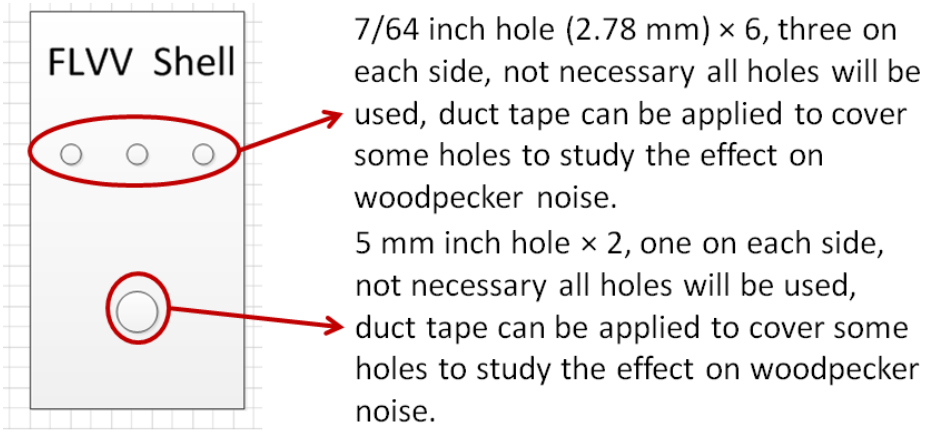

Figure 5-31: FLVV modified, small holes drilled on the both side

For the second thoughts, various parts were added on the bottom part of the FLVV as extension to test if it would help enhance the damping effect of the FLVV float movement (shown in Figure 5-32 below). However, preliminary testing results were not promising. Thus this option was not further explored. The preliminary testing utilized readily available parts instead of the parts shown in Figure 5-32.

Figure 5-32: FLVV extension for damping

However, after consulting with the OEM, it was determined that modifying FLVV could have big implications. It was thus dropped as a feasible option at this stage. Nevertheless, it is worthwhile to include this concept and present the test results in the report for potential future review. This proposal is also included in the final conclusions and recommendations.

5.7 CPV Modifications

The scope of this project initially excluded the possibilities of any modifications done on the CPV, for the same reason with the FLVV modification. The CPV has a very dedicated design meeting different functional specs. As a result, changes were very constrained. For example, it will cause big complication on the vehicle calibration if the CPV operating frequency changes. The current calibration parameter for CPV frequency is 20Hz or 17Hz, depending on the model specs.

Towards the final phase of the project, the OEM decided to explore the possibility of modifying the CPV design for different purposes. Springs with different stiffness on the CPV were tested in an attempt to resolve CPV durability issue. The OEM was very interested to see if such design changes would have some effects, if any, on the woodpecker noise issue. The OEM provided two CPV prototypes with stiffer springs to be tested on the existing rig. The two CPV prototypes obtained from the OEM has 1.5N and 2.0N spring constants respectively with the baseline CPV design having 1.0N spring stiffness. The two CPV prototypes are shown in Figure 5-33.

Figure 5-33: CPV prototypes, 1.5N and 2.0N

5.7.1 Flow Rate

Following the same testing procedures, the change on the flow rate was investigated at first. In order to eliminate other effects, the stand-alone flow rate testing methodology was utilized. The results showed that the 1.5N CPV prototype had very similar flow rate compared with the baseline CPV design, while the 2.0N CPV prototype caused restrictions in the flow.

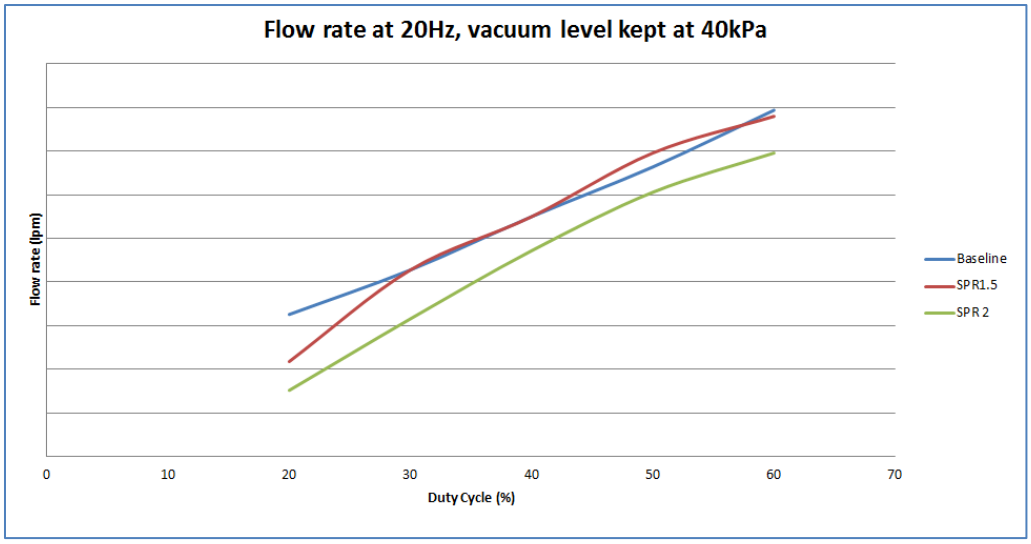

Figure 5-34: Flow rate for different CPV prototypes, constant CPV frequency, and different duty cycles

Another interesting observation was made when testing the flow rate under different CPV frequencies while keeping the duty cycle constant. The results are shown in Figure 5-35 below. It is counter-intuitive that the 2.0N spring constant CPV prototype yields a decreasing trend in flow rate at increasing CPV frequencies. One possible explanation for this phenomenon might be that due to higher spring stiffness, the CPV opening mechanism became less "sensitive" to the CPV driving frequency. By deduction, the slight drop of flow rate in 1.5N CPV prototype compared with the baseline could be explained as well.

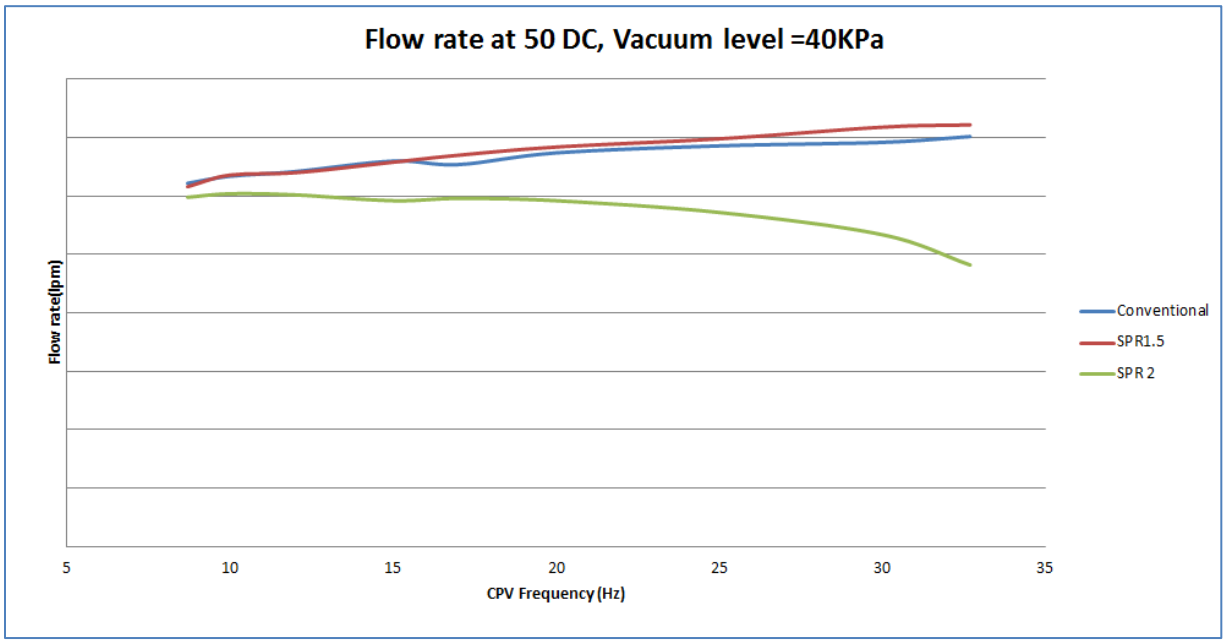

Figure 5-35: Flow rate for different CPV prototypes, constant duty cycle, and different CPV frequencies.

5.7.2 Woodpecker Noise

Testing results showed that woodpecker noise still persisted while the two CPV prototypes were installed onto the system to replace the baseline CPV. However, it was found that the number of occurrences of woodpecker noise became less. In other words, the woodpecker noise occurred at narrower operational conditions with increasing spring stiffness. Figure 5-36 showed the results. It is clear that 2.0N CPV has a smaller range for the woodpecker noise to occur. The system running condition is the baseline condition.

Baseline CPV Design with 1.0N Spring

CPV Duty Cycle (%)	CPV Frequency (Hz) 8.7	10	12	15	17	20	25	30	32.7
20									
30									
40									
50									
60									

SPR1.5 CPV Design with 1.5N Spring

CPV Duty Cycle (%)	CPV Frequency (Hz) 8.7	10	12	15	17	20	25	30	32.7
20									
30									
40									
50									
60									

SPR2.0 CPV Design with 2.0N Spring

CPV Duty Cycle (%)	CPV Frequency (Hz) 8.7	10	12	15	17	20	25	30	32.7
20									
30									
40									
50									
60									

	Blank Not Tested
	Tested but no woodpecker noise
	Tested with woodpecker noise

Figure 5-36: Operation conditions that woodpecker noise occurred at different CPVs

The CPV prototypes had an L-shaped design, which was different from the baseline CPV's "straight line" design. It was thus speculated that the L-shaped may contribute to the reduction of the woodpecker noise [31]. The pressure pulsations are being projected from the CPV and being sent to the rest of the EVAP system. In the case of the CPV prototype L-shaped design the pressure pulsations hit the flat wall first, thus the pressure pulsations decrease in magnitude compared with the baseline CPV straight-line design which has nothing standing in the way of the pressure pulsation transmission path.

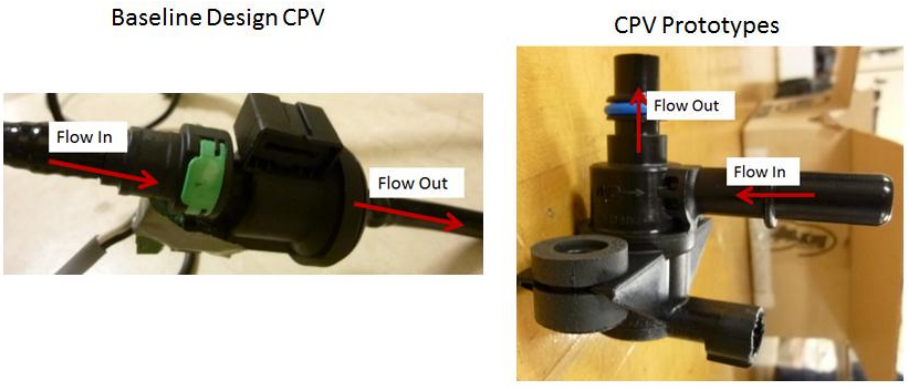

Figure 5-37: Baseline vs. prototype CPVs design difference

The pressure readings taken at location 4, which was on the big vapor line close to the CPV side, are shown in Table 5-3. It is clear that both of the CPV prototypes caused decrease in system vacuum level

from -3.02kPa to -2.6kPa. More importantly, the peak-to-peak fluctuation were reduced when CPV prototypes were used compared with the baseline CPV. The reduction in pulsation was over 22%. This percentage reduction was apparently not enough to completely eliminate the noise. However, it does show that the CPV prototypes were beneficial in terms of pressure pulsation attenuation.

Table 5-3: Pressure comparison, CPV modifications, located at big vapor line CPV side

	Baseline	SPR1.5	SPR2.0
AVG(kPa)	-3.0	-2.7	-2.6
PP(kPa)	16.1	12.4	12.4

5.8 Modifications Added on Tank-to-Canister Line

Previous studies did not discuss where to install the pressure pulsation attenuation devices in the system. Mizuno et al. [31] explained that the pressure pulsation damper was installed at the inlet of the fuel rail, which is the pressure pulsation source. Later researchers followed the same pattern without going into details to explore the effect of location change [24], [28], [32], [39], [47], [57]. Thus, this project explored adding the same pressure pulsation attenuation device from method 1 to 5 onto the tank-to-canister line. This location is furthest from the pressure pulsation source CPV, but closest to the noise source which is FLVV.

Porous material used in Proposal #1 was added on the tank-to-canister line. There were many different packed porous material arrangements as discussed previously in Section 5.1. The one tested was 5 inch tube with 5/8 inches ID tube densely packed steel wool. Figure 5-38 shows the porous material added onto the tank-to-canister line. Preliminary results showed that the noise was eliminated. However, due to this arrangement, no pressure readings could be obtained.

Figure 5-38: Porous material added onto tank-to-canister line

Same sized nozzle and convoluted pipes proposed in previous sections were also installed on the same tank-to-canister line location to test if they could eliminate the woodpecker noise. The results were rather surprising: with nozzle added onto the tank-to-canister line, the woodpecker noise still persisted; same with convoluted pipes. Different lengths of the same convoluted pipes (5/8 inches ID) were tested (4.5, 9, 18, and 36 inches). However, none was able to eliminate the woodpecker noise.

5.8.1 Pressure Readings taken at Tank-to-Canister line

At the beginning of the experimental data gathering, many pressure readings were taken at tank-to-canister line. With data analysis, initial attempts were made to find a "threshold" for the pressure at tank-to-canister line. That is where the pressure pulsation becomes big enough for the woodpecker noise to occur. However, such threshold could not be clearly identified. It could be partially due to the pressure pulsation flow direction discussed in Causality (Section 4.1.2).

This report only presented one set of data for illustration purposes to show the trend. For this particular experiment set up, same nozzle in Section 5.2 was added onto tank-to-canister line. Pressure readings on location ② were taken, as shown in Figure 5-39 below.

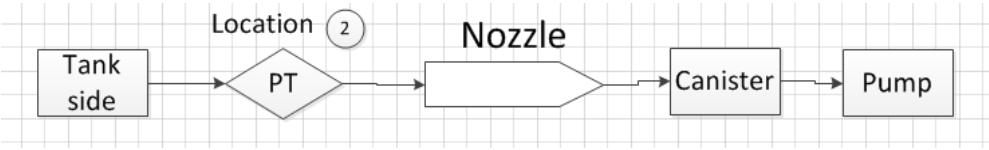

Figure 5-39: Nozzle added onto tank to canister line

The test running condition is at benchmark (baseline) condition as discussed in Section 3.8. The CPV frequency was 20Hz, duty cycle was at 50%, and the vacuum level was kept at 40kPa. It was observed that both benchmark condition (no components attached) and nozzle added (both directions) would produce woodpecker noise. Figure 5-40 through Figure 5-42 show the pressure readings in frequency domain. It was noticed that there was little noticeable differences, which is confirmed by data shown in Table 5-4 below.

Table 5-4: Nozzle added on tank-to-canister line pressure readings comparison

	BenchMark	Nozzle-pointing tank	Nozzle-pointing CPV
AVG(Kpa)	-1.1	-1.0	-1.0
PP(Kpa)	1.8	1.8	1.4

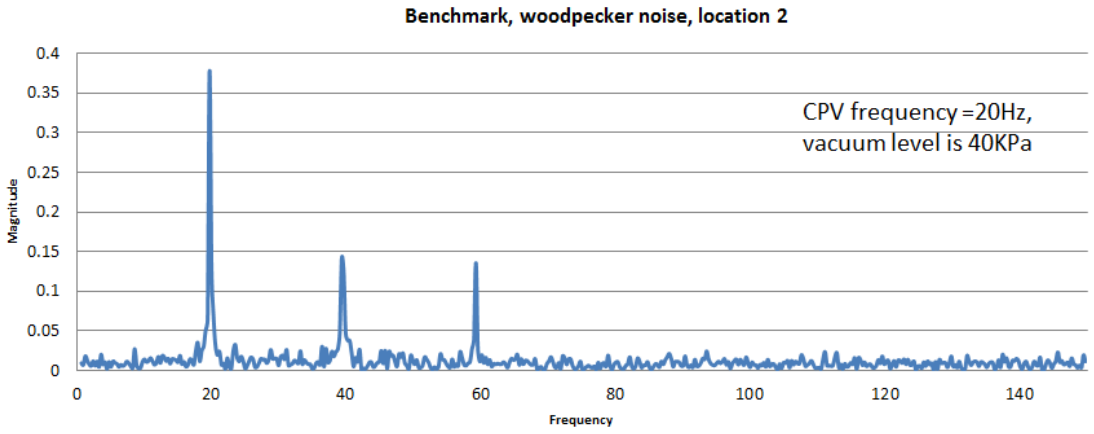

Figure 5-40: Benchmark woodpecker noise, frequency domain

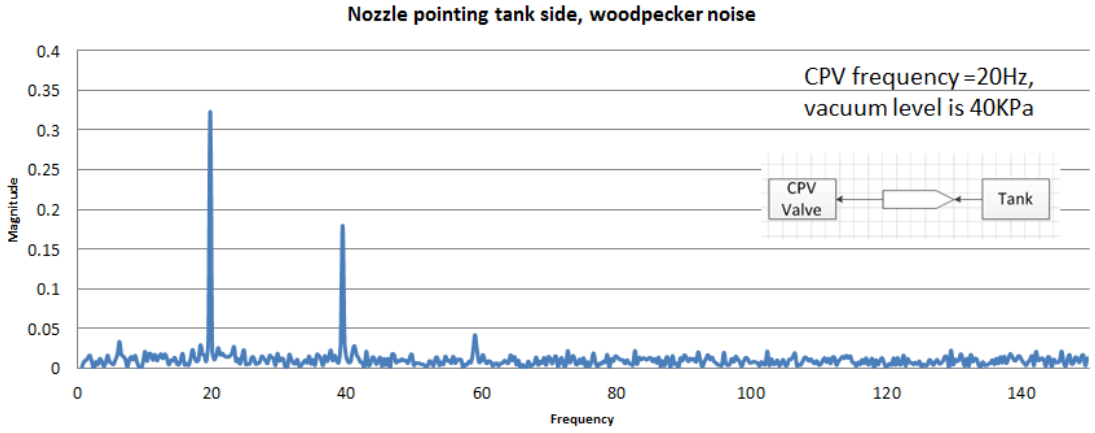

Figure 5-41: Nozzle pointing tank side, woodpecker noise, frequency domain

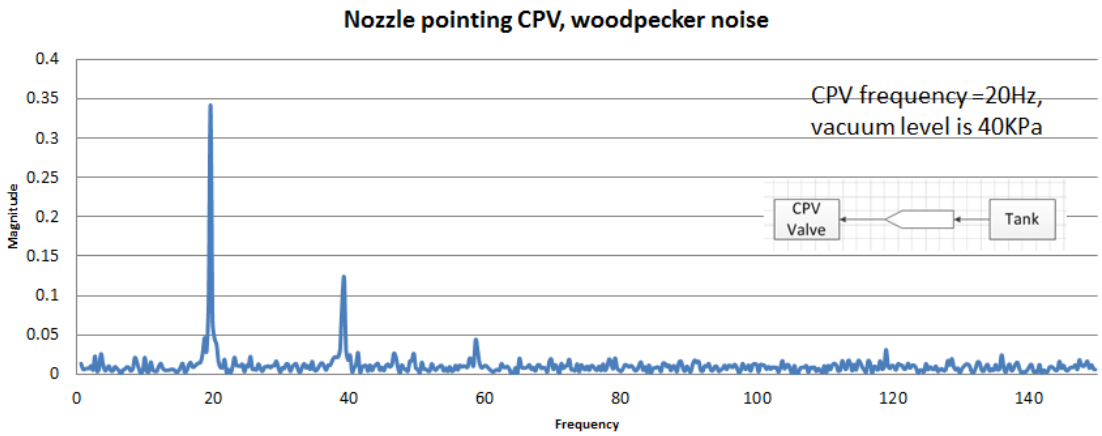

Figure 5-42: Nozzle pointing CPV, woodpecker noise, frequency domain

Another extra piece of information came later during weekly meeting with the OEM. Due to design constraints, there should not be any components added on the tank-to-canister line to cause resistance for the gas vapor to flow from tank to canister during normal non-purging conditions. Based on these information discussed above, it was decided not to pursue adding components on tank-to-canister line further.

Chapter 6
Summary and Recommendations

This chapter summarizes the work done in this research which consisted of two parts and makes recommendations for potential future researches. First part is observations and findings obtained during noise re-creation. This is covered in Chapter 4, and corresponds to the first two objectives listed in Section 1.3. Second part is assessing potential solutions to address the noise issue, either qualitatively or quantitatively. This corresponds to the 3rd and 4th objectives and is covered in Chapter 5. Thus all the objectives of this thesis have been achieved.

6.1 Noise Re-creation Summary

Pressure readings obtained from the two pressure transducers were the primary data collected and analyzed. The data, once obtained, was analyzed in both time and frequency domains. It provided many insights about the noise phenomenon. In the time domain, the peak-to-peak values of the pressure readings were used to quantify the pressure pulsation. Timed averages of the pressure readings were also presented. In the frequency domain, the pressure readings were treated by FFT. The pressure FFT plots confirmed that the CPV frequency, which is controlled by the PWM driver, is the dominant frequency in the system.

It was observed that the in frequency domain, there was one dominant peak occurring at the driving CPV frequency, which was expected. However, smaller peaks at the harmonics of the driving frequency were present as well. In one previous research [31], the same phenomenon was evident, however it was not noted by the authors.

The pressure pulsation transmission path is from CPV to fuel tank, and it was deduced that the pressure affecting the system is always the "downstream" pressure. The pressure that is closer to the fuel tank exerts greater influence on its behavior. This observation is especially important in Chapter 5 as the main focus was on the pressure reading going to the fuel tank. It also explains why re-circulation line does not impact the noise.

A different kind of noise less audible was identified and named "satellite disc" noise. The main tapping noise was subsequently named woodpecker noise for differentiation. The naming convention of the satellite disc noise was based on the speculation that it was initiated by the satellite disc. The satellite disc is a small sealing piece sitting on top of the float inside FLVV.

It was also observed that the noise would not necessarily occur even at the supposed noise occurring operating conditions. This had led to the theory of noise initialization. The sloshing effect of the liquid inside the fuel tank and the satellite disc's movement may initiate the noise, which turns into a self-sustaining effect. However, this was not proved in this thesis.

This research confirmed that the GVV does not have noticeable effects on the noise, and disproved the theory that the FLVV and GVV are acting together driven by the pressure buildup inside the fuel tank valve system. The GVV's float, whether it is at its top position or not, does not create a ripple effect that affects the FLVV.

The use of inspection camera enabled inspection inside the fuel tank on the rig level testing, while preliminary tests allowed inspection on the individual valve level. The main observation is the water level, which affects the float position of the FLVV and GVV. If the float is at its top position, the valve is considered closed and may cause restriction on the flow. The visualization confirmed that the GVV's open/closed state does not affect the noise. Also it provided information about the water level inside the fuel tank with respect to each valve when the fuel tank is at various orientations.

6.2 Noise Reduction Summary

The main focus on addressing the noise issue was to reduce or eliminate the pressure pulsation on its transmission path. In this report, this was achieved by either adding extra components on the EVAP line, or changing the pipe line dimensions and configurations. The earlier includes method to add porous material, nozzle, and an empty chamber, while the latter includes changing the pipe diameters, and switching to convolute pipe.

The measured parameters were flow rate, pressure readings, as well as a subjective assessment of noise occurring. These parameters were used as indicators to compare each proposal. The flow rate was used to compare the effect it has on the flow by adding one component. The pressure pulsation was quantified by peak-to-peak values. Pressure FFT plots were included to analyze the data in frequency domain. The timed-average of the pressure readings was calculated as well.

The numbers were compared between the baseline data with each method. Table 6-1 shows all the tabulated data. This table only included the methods that successfully eliminated the noise. Due to facility constraint, noise could only be identified subjectively as being eliminated or persistent. The pressure readings shown in the table only include the tank side reading. The reason is that the pressure pulsation traveling direction which is covered in Causality in Section 4.1.2.

Table 6-1: Pressure Pulsation Attenuation Summary-Transmission Path

Proposal	Description	Flow	Pressure Pulsation (Peak-to-peak)	Pressure	Noise?
Porous Material	2" length, 3/8"ID tubing, with densely packed steel wool	7.5% reduction	49% reduction	33% reduction in negative pressure	No
Nozzle	non-standard size, 14.96mm to 2.36mm, not concentric	10% reduction	37% reduction	65% reduction in negative pressure	No
	standard size, 3/8" to 1/8", concentric	40% reduction	42% reduction	18% reduction in negative pressure	No
Varying ID pipe	5/8" ID	9% increase	43.5% reduction	6% reduction in negative pressure	No
	3/16" ID	31% reduction	65% reduction	19% reduction in negative pressure	No
Convolute pipe	5/8" ID convolute pipe	-----*	56.5% reduction	6% increase in negative pressure	No
Chamber	65ml internal volume, roughly a rectangular boxed shape	-----**	35% reduction	13% reduction in negative pressure	No

* information was not recorded

**information was not recorded

It can be seen that the common trait for all the proposals that successfully eliminating the noise is reduction in pressure pulsation. The maximum reduction is 65% in 3/16” ID pipe case, and the minimum reduction is 35%. This is consistent with the observation regarding the noise generation mechanism. The flow rate was reduced in most of the cases, while the negative pressure applied to the system also reduced except for one case.

The two CPV prototypes with different spring stiffness did not eliminate the noise. It was observed that the noise would occur less because the operating conditions that created the noise became less. This may be due to the prototypes' L-shaped design as oppose to the baseline design of straight line. However, further investigations are needed.

Modifications on the FLVV were carried out on the two separate FLVV/GVV sets provided by the OEM. Two approaches were investigated. First was to drill holes on the FLVV casing, allowing the pressure to equalize. This provided promising results on the individual valve level test. The second approach was to modify the casing to create damping effect on the float, preventing its up-and-down motion induced by the pressure pulsations. However, preliminary test did not show any improvements.

This report did not fully explore the effects of the location change on the pressure pulsation change. But an extreme case scenario was tested, which was to have the components added on the tank-to-canister line – the other end of the pressure pulsation transmission path. This was covered in Section 5.8. A sensitivity study could be conducted on where the pulsation reduction effect is the most. This can be done either experimentally or through computer simulation.

6.3 Recommendations

All four of the objectives stated in this research have been met. However, this project still has great potentials to be investigated further. Based on the work and research done in this thesis, below is a list of recommended future works that can help further understand this noise issue and may lead to eventual discovery of the "ultimate" solution that can both address the noise issue but also takes real-world engineering design constraints into consideration.

- A "round robin" test to validate both the quantitative and qualitative conclusions drawn from this thesis, preferably more sensible and accurate equipment used.
- If possible, re-run the test in an anechoic chamber. This allows an accurate capture of noise and provides new understandings on the "satellite disc" noise.
- Perform assessment on the proposals covered in Table 6-1 with focus on the feasibility in engineering perspective. Although all of those proposals provide sufficient pressure pulsation reduction to reduce the noise, the system suffers either flow restriction or packaging issue, or both.

- Further investigation on CPV or FLVV modifications. Although it was decided that this is not feasible at this stage, they are the sources of the noise issue. CPV is the pressure pulsation source, and FLVV is the noise source.
- A closer look at the harmonic peaks occurring in frequency domain is recommended as was covered in Section 4.1.1. If pressure readings collected from previous researches focusing on pressure pulsations can be obtained, a frequency domain analysis should be carried to either confirm or dismiss this phenomenon.
- Parametric and sensitivity studies to further quantify findings and proposals. This is especially important as the proposal needs to be integrated into the actual production vehicle.
- A numerical simulation can complement the experimental work in better understanding of this phenomenon. This is especially crucial in noise prevention during design phase.
- More detailed statistical analyses are required to examine the relationship or correlations among all the data collected.

Bibliography

[1] "OCIA stats online sources," *http://www.oica.net/category/production-statistics/*.

[2] "AECA stats online sources," *Http://www.acea.be/statistics/tag/category/vehicles-in-use*.

[3] "Arbitron in-car study 2009," *http://www.arbitron.com/downloads/InCarStudy2009.pdf*, 2009.

[4] P. Oliveira, A. Alto, and A. Prechtel, "Impact of new evaporative emission requirements (Euro III/IV) on gasoline fuel systems," *SAE Tech. Pap. 2007-01-2661*, 2007.

[5] H. Huo, K. He, M. Wang, and Z. Yao, "Vehicle technologies, fuel-economy policies, and fuel-consumption rates of Chinese vehicles," *Energy Policy*, vol. 43, pp. 30–36, Apr. 2012.

[6] K. S. Kumar, S. Pal, and R. C. Sethi, "Objective evaluation of ride quality of road vehicles," *SAE Tech. Pap. 990055*, Jan. 1999.

[7] A. Soliman, A., Moustafa, S., and Shogae, "Parameters affecting vehicle ride comfort using half vehicle model," *SAE Tech. Pap. 2008-01-1146*, 2008.

[8] C. Chavan, D. Kb, R. Babu, and M. Shaikh, "Ride comfort analysis of motorcycle using virtual prototype," *SAE Tech. Pap. 2011-32-0537*, 2011.

[9] S. Kim, S. Hwang, K. Lee, and J. Pyun, "New anthropometry of human body models for riding comfort simulation," *SAE Tech. Pap. 2007-01-2457*, 2007.

[10] K. S. Hatti, V. A. John Britto, and S. Sankaranarayana, "NVH attribute - roadmap for competitive advantage," *SAE Tech. Pap. 2013-01-2851*, Nov. 2013.

[11] S. Park, B. Min, J. Lee, and E. Kang, "Development of the evaluating system for ride comfort and fatigue in vehicle," *SAE Tech. Pap. 2001-01-0388*, 2001.

[12] A. de Miranda and J. Germaine, "New direction and trends for vehicle entertainment systems," *SAE Tech. Pap. 2012-36-0518*, 2012.

[13] A. de Miranda, "New designs and concepts for vehicle entertainment systems," *SAE Tech. Pap. 2006-01-2828*, 2006.

[14] A. M. Mufid, "Future automotive multimedia subsystem interconnect technologies," *SAE Tech. Pap. 2000-01-C028*, 2000.

[15] G. Mastinu, M. Gobbi, and M. Pennati, "Theoretical and experimental ride comfort assessment of a subject seated into a car," *SAE Int. Journal, Passeng. Cars-Mechanical Syst.*, vol. 3, no. 1, pp. 607–625, 2010.

[16] A. Heydari and S. Jani, "Entropy-minimized optimization of an automotive air conditioning and HVAC system," *SAE Tech. Pap. 2001-01-0592*, 2001.

[17] N. Orand and R. Rhote-Vaney, "Modeling, validation and analysis of the fuel supply and injection system for NVH improvement," *SAE Tech. Pap. 2009-01-2055*, 2009.

[18] H. Du, J. Chen, K. Moss, and J. Zamora, "NVH analysis of balancer chain drives with the compliant sprocket of the crankshaft with a dual-mass flywheel for an inline-4 engine," *SAE Tech. Pap. 2007-01-2415*, 2007.

[19] C. La, M. Poggi, P. Murphy, and O. Zitko, "NVH considerations for zero emissions vehicle driveline design," *SAE Tech. Pap. 2011-01-1545*, May 2011.

[20] B. Avutapalli, S. Vallurupalli, and H. Keshtkar, "Road-shake and impact Harshness(NVH) response multi- function optimization for a body-on-frame vehicle," *SAE Tech. Pap. 2003-01-1713*, 2003.

[21] S. Amman, B. Gulker, and S. Abhyankar, "Subjective quantification of wind buffeting noise," *SAE Tech. Pap. 1999-01-1821*, 1999.

[22] R. Williams, M. Allman-Ward, P. Jennings, and M. Batel, "Using an interactive NVH simulator to capture and understand customer opinions about vehicle sound quality," *SAE Tech. Pap. 2007-26-036*, Jan. 2007.

[23] J. Headley, K. Liu, and R. Shaver, "Validation of vehicle NVH performance using experimental modal testing and in-vehicle dynamic measurement," *SAE Tech. Pap. 2007-01-2320*, 2007.

[24] R. Izydorek and G. Maroney, "A standard method for measuring fuel system pulse damper attenuation," *SAE Tech. Pap. 2000-01-1086*, 2000.

[25] A. Pittel and A. Weimer, "High vacuum purge and vapor canister performance," *SAE Tech. Pap. 2004-01-1435*, 2004.

[26] T. Arase, T. Ishikawa, M. Kobayashi, Y. Hyodo, and M. Kasai, "Development of vapor reducing fuel tank system," *SAE Tech. Pap. 2001-01-0729*, 2001.

[27] Y. Nuiya, H. Uto, and T. Suzuki, "Reduction technologies for evaporative emissions in zero level emission vehicle," *SAE Tech. Pap. 1999-01-0771*, 1999.

[28] R. a. Roberts and J. Cui, "Numerical analysis of a pulsation damper in fuel injection rails," *Int. J. Veh. Syst. Model. Test.*, vol. 1, no. 4, pp. 312–328, 2006.

[29] J. Kim, S. Oh, K. Lee, and M. Sunwoo, "Individual cylinder air-fuel ratio estimation algorithm for variable valve lift (VVL) engines," *SAE Tech. Pap. 2010-01-0785*, 2010.

[30] C. S. Potts, “A case of probable encephalitis due to the inhalation of the fumes of gasoline,” *J. Nerv. Ment. Dis.*, vol. 42, no. 1, pp. 24–27.

[31] K. Mizuno, S. Usui, I. Imura, and T. Ogata, “Fuel rail with integrated damping effect,” *SAE Tech. Pap. 2002-01-0853*, 2002.

[32] S. M. Tariq and M. Tripathi, “Robust Engineering Methodology for pulsation noise reduction in gasoline vehicles,” *SAE Tech. Pap. 2013-01-2740*, Nov. 2013.

[33] H. Scheuerer, K. Braess, “Transportation fuels of the future,” *SAE Tech. Pap. 2006-21-0089*, 2006.

[34] C. Marriott, M. Wiles, J. Gwidt, and S. Parrish, “Development of a naturally aspirated spark ignition direct-injection flex-fuel engine,” *SAE Int. J. Engines*, vol. 1, no. 1, pp. 267–295, 2009.

[35] J. Cohen, D. Eichelberger, and D. Guro, “Determining the optimum hydrogen fueling pressure,” *SAE Tech. Pap. 2007-01-0695*, 2007.

[36] P. Chinnasamy, H. Sauter, A. Zeller, and J. Schwinge, “Air intake system evaporation emissions: physical description and solutions,” *SAE Tech. Pap. 2008-01-0627*, 2008.

[37] M. Sultan, M. Kushion, and R. Wind, “Closed-loop canister purge control system,” *SAE Tech. Pap. 980206*, 1998.

[38] J.-S. Lin, M. Dong, S. Ali, M. Hipp, and C. Schnepper, “Vehicular emission performance simulation,” *SAE Tech. Pap. 2012-01-1059*, Apr. 2012.

[39] M. Cortese, “A study of rail pressure variation for various fuel injectors on a simple rail design over the engine operation range,” *SAE Tech. Pap. 2004-01-2937*, 2004.

[40] H. D. S. Ho Nam Chang, Ji Soo Ma, Joony Kon Park, In Ho Kim, “Velocity field of pulsatile flow in a porous tube,” *J. Biomech.*, vol. 22, no. 11/12, pp. 1257–1262, 1989.

[41] R. J. Pearson and J. W. G. Turner, “Exploitation of energy resources and future automotive fuels,” *SAE Tech. Pap. 2007-01-0034*, 2007.

[42] G. E. Barter, D. Reichmuth, T. H. West, and D. K. Manley, “The future adoption and benefit of electric vehicles: a parametric assessment,” *SAE Int. Journal, Altern. Power*, vol. 2, no. 1, pp. 82–95, Apr. 2013.

[43] A. Pant, C. P. Jain, and D. K. Panda, “Numerical modeling of critical path contributions for NVH prediction of vehicle,” *SAE Tech. Pap. 2013-01-2802*, Nov. 2013.

[44] V. A. John Britto, S. Sivasankaran, E. Loganathan, S. Kupplili Saisankaranarayana, and K. Sidram Hatti, "Commercial vehicle NVH refinement through test-CAE development approach," *SAE Tech. Pap. 2013-01-1006*, Apr. 2013.

[45] Otto N. and Feng B., "Wind noise sound quality," *SAE NVH Conf. Travers. City, MI*, no. Paper 951369, 1995.

[46] "Method for calculating loudness level," *ISO 532*, 1975.

[47] T. Ogata, Y. Serizawa, and H. Tsuchiya, "Further pressure pulsation reduction in fuel rails," *SAE Tech. Pap. 2003-01-0407*, 2003.

[48] C. Chen, J. Lin, and C. Le, "Integrate structural optimization into upfront carbon canister component design process," *SAE Tech. Pap. 2005-01-1066*, 2005.

[49] G. Delaire and D. Balsdon, "Mathematical modeling of a balanced canister purge solenoid valve," *SAE Tech. Pap. 1999-01-1080*, 1999.

[50] H. Servati, S. Marshall, J. Murphy, M. F. Sanei, W. Zhou, and W. L. Jr, "Carbon canister-based vapor management system to reduce cold-start hydrocarbon emissions," *SAE Tech. Pap. 2005-01-3866*, 2005.

[51] H. Viswanathan, A. Awasthi, C. Ageorges, and M. Bohl, "Shock waves in canister purge valves," *SAE Tech. Pap. 2013-26-0040*, 2013.

[52] D. Mancini, "The design for Six Sigma approach for the development of a carbon canister for Tier II, LEV II and PZEV emission levels," *SAE Tech. Pap. 2007-01-1090*, 2007.

[53] S. Reddy, "Understanding and designing automotive evaporative emission control systems," *SAE Tech. Pap. 2012-01-1700*, Sep. 2012.

[54] J. Chen and W. Yang, "Pressure pulsation and fuel injction noise of a fuel delivery system-applications of FuelNet," *SAE Tech. Pap. 981416*, 1998.

[55] Huang D. and Lai M.C., "Experimental investigation of characteristics of pressure modulation in a fuel injection system," *Int. J. Automot. Technol.*, vol. 10, no. 1, pp. 9–16, 2009.

[56] Q. Hu, S. Wu, M. Lai, S. Stottler, and R. Raghupathi, "Prediction of pressure fluctuations inside an automotive fuel rail system," *SAE Tech. Pap. 1999-01-0561*, 1999.

[57] H. S. Heo, S. J. Bae, H. K. Lee, and K. S. Park, "Analytical study of pressure pulsation characteristics accroding to the geometries of the fuel rail of an MPI engine," *Int. J. Automot. Technol.*, vol. 13, no. 2, pp. 167–173, 2012.

[58] T. D. Spegar, "Minimizing Gasoline Direct Injection (GDi) fuel system pressure pulsations by Robust Fuel Rail Design," *SAE Tech. Pap. 2011-01-1225*, Apr. 2011.

[59] D. R. Rogers, “Engine combustion: pressure measurement and analysis,” *"A Br. Hist. Engine Indic. Engine Combust. Press. Meas. Anal.*

[60] S. Wheatley, “Using pulsation dampers to reduce pipework vibrations,” *World Pumps*, no. January, pp. 32–35, 2002.

[61] J. Chai, J., Munukutla, S. and Peddieson Jr., “Fuel system pulsation analysis,” *Tech. Rep. Submitt. to EPRI Inc.*, 1999.

.